Unified Continuum Modeling of Fully Coupled Thermo-Electro-Magneto-Mechanical Behavior, with Applications to Multifunctional Materials and Structures

Dissertation

Presented in Partial Fulfillment of the Requirements for the Degree Doctor of Philosophy in the Graduate School of The Ohio State University

By

Sushma Santapuri,

Graduate Program in Department of Mechanical Engineering

The Ohio State University

2012

Dissertation Committee:

Prof. Stephen Bechtel, Advisor

Prof. Marcelo Dapino, Co-Advisor

Prof. Joseph Heremans

Prof. Rama Yedavalli

© Copyright by

Sushma Santapuri

2012

Abstract

Multifunctional structures based on active or smart materials are being implemented in a wide range of aerospace, infrastructural, automotive, and biomedical applications. However, smart materials are underutilized in these applications, as majority of the modeling and characterization techniques of smart materials limit the understanding of material behavior to low-signal, small-deformation ranges of operation, or regimes where only a subset of the thermal, electrical, magnetic, and mechanical interactions are dominant. By modeling smart materials in their fully coupled, nonlinear, three-dimensional, multiphysics process domain rather than in a specific regime of behavior, design of the next-generation of load-carrying smart structures with superior performance capabilities can be enabled. The objective of this work is to develop mathematical and computational models for modern multifunctional materials and devices.

This dissertation focuses on development of a first-principle based theoretical framework for modeling and characterization of fully coupled thermo-electro-magneto-mechanical behavior in a multiphysics process domain, that can be utilized to (i) develop constitutive models and free energy functions for a broad range of smart materials using the fundamentals of equilibrium and non-equilibrium thermodynamics, (ii) develop asymptotic models for design and analysis of load-bearing antenna, which

is a multifunctional actuating and receiving device integrated with a load-bearing structure.

The first part focuses on development of a unifying thermodynamic framework for multifunctional materials with fully coupled thermo-electro-magneto-mechanical response. This framework consists of a comprehensive catalogue of all possible state variables, thermodynamic potentials, and state equations that characterizes TEMM processes. This unifying framework applicable to a general polarizable, magnetizable and deformable media, is then utilized to develop material response functions for a wide range of materials, i.e., (i) elastic, lossless dielectric, piezoelectric materials (approximately reversible), (ii) ferroic materials exhibiting dissipation, (iii) materials exhibiting transport properties.

The second part of this dissertation is focused on development of mathematical models that will enable the design and analysis of multifunctional structures. Existing models for smart material based applications assume quasi-static electric or magnetic fields, which is not an accurate assumption for high frequency based antenna applications. In order to model this dynamic electromagnetic behavior coupled with the structural behavior of load-bearing antennas, a two-dimensional plate theory for coupled electro-magneto-mechanical plates has been developed in high frequency electromagnetic field regime, and finite element method has been used to simulate this behavior. Simulations are performed for a prototype design of the load-bearing antenna structure consisting of regular dielectric-honeycomb sandwich structure and the results are compared to suggest improvements in load-bearing antenna designs. The mathematical framework presented here is fairly general and can be used to model a broad range of materials and devices.

To my parents ... for their endless love and support

Acknowledgments

I am truly indebted and thankful to my Advisor Prof. Stephen Bechtel for his support and guidance throughout the course of my graduate study. His passion towards research, teaching, and amazing technical documentation skills will always be an inspiration to me. I owe sincere and earnest thankfulness to my Co-Advisor Prof. Marcelo Dapino, for giving invaluable advice on my research work, that has helped greatly in improving this dissertation. I sincerely appreciate all his support and encouragement which has helped me in working towards my development as a researcher.

I would like to express my gratitude to Prof. Heremans for agreeing to be on my doctoral committee and for sharing his thoughts and providing valuable inputs on the thermodynamic framework development. I would also like to thank to Prof. Yedavalli for agreeing to be on my committee and also for giving me valuable advice on research and graduate life.

I would like to take this opportunity to thank my undergraduate professor and mentor Prof. Babu for guiding me through some of the most difficult times. I would also like to thank my labmate and my friend Robert Lowe, who has always been willing to lend a helpful hand. I have truly enjoyed working with him and learning from him.

I would like to thank my friends Swapna, Nafeesa, Amita, Siddhesh, Emily, and Surya, for showing their support and making my graduate school life memorable. Most importantly, I would like to thank my best friend Praneeth for giving me the much needed emotional support and listening to my ramblings during the difficult times.

Finally, I would like to thank my parents and my sister, for their endless love and affection. My graduate life and this dissertation would not have been possible without their encouragement and support. I will always be grateful to my parents for teaching me to appreciate the important things in life.

Vita

June 15, 1985 ..... Born - Hyderabad, India

2007 ..... B.Tech. Mechanical Engineering

2007-present ..... Graduate Research Assistant,
The Ohio State University.

Publications

Research Publications

S. Santapuri and S.E. Bechtel, "A Two-Dimensional Theory of Coupled Electro-Magneto-Mechanical Plates as an Application to Load-Bearing Antenna Structures," SPIE Proceedings, Vol. 7978, 6-10 March 2011, San Diego, CA, USA.

S. Santapuri and S.E. Bechtel., "Model-Based Optimization of Coupled Electro-Magneto-Thermo-Mechanical Behavior of Load-Bearing Antennas," Proceedings of ASME IMECE, 12-18 November 2010, Vancouver, BC, Canada.

Fields of Study

Major Field: Mechanical Engineering

Table of Contents

Page

List of Tables

List of Figures

Chapter 1: Introduction

1.1 Multifunctional Materials and Structures

Multifunctional materials can be described as materials that are designed to accomplish multiple performance objectives (e.g., structural integrity, sensing and actuating capabilities) in a single material system [45]. The novel capabilities afforded by multifunctional materials promise to (i) improve existing actuating and sensing technologies and (ii) expand the performance space of the next generation of intelligent systems, structures, and devices [69]. They are generally fabricated by layering a constituent set of active materials into a composite, or by embedding small particles in a matrix [11], and can be tailored to attain a desired set of performance objectives that would be realized less optimally, or even be improbable to achieve, with a single smart material.

Some examples of modern multifunctional structures are highlighted in Fig. 1.1 [65]. One such example includes modern aerospace technology called conformal load-bearing antenna, designed by embedding sensing and actuating device (antenna) in a load-bearing structure, to accomplish multifunctionality and weight reduction (Fig. 1.1) [81]. This multifunctional system can simultaneously support aerodynamic loads in addition to radiating and receiving electromagnetic signals. Other examples of

novel multifunctional devices and applications include devices like crystal oscillators [79], photoelectric sensors, macrofiber composites [74, 80], and micro antenna devices [71].

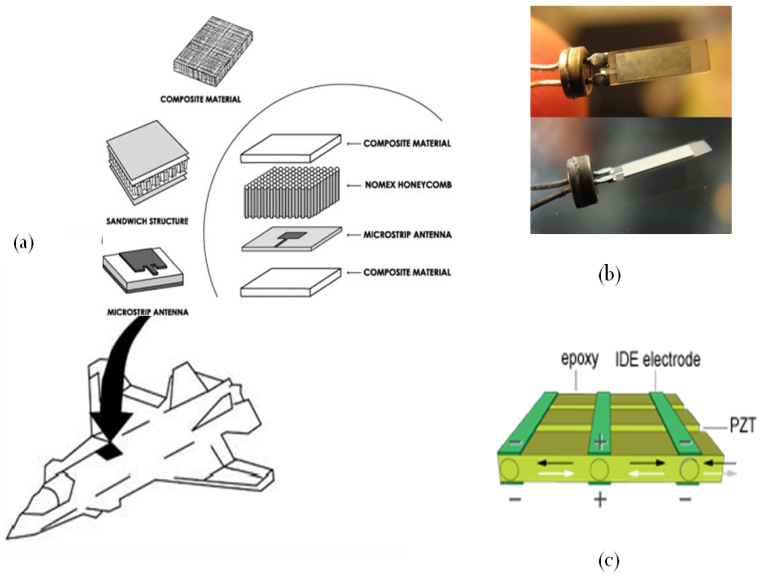

Figure 1.1: Examples of modern multifunctional structures: (a) load-bearing antenna (b) crystal oscillator (c) macrofiber composite

A sufficiently general description of a multifunctional structure would include a composite (beam, plate, shell, or any other structural elements) with embedded or surface mounted smart material layers designed to sense and take corrective action [65]. By appropriately choosing the constituent materials and geometry of the composite, the multifunctional structure can be designed to perform optimally for the particular application. Some well-known smart materials used for multifunctional applications include piezoelectric materials, electrostrictive materials, magnetostrictive materials, and shape memory alloys, to name a few. If utilized to their maximum

potential, these smart materials can be used to develop sophisticated adaptive and multifunctional technologies with self-sensing, healing, actuating, and active vibration controlling capabilities.

Experimental investigations to construct multifunctional material systems and structures with these materials can be very expensive and therefore they should be complemented with appropriate theoretical analysis. Unfortunately, much of the early literature on modeling and characterization of smart materials confined the understanding of material behavior to low-signal, small-deformation ranges of operation or regimes where only a subset of the thermomechanical and electromagnetic interactions are dominant [72]. Also, these models often neglect complex effects like dynamic nature of electromagnetic fields, anisotropy, and material nonlinearity.

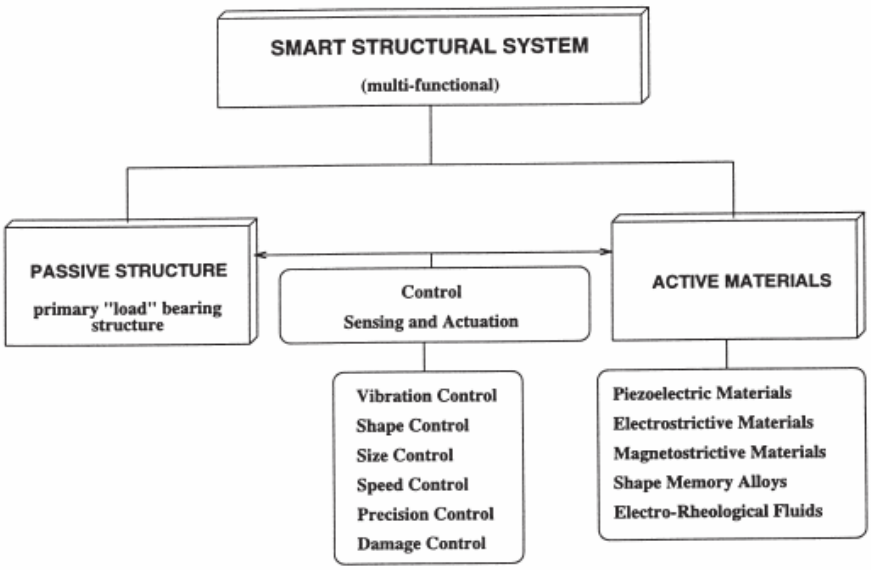

Figure 1.2: Smart Structural Systems

These models are not always sufficient for design and analysis of modern multifunctional materials with complex thermal, electrical, magnetic and/or mechanical coupling. For instance, the customary quasi-static electromagnetic field approximation breaks down for devices like load-bearing antennas, macrofiber composites, and micro antennas, which operate at higher frequencies (MHz - GHz). By placing a priori restrictions and ignoring some of the physics effects in modeling, the breadth of the design space is often limited. In order to progress towards the next generation of intelligent structural systems with embedded multifunctionality, fundamental advancements in the continuum modeling architecture are required. This architecture must be broad enough to enable design and optimization. In particular, a general 3-D multi-physics model that accommodates fully coupled thermo-electro-magneto-mechanical (TEMM) behavior, finite deformations, nonlinear constitutive behavior, dynamic fields, etc. is needed.

A unifying continuum framework for fully coupled TEMM behavior as described above promises to not only improve existing multifunctional technologies and designs, but can also provide the necessary mathematical background to design new man-made materials with customized material properties. Some examples of existing man-made materials designed to have tailored material properties like permittivity and permeability include metamaterials [70], and photonic crystals [38].

The main objective of this dissertation is to develop advanced mathematical and computational tools that enable the modeling and characterization of multifunctional materials and structures. The first part of this dissertation focuses on the development of a unifying thermodynamic framework for multifunctional materials with fully coupled thermo-electro-magneto-mechanical response. This framework consists of a

comprehensive catalogue of all possible state variables, thermodynamic potentials, and state equations that characterize TEMM processes. This unifying framework for a general polarizable, magnetizable and deformable medium is then utilized to develop material response functions for a wide range of materials, i.e., (i) approximately reversible, e.g., elastic, lossless dielectric, piezoelectric materials (ii) hysetertic materials, e.g., ferroic materials, magnetostrictives, and (iii) materials exhibiting transport properties, e.g., metals.

The second part of this dissertation is focused on the development of mathematical models that will enable the design and analysis of multifunctional structures. Asymptotic models are developed for multifunctional structures operating in a specified regime of behavior, or consisting of specialized geometries like beam, shell, plate, etc., using nondimensionalization and perturbation techniques. This dissertation focuses on one such multifunctional structure, i.e., a load-bearing antenna. Governing equations are developed for a load-bearing antenna structure and solved for some of its existing designs. This framework is then extended to develop a general 2-D plate theory for dynamic fully coupled electro-magneto-mechanical behavior. The theory and its weak formulation are developed, and the finite element formulation is set up for this problem. This framework is fairly general and can be utilized to model a wide variety of applications.

1.2 Research Objectives

A brief description of each of these research objectives is presented in the following section, along with the associated literature survey, the methodology used, and the expected outcomes.

1. Development of a Unifying Thermodynamic Framework for Fully Coupled Thermo-Electro-Magneto-Mechanical Behavior with Applications to Multifunctional Materials

As discussed earlier, the early literature on modeling and characterization of smart materials like piezoelectrics, electrostrictives, magnetostrictives, and shape memory alloys confines the understanding of material behavior to low-signal, small-deformation ranges of operation, or regimes where only a subset of the thermal, electrical, magnetic, and mechanical interactions are dominant (see, for instance, [8]). With the advent of new technologies and increasingly demanding operating environments, these early models have been advanced to accommodate some of the more complex effects like large deformations, strong electromagnetic fields, constitutive nonlinearities, hysteresis, and anisotropy, to name a few. For instance, Smith & Dapino [73] and Evans & Dapino [21, 20] characterize the three-dimensional, nonlinear, anisotropic, hysteretic, magneto-mechanical constitutive behavior of magnetostrictives like Terfenol-D and Galfenol. Models for ferroelectrics developed by Hwang & McMeeking [35, 36] incorporate three-dimensional, nonlinear, anisotropic, electromechanical response. Recent papers by Dorfmann & Ogden [16, 17] and Kankanala & Triantafyllidis [40] on magnetorheological elastomers, and by Rajagopal & Růžička [64] on electrorheological fluids, reflect the dynamic coupling of the electromagnetic and thermomechanical fields. Although advanced, these models are applicable only to the particular material in its regime of operation.

To facilitate the characterization and design of novel multifunctional materials, a more general approach is needed, i.e., one that (i) describes a general deformable, magnetizable, polarizable continuum, and (ii) incorporates many of the features of

the state-of-the-art models discussed above by nonlinearly, dynamically, and three-dimensionally fully coupling the thermal, electrical, magnetic, *and* mechanical effects. To this end, in this disertation, a multiphysics framework is developed and deployed for modeling and characterizing fully coupled thermo-electro-magneto-mechanical behavior, from the perspective of a general thermodynamic process. This methodology differs fundamentally from existing approaches in that the smart materials are modeled in their fully nonlinear, three-dimensional, multiphysics *process domain* rather than in a specific *regime of behavior.*

In particular, the principles of classical thermodynamics [9] are integrated with the pioneering continuum electrodynamics work of Eringen & Maugin [18, 19], Hutter [34, 32, 31, 33], Pao [60, 61], and Truesdell & Toupin [78, 76]. In these continuum electrodynamics models, the first principles (i.e., Maxwell's equations, conservation of mass, balance of linear momentum, balance of angular momentum, and the first law of thermodynamics), boundary conditions, and *coupling models* were well-developed and studied extensively. The coupling models describe the electromagnetic interaction terms (namely, the electromagnetic body force, body couple, and energy supply) that couple the thermomechanical balance laws to Maxwell's equations. Some well-known theories in literature that describe these electromagnetic interaction terms are Minkowski, Chu, Statistical [22]. Further development of these theories is needed, however, particularly in regards to aspects of constitutive modeling and material characterization, since these theories do not always appeal to the principles of classical thermodynamics, nor are they comprehensive. The Legendre transforms developed by these authors are not always consistent with the intensive-extensive formalism commonly used in classical thermodynamics. Also, auxiliary variables like electric

displacement vector, magnetic induction vector, are inaccessible as independent variables in a free energy via the customary formalism of Legendre transformations.

These needs are addressed and the necessary first steps are taken towards creating a unified and comprehensive TEMM framework for modeling, designing, and optimizing novel multifunctional materials. This thermodynamic framework is developed by drawing analogies from classical thermodynamics principles. Also, it is identified that the electromagnetic conjugate pairs follow from the choice of coupling model which describes the electromagnetic energy. This electromagnetic energy contributes to the evolution of the internal energy, as quantified by the first law of thermodynamics. The electromagnetic conjugate pairs differ from one interaction model to another and, hence, are not unique. In order to address this ambiguity, the framework is developed by making a particular choice of coupling theory and identifying the corresponding conjugate pairs, which gives a description for Legendre transforms.

Following these guidelines, a comprehensive catalogue consisting of thermodynamic potentials, state variables (i.e., independent and dependent variables), and state equations is developed. This framework enables the characterization of fully coupled TEMM processes. To generate this comprehensive catalogue, a complete combinatorial analysis is performed such that all possible combinations of thermal, electrical, magnetic, and mechanical independent variables that appear in the first principles are considered. Each of these combinations corresponds to a particular TEMM process, and each process, in turn, correlates with a set of experiments, the independent variables being controlled and the dependent variables being the measured responses. Each such experiment is characterized by a thermodynamic potential and a set of state equations. New thermodynamic potentials are introduced

through a battery of Legendre and Legendre-type (for introducing auxiliary independent variables) transformations, many appearing in the literature for the first time. The breadth of this catalogue is intended to provide engineers, applied physicists, and material scientists with optimal flexibility in their approach to characterizing and designing novel multifunctional materials: material properties can be deduced by working with a set of state equations that corresponds to a particular set of experiments, or energy and entropy landscapes can be constructed to achieve targeted performance properties expressed in terms of any set of TEMM quantities.

This unified thermodynamic framework is then utilized to develop response functions for a broad range of multifunctional materials and processes exhibiting coupling, namely, (i) linear reversible processes, (ii) transport processes, and (iii) hysteretic processes. Equilibrium thermodynamics principles are used for the characterization of reversible, linear processes. When extended to materials exhibiting hysteresis, an internal evolution term was introduced to accommodate for the hysteretic energy losses. To accommodate these processes, a formalism developed by Gurtin and Fried [23, 24] was utilized and extended to fully coupled TEMM behavior. This formalism requires the second law of thermodynamics to be modified to include evolution of this internal variable and the associated hystersis.

This framework can be applied to calculate energy landscapes that describe a broad range of material behavior including anisotropy, hysteresis and transport phenomena. These energy landscapes can be used for design and analysis of novel multifunctional materials and structures. Other applications of this work will be discussed in detail in the later part of the dissertation.

2. Development of Asymptotic 2-D Models for Multifunctional Structures, with Application to Load-Bearing Antennas

The second part of this dissertation will focus on developing mathematical models and computational tools that can be used to model a broad range of multifunctional materials and structures. This work details the mathematical framework to derive regime and structure specific models using nondimensionalization and perturbation techniques [58]. Perturbation techniques were used by Bechtel et al. [5, 4] to predict the behavior of viscoelastic jets by exploiting their slender 1-D axisymmetric geometry. Similarly the thin geometry of plates was exploited by Mindlin [55] to develop 2-D models for elastic, piezoelectric plates.

Similar techniques are used in this work to develop asymptotic models for multifunctional materials and structures that exhibit TEMM coupling. The complete set of TEMM governing equations are presented in a nondimensionalized form and the corresponding nondimensional groups are derived to quantify the competition between various physical effects in the operation of the particular material or structure. Depending on the design of the structure and nature of the excitation, only a subset of the physical effects are dominant, which dictates the appropriate computational model. A fixed relative ordering of all competing effects as quantified by nondimensional groups determines a *regime* of structure-environment interaction. This formalism is used for modeling and analysis of load-bearing antennas.

Load-bearing antennas are multifunctional structures with sensing and actuating capabilities integrated within a load-bearing structure. These antennas are appealing for military applications like unmanned aerial vehicles (UAV), and have superior structural and electromagnetic radiation properties compared to conventional aircraft

antennas. The antenna structure is subjected to mechanical forces, temperature gradients, and electromagnetic fields, giving rise to highly-coupled nonlinear thermo-electro-magneto-mechanical (TEMM) behavior.

In the present work, analytical techniques and computational tools are developed for multi-scale, multi-physics modeling of composite load-bearing antennas, specific to UAV applications. This work is one of the early attempts to develop a fully coupled theory for multifunctional structures like load-bearing antennas, that operate in high frequency electromagnetic fields. In order to develop models for load-bearing antennas consisting of smart or adaptive materials, the existing theories in literature are insufficient since smart materials have been traditionally modeled in the quasi-static regime, which is not a valid assumption for high frequency devices like antennas.

As described earlier, multifunctional systems like those described in Fig. 1.1 are usually designed as composite smart structures of different geometries, among which a thin geometry (plate or shell) is very frequently used (e.g., macrofiber composites, load-bearing antennas). For these applications, a coupled electro-magneto-mechanical plate theory is developed for thin geometries, where the dynamic electromagnetic behavior is coupled with the mechanical field. Some well-known plate theories used for analysis in current literature are Mindlin's plate theory [55], classical plate theory, and Reddy's third order theory [66], but all of these theories are developed for piezoelectric or piezomagnetic materials under quasi-static field assumption. In this work, an asymptotic plate theory with fully dynamic electro-magneto-mechanical coupling is developed for the first time, and the appropriate weak form is formulated using variational principles. The finite element formulation of this theory is then developed.

The use of this theory in the design of multifunctional systems is then demonstrated via a simple optimization problem.

1.3 Outline of the Dissertation

This dissertation is structured as follows: In Chapter 2 the continuum theory of electromagnetic solids is presented in a deformable, polarizable, and magnetizable medium. In this chapter, the classical continuum electrodynamics theories are explored in detail[34]. This chapter begins with explicitly stating the first principles for a deformable TEMM material (i.e., Maxwell's equations, conservation of mass, balance of linear momentum, balance of angular momentum, and the first law of thermodynamics). The first principles include terms (i.e., the electromagnetic body force, body couple, and energy supply) that model the interaction between electromagnetic and thermomechanical effects, consequently fully coupling Maxwell's equations and the thermomechanical balance laws. These coupling terms are described and quantified in Section 2.3.1. Finally, a brief discussion on coupled processes and the materials that undergo these processes is presented in Section 2.4.

This background is then utilized to develop a unifying thermodynamic framework for TEMM materials in Chapter 3. In Section 3.2, the principles of classical thermodynamics are revisited and are subsequently used as guidelines to develop an analogous continuum thermodynamic framework. In Sections 3.3 - 3.5, a comprehensive catalogue of all possible state variables, thermodynamic potentials, and state equations that characterize TEMM processes is developed. According to classical thermodynamics [9], a *fundamental* energetic process involves specific internal energy as a function of *extensive* TEMM variables; the *conjugate intensive* quantities are

the dependent variables. Thus, new energy potentials that utilize any or all of the conjugate intensive quantities as independent variables are introduced as Legendre transformations of the internal energy. In Section 3.4, energy potentials that utilize non-conjugate or auxiliary electromagnetic quantities as independent variables are introduced as Legendre-type transformations of the internal energy. At this point, a connection is established with Green and Naghdi's work on TEMM processes where these auxiliary variables were instead used as independent variables [26]. In Section 3.5, the formalism of Sections 3.3 and 3.4 is extended to TEMM processes employing entropy rather than energy as the characterizing thermodynamic potential.

The second part of this chapter focuses on development of constitutive equations for various classes of materials and processes. In Section 3.6 invariance and angular momentum restrictions are applied to the state equations. The potential function is then expanded using Taylor series, and this polynomial function is truncated after second-order terms. This expression is used to deduce a linear form for constitutive equations. The materials and the corresponding coupled effects that can be characterized with these equations are then cataloged in detail through the use of Multiphysics Interaction Diagrams (MPIDs) in Section 3.7. These interaction diagrams were developed to describe all of the linear thermo-electro-magneto-mechanical processes in [49]. These constitutive equations are further restricted in Section 3.7.1 by accommodating the symmetry of crystal structure in thermodynamic equilibrium.

Unlike the analysis of linear processes, this procedure is not straightforward and requires additional independent variables characterizing additional effects. Two kinds of irreversible behavior are addressed here: (i) transport processes, (ii) hysteretic processes. In Section 3.8.1, general linearized equations are developed for materials

exhibiting transport processes (e.g., conductivity, thermo-electric effects) and the corresponding MPIDs. In Section 3.9, an order-parameter based framework developed by Gurtin & Fried [23, 24] is extended to characterize fully coupled TEMM materials exhibiting hysteresis. To conclude, the applications and consequences of this unified framework are addressed in Section 3.10.

In Chapter 4, asymptotic models are developed for multifunctional structures with specialized geometries (beam, shell, plate etc), or a specified regime of behavior. In Section 4.3, the TEMM governing laws (discussed in Chapter 2) are presented in nondimensional form and the resulting nondimensional quantities are derived. Depending on the design of the particular structure and the restrictions on the process, some of the physical effects are more dominant than others. These dominant effects can be determined by the order of the nondimensional quantities involved. In the first part of this chapter, the use of this methodology is demonstrated for a particular application, i.e., load-bearing antenna structures.

In Section 4.2, the design and working of load-bearing antenna is described, and characteristic scales are assigned to the involved physical parameters. In Section 4.5 these characteristic scales are utilized to develop the operating regime and the leading-order model for load-bearing antennas. The leading-order model is solved analytically, and the formalism is extended to a multilayer structure in Section 4.6. These analytical solutions are then utilized to calculate deflections and antenna gain for various materials, and the results are compared. This model is applicable to materials with uncoupled constitutive behavior. In order to extend the framework to accommodate coupled constitutive behavior (e.g., piezoelectric, magnetostrictive materials etc.), a coupled electro-magneto-mechanical plate theory is developed, wherein, the dynamic

nature of electromagnetic fields in an antenna are coupled with the mechanical structure. In Section 4.7, a novel electro-magneto-mechanical plate theory is developed, and its finite element formulation is presented.

Chapter 2: Continuum Electrodynamic Theory for Deformable, Polarizable, and Magnetizable media

2.1 Introduction

Electrodynamics and continuum mechanics have traditionally been considered as two separate branches of physics since electrodynamics deals with study of electric charges in motion, whereas continuum mechanics deals with deformation and flow of matter [52]. Electrodynamics governed by Maxwell equations and continuum mechanics governed by thermo-mechanical conservation laws (i.e., mass, momentum, angular momentum, and energy conservation laws) cover a broad range of phenomena occurring at different time scales, and were traditionally used to model widely disparate applications. With the advent in technology and growing interest in applications of multifunctional materials with coupled electromagnetic and mechanical properties, there is need to explore the fully coupled theories that describe the unification of these two branches of physics.

As recognized by J.C. Maxwell, the matter of continuum mechanics is made of constituents which are also the object of study of electrodynamics, i.e., the moving charges [54]. Moving charges create electromagnetic fields which give rise to Lorentz forces at the microscopic level. When averaged to macroscopic continuum,

these forces contribute to continuum conservation laws through electromagnetic body forces. These forces are often referred to in literature as the Maxwell stress tensor [53]. Depending on the material being modeled, these forces may or may not be dominant. Another possible coupling of electromagnetic and thermomechanical fields occurs through material specific phenomena like piezoelectric effect (application of stress produces polarization), magnetostriction (stresses producing magnetization). These phenomena are described by *constitutive equations*, i.e., the additional mathematical relations that describe the macroscopic material behavior and close the differential system of balance laws. Both these phenomena will be addressed in this dissertation.

This chapter will focus on presenting the continuum theory of electromagnetic solids in a deformable, polarizable, and magnetizable media. Various electrodynamic continuum theories existing in literature are explored and a comparison of these theories is presented in Sections 2.2 - 2.3 [34, 60, 19]. A brief overview of fully coupled thermo-electro-magneto-mechanical processes is presented in Section 2.4 with the aid of multiphysics interaction diagrams [49]. This background will be used in the following chapters for development of the unified TEMM framework.

2.2 First-Principle Equations for TEMM Processes

The first-principle expressions for a deformable thermo-electro-magneto-mechanical (TEMM) material in their most primitive form are:

- The magnetic flux through any closed material surface is zero (Gauss' law for magnetism);

- The electromotive force induced in any closed material curve is equal and opposite the rate of change of the magnetic flux through the surface enclosed by that curve (Faraday's law);

- The electric flux through any closed material surface is equal to the free charge enclosed by that surface (Gauss' law for electricity);

- The magnetic field induced in any closed material curve is equal to the total current passing through the surface enclosed by that curve (Ampère's law);

- The mass of any material volume is constant throughout its motion, or, equivalently, the rate of change of the mass of any material volume is zero (conservation of mass);

- The rate of change of the linear momentum of any material volume is equal to the resultant external force acting on that volume (balance of linear momentum);

- The rate of change of the angular momentum of any material volume about the origin is equal to the resultant external moment acting on that volume about the origin (balance of angular momentum);

- The rate of change of the kinetic and internal energies of any material volume is equal to the rate of mechanical work generated by the resultant external force acting on that volume plus all other energies entering or exiting that volume (first law of thermodynamics).

These primitive statements are valid for the body as a whole and all subsets. Specializing to a continuum gives a set of integral equations,[1] presented here in Eulerian form [34, 61]:

Gauss-Faraday

$$\int_{\partial\mathcal{V}} \mathbf{b}^* \cdot \mathbf{n}\, da \;=\; 0, \tag{2.1}$$

Faraday-Maxwell

$$\frac{d}{dt}\int_{\mathcal{S}} \mathbf{b}^* \cdot \mathbf{n}\, da \;=\; -\int_{\partial\mathcal{S}} \mathbf{e}^* \cdot \mathbf{l}\, dl, \tag{2.2}$$

Gauss-Coulomb

$$\int_{\partial\mathcal{V}} \mathbf{d}^* \cdot \mathbf{n}\, da \;=\; \int_{\mathcal{V}} \sigma^*\, dv, \tag{2.3}$$

Ampère-Maxwell

$$\frac{d}{dt}\int_{\mathcal{S}} \mathbf{d}^* \cdot \mathbf{n}\, da \;+\; \int_{\mathcal{S}} \mathbf{j}^* \cdot \mathbf{n}\, da \;=\; \int_{\partial\mathcal{S}} \mathbf{h}^* \cdot \mathbf{l}\, dl, \tag{2.4}$$

conservation of mass

$$\frac{d}{dt}\int_{\mathcal{V}} \rho\, dv \;=\; 0, \tag{2.5}$$

balance of linear momentum

$$\frac{d}{dt}\int_{\mathcal{V}} \rho\mathbf{v}\, dv \;=\; \int_{\mathcal{V}} \rho(\mathbf{f}^{ext} + \mathbf{f}^{e})\, dv \;+\; \int_{\partial\mathcal{V}} \mathbf{t}\, da, \tag{2.6}$$

balance of angular momentum

$$\frac{d}{dt}\int_{\mathcal{V}} \mathbf{x} \times \rho\mathbf{v}\, dv \;=\; \int_{\mathcal{V}} \mathbf{x} \times \rho(\mathbf{f}^{ext} + \mathbf{f}^{e})\, dv \;+\; \int_{\mathcal{V}} \rho\mathbf{c}^{e}\, dv \;+\; \int_{\partial\mathcal{V}} \mathbf{x} \times \mathbf{t}\, da, \tag{2.7}$$

[1]The convention employed in this work: lowercase Greek letters denote scalars, bold lowercase Latin letters denote first-order tensors (vectors), and bold uppercase Latin letters denote second-order tensors (tensors). Accordingly, the notation for the various electromagnetic vector fields is lowercase, which departs from the uppercase notation appearing in much of the literature.

first law of thermodynamics

$$\frac{d}{dt}\int_{\mathcal{V}}\rho(\varepsilon+\frac{1}{2}\mathbf{v}\cdot\mathbf{v})dv \;=\; \int_{\mathcal{V}}\rho(\mathbf{f}^{ext}+\mathbf{f}^{e})\cdot\mathbf{v}\,dv+\int_{\partial\mathcal{V}}\mathbf{t}\cdot\mathbf{v}\,da+\int_{\mathcal{V}}\rho(r^{ext}+r^{e})dv-\int_{\partial\mathcal{V}}h\,da, \tag{2.8}$$

The continuum approach to modeling assumes that the quantities in the integral statements (2.1)-(2.8) are continuous, bounded fields. These integral statements are global, i.e., valid for any open material volume $\mathcal{V}$ bounded by a closed surface $\partial\mathcal{V}$, and any open material surface $\mathcal{S}$ bounded by a closed curve $\partial\mathcal{S}$.

In (2.1)-(2.8), $\mathbf{l}$ is the unit tangent along $\partial\mathcal{S}$, $\mathbf{n}$ is an outward unit normal, $(\,)\cdot(\,)$ denotes an inner product, $(\,)\times(\,)$ denotes a vector cross product, and d/dt denotes the derivative of a function of a single variable t. $\mathbf{e}^*$, $\mathbf{d}^*$, $\mathbf{h}^*$, $\mathbf{b}^*$, σ^*, and $\mathbf{j}^*$ are the effective electric field intensity, effective electric displacement, effective magnetic field intensity, effective magnetic induction, effective free charge density, and effective free current density, respectively. ρ is the present density, $\mathbf{v}$ is the velocity, $\mathbf{f}^{ext}$ and $\mathbf{f}^{e}$ are the mechanically and electromagnetically induced specific body forces, $\mathbf{t}$ is the traction, $\mathbf{c}^{e}$ is the specific body couple, ε is the specific internal energy, r^{ext} and r^{e} are the thermally and electromagnetically induced specific energy supply rates, and h is the heat flux. All fields are Eulerian, i.e., functions of the present position $\mathbf{x}$ of a continuum particle and time t.

It is important for the proposed continuum model to first give the integral expressions (2.1)-(2.8), rather than starting directly with a set of pointwise equations, because the pointwise equations must be derivable from an integral set, and the assumptions for continuum models are imposed on the integral form. For instance, electromagnetic effects in the balance laws (2.6)-(2.8) can be modeled as inertial terms,

incorporated into the constitutive response, or introduced through an electromagnetically induced body force, body couple, and energy supply. In this dissertation, the lattermost approach is adopted.

The continuous, bounded nature of the integrands in (2.1)-(2.8) enables the transport and divergence theorems, and the requirement that (2.1)-(2.8) be global, i.e., true for the entire body and all subsets, enables the localization theorem. Assuming that the traction $\mathbf{t}$ and heat flux h are dependent on surface geometry only through the outward unit normal $\mathbf{n}$, so that $\mathbf{t} = \mathbf{T}\mathbf{n}$ and $h = \mathbf{q} \cdot \mathbf{n}$, application of the transport, divergence, Stokes, and localization theorems to the global equations (2.1)-(2.8) leads to the pointwise (local) equations

$$\operatorname{div} \mathbf{b}^* = 0, \tag{2.9}$$

$$\operatorname{curl} \mathbf{e}^* = -(\mathbf{b}^*)' - \operatorname{curl}(\mathbf{b}^* \times \mathbf{v}), \tag{2.10}$$

$$\operatorname{div} \mathbf{d}^* = \sigma^*, \tag{2.11}$$

$$\operatorname{curl} \mathbf{h}^* = (\mathbf{d}^*)' + \operatorname{curl}(\mathbf{d}^* \times \mathbf{v}) + \sigma^* \mathbf{v} + \mathbf{j}^*, \tag{2.12}$$

$$\dot{\rho} + \rho \operatorname{div} \mathbf{v} = 0, \tag{2.13}$$

$$\rho \dot{\mathbf{v}} = \rho(\mathbf{f}^{ext} + \mathbf{f}^e) + \operatorname{div} \mathbf{T}, \tag{2.14}$$

$$\rho \boldsymbol{\Gamma}^e + \mathbf{T} - \mathbf{T}^{\mathrm{T}} = \mathbf{0}, \tag{2.15}$$

$$\rho \dot{\varepsilon} = \mathbf{T} \cdot \mathbf{L} + \rho(r^{ext} + r^e) - \operatorname{div} \mathbf{q}, \tag{2.16}$$

where $\mathbf{T}$ is the Cauchy stress tensor, $\mathbf{q}$ is the Eulerian heat flux vector (energy per time per present area), $\mathbf{L} = \operatorname{grad} \mathbf{v} = \partial \mathbf{v} / \partial \mathbf{x}$ is the Eulerian velocity gradient, $\boldsymbol{\Gamma}^e$ is a skew tensor whose axial vector is $\mathbf{c}^e$, i.e., $\boldsymbol{\Gamma}^e \mathbf{u} = \mathbf{c}^e \times \mathbf{u}$ for any vector $\mathbf{u}$, and

$$\mathbf{v}' \stackrel{\text{def}}{=} \frac{\partial}{\partial t} \tilde{\mathbf{v}}(\mathbf{x}, t), \qquad \dot{\mathbf{v}} \stackrel{\text{def}}{=} \frac{\partial}{\partial t} \hat{\mathbf{v}}(\mathbf{X}, t)$$

denote the Eulerian and material time derivatives,[2] respectively, related by $\dot{\mathbf{v}} = \mathbf{v}' + (\text{grad}\,\mathbf{v})\,\mathbf{v}$. In (2.9)-(2.16), div ( ) denotes the Eulerian divergence, curl ( ) denotes the Eulerian curl, and $\mathbf{T}^{\mathrm{T}}$ denotes the transpose of $\mathbf{T}$. *It is emphasized that the pointwise equations (2.9)-(2.16) are valid statements of the first principles because they are progenies of the global equations (2.1)-(2.8).*

The effective fields $\mathbf{e}^*$, $\mathbf{d}^*$, $\mathbf{h}^*$, $\mathbf{b}^*$, σ^*, and $\mathbf{j}^*$ are the electromagnetic fields acting on the deforming continuum as seen in its present configuration, measured with respect to a co-moving frame [60, 19]. The relations between the effective (starred) fields and the primary (unstarred) fields, the latter being measured with respect to a stationary frame rather than a co-moving frame, depend on the transformation properties of the particular theory.

In addition to the pointwise first principles (2.9)-(2.16), three sets of equations must be supplied to complete the TEMM model. The first two sets describing the two-way electromagnetic and thermomechanical interactions, are described in the next two sections. The third set, discussed and developed in the following chapter, are the constitutive equations that characterize a general TEMM process by relating the independent and dependent variables in the first-principle equations.

2.3 Constitutive Assumptions on Effective Fields and Electromagnetically Induced Forces, Couples, and Energies

Material deformation and electromagnetic body forces result in a two-way coupling between expressions (2.9)-(2.12) and (2.13)-(2.16) (or, equivalently, (2.1)-(2.4) and (2.5)-(2.8)). In this section, this coupling is characterized with two sets of constitutive

[2]The superscript tilde and hat are used to differentiate a function from its value, with the tilde representing a spatial description of a function, and the hat a referential description.

equations, labeled C1 and C2. C1 postulates the *effective* electromagnetic fields appearing in (2.9)-(2.12) in terms of the *primitive* electromagnetic fields and the time-dependent deformation. C2 postulates the electromagnetically induced body force, body couple, and energy supply rate appearing in (2.13)-(2.16) in terms of the effective electromagnetic fields.

2.3.1 C1: Effective electromagnetic fields

Recall that the effective electromagnetic fields capture the effect of the deforming continuum on the primitive electromagnetic fields. Various models have been presented in the literature to relate the effective fields to the primitive fields, each based on a different set of principles and postulates. Four such models – namely, the Minkowski, Lorentz, Statistical, and Chu models – are briefly described and compared in this section.

Minkowski Model

The Minkowski model [19, 60, 34] is motivated by Einstein's special theory of relativity. In this approximation, the effective fields are related to the primitive fields through semi-relativistic inverse Lorentz transformations:

$$\mathbf{e}^* = \mathbf{e}_M + \mathbf{v} \times \mathbf{b}_M, \qquad \mathbf{h}^* = \mathbf{h}_M - \mathbf{v} \times \mathbf{d}_M, \qquad \mathbf{d}^* = \mathbf{d}_M, \qquad \mathbf{b}^* = \mathbf{b}_M,$$

$$\mathbf{p}^* = \mathbf{p}_M, \qquad \mathbf{m}^* = \mathbf{m}_M + \mathbf{v} \times \mathbf{p}_M, \qquad \mathbf{j}^* = \mathbf{j}_M - \sigma_M \mathbf{v}, \qquad \sigma^* = \sigma_M, \tag{2.17}$$

where $(\cdot)_M$ represents a primitive electromagnetic field corresponding to the Minkowski model.

Lorentz Model

The Lorentz model is motivated by Lorentz's theory of electrons [48], which postulates that a body consists of an infinitely large number of rapidly moving charged particles called electrons whose motion generates rapidly fluctuating microscopic electromagnetic fields. These microscopic fields averaged over a small time interval and an infinitesimal volume containing a sufficiently large number of electrons are defined as the corresponding macroscopic fields. The aforementioned postulates lead to the following relationships:

$$\mathbf{e}^* = \mathbf{e}_L + \mathbf{v} \times \mathbf{b}_L, \qquad \mathbf{h}^* = \mathbf{h}_L - \epsilon_o \mathbf{v} \times \mathbf{e}_L, \qquad \mathbf{d}^* = \mathbf{d}_L, \qquad \mathbf{b}^* = \mathbf{b}_L,$$

$$\mathbf{p}^* = \mathbf{p}_L, \qquad \mathbf{m}^* = \mathbf{m}_L, \qquad \mathbf{j}^* = \mathbf{j}_L - \sigma_L \mathbf{v}, \qquad \sigma^* = \sigma_L, \tag{2.18}$$

where $(\cdot)_L$ represents a primitive electromagnetic field corresponding to the Lorentz model.

Statistical Model

The Statistical model [15] is a modification of Lorentz's theory of electrons, wherein the electrons are grouped into stable systems such as atoms, molecules, or ions. The field effects of the electrons within each stable atom are represented by microscopic electric and magnetic multipole moments (e.g., dipole, quadrupole, and octupole moments), and the macroscopic polarization and magnetization fields are defined as statistical averages of these multipole moments over a large number of stable atoms. The transformations presented in this model are identical to Minkowski's, i.e.,

$$\mathbf{e}^* = \mathbf{e}_S + \mathbf{v} \times \mathbf{b}_S, \qquad \mathbf{h}^* = \mathbf{h}_S - \mathbf{v} \times \mathbf{d}_S, \qquad \mathbf{d}^* = \mathbf{d}_S, \qquad \mathbf{b}^* = \mathbf{b}_S,$$

$$\mathbf{p}^* = \mathbf{p}_S, \qquad \mathbf{m}^* = \mathbf{m}_S + \mathbf{v} \times \mathbf{p}_S, \qquad \mathbf{j}^* = \mathbf{j}_S - \sigma_S \mathbf{v}, \qquad \sigma^* = \sigma_S, \tag{2.19}$$

where $(\cdot)_S$ represents a primitive electromagnetic field corresponding to the Statistical model.

Chu Model

The Chu model [22] is based on the postulate that deforming bodies contribute to electromagnetic phenomena by acting, in a macroscopic sense, as electric and magnetic dipole sources for the electromagnetic fields. The transformations for the Chu model are

$$\mathbf{e}^* = \mathbf{e}_C + \mu_o \mathbf{v} \times \mathbf{h}_C, \qquad \mathbf{h}^* = \mathbf{h}_C - \epsilon_o \mathbf{v} \times \mathbf{e}_C, \qquad \mathbf{d}^* = \mathbf{d}_C, \qquad \mathbf{b}^* = \mathbf{b}_C,$$
$$\mathbf{p}^* = \mathbf{p}_C + \mathbf{m}_C \times \frac{\mathbf{v}}{c^2}, \qquad \mathbf{m}^* = \mathbf{m}_C, \qquad \mathbf{j}^* = \mathbf{j}_C - \sigma_C \mathbf{v}, \qquad \sigma^* = \sigma_C, \tag{2.20}$$

where $(\cdot)_C$ represents a primitive electromagnetic field corresponding to the Chu model.

A Comparison of the Four Models

Table 2.1 catalogues Maxwell's equations for each of the four models, deduced by substituting each choice of C1 (i.e., (2.17), (2.18), (2.19), or (2.20)) into Eqs. (2.9)-(2.12). Recall that in our notation, $\mathbf{b}'_M = \partial \tilde{\mathbf{b}}_M(\mathbf{x}, t)/\partial t$.

Since each of the four models is based on a different set of postulates, the primitive electromagnetic fields may have different physical connotations depending on the model. The relationships between the primitive variables allow us to establish equivalence among the four models. For instance, the Minkowski and Statistical models,

Table 2.1: Maxwell's Equations for Different Choices of C1

Model for C1	Maxwell's Equations	
Minkowski	$\operatorname{curl} \mathbf{e}_M = -\mathbf{b}'_M$	$\operatorname{div} \mathbf{d}_M = \sigma_M$
	$\operatorname{curl} \mathbf{h}_M = \mathbf{d}'_M + \mathbf{j}_M$	$\operatorname{div} \mathbf{b}_M = 0$
Lorentz	$\operatorname{curl} \mathbf{e}_L = -\mathbf{b}'_L$	$\operatorname{div} \mathbf{d}_L = \sigma_L$
	$\operatorname{curl} \mathbf{h}_L = \mathbf{d}'_L - \operatorname{curl}(\mathbf{v} \times \mathbf{p}_L) + \mathbf{j}_L$	$\operatorname{div} \mathbf{b}_L = 0$
Statistical	$\operatorname{curl} \mathbf{e}_S = -\mathbf{b}'_S$	$\operatorname{div} \mathbf{d}_S = \sigma_S$
	$\operatorname{curl} \mathbf{h}_S = \mathbf{d}'_S + \mathbf{j}_S$	$\operatorname{div} \mathbf{b}_S = 0$
Chu	$\operatorname{curl} \mathbf{e}_C = -\mathbf{b}'_C + \mu_o \operatorname{curl}(\mathbf{v} \times \mathbf{m}_C)$	$\operatorname{div} \mathbf{d}_C = \sigma_C$
	$\operatorname{curl} \mathbf{h}_C = \mathbf{d}'_C - \operatorname{curl}(\mathbf{v} \times \mathbf{p}_C) + \mathbf{j}_C$	$\operatorname{div} \mathbf{b}_C = 0$

although developed from different perspectives, are mathematically equivalent[3] (i.e., $\mathbf{m}_M = \mathbf{m}_S$, $\mathbf{p}_M = \mathbf{p}_S$, etc.).

$$
\begin{aligned}
&\textit{magnetization}: && \mathbf{m}_M = \mathbf{m}_S = \mathbf{m}_L + \mathbf{p}_L \times \mathbf{v} = \mathbf{m}_C + \mathbf{p}_C \times \mathbf{v} \\
&\textit{polarization}: && \mathbf{p}_M = \mathbf{p}_S = \mathbf{p}_L = \mathbf{p}_C - \frac{1}{c^2}\, \mathbf{m}_C \times \mathbf{v} \\
&\textit{magnetic induction}: && \mathbf{b}_M = \mathbf{b}_S = \mathbf{b}_L = \mathbf{b}_C \\
&\textit{electric displacement}: && \mathbf{d}_M = \mathbf{d}_S = \mathbf{d}_L = \mathbf{d}_C \\
&\textit{electric field}: && \mathbf{e}_M = \mathbf{e}_S = \mathbf{e}_L = \mathbf{e}_C + \mu_o\, \mathbf{m}_C \times \mathbf{v} \\
&\textit{magnetic field}: && \mathbf{h}_M = \mathbf{h}_S = \mathbf{h}_L - \mathbf{p}_L \times \mathbf{v} = \mathbf{h}_C - \mathbf{p}_C \times \mathbf{v}
\end{aligned}
$$

In this work, Minkowski's transformations (2.17) are adopted. This choice of C1, in turn, impacts the electromagnetic body force $\mathbf{f}^e$, body couple $\mathbf{c}^e$, and energy supply r^e, which are presented in the following section as the constitutive set C2.

[3]For the Minkowski and Statistical models, Maxwell's equations for a deforming continuum (refer to Table 2.1) are formally identical to Maxwell's equations for a stationary, rigid continuum.

2.3.2 C2: Modeling of the Electromagnetically Induced Coupling Terms

The terms $\mathbf{f}^e$, $\mathbf{\Gamma}^e$, and r^e appearing in equations (2.14)-(2.16) arise due to moving charges and concomitantly depend on the electromagnetic fields. Hence, $\mathbf{f}^e$, $\mathbf{\Gamma}^e$, and r^e are interaction terms, i.e., they couple the thermomechanical equations (2.13)-(2.16) to the electromagnetic equations (2.9)-(2.12).

In principle, these coupling terms are part of the solution of the atomic-scale problem [19]: Knowledge of the position, velocity, and charge of each discrete particle enables calculation of the electromagnetic fields acting on each charged particle. With these atomic-scale electromagnetic fields known, the continuum-scale (or macroscopic-scale) electromagnetic fields $\mathbf{e}^*$, $\mathbf{d}^*$, $\mathbf{h}^*$, and $\mathbf{b}^*$ are deduced by statistically averaging the values of their discrete microscopic counterparts over an infinitesimal volume element as described in [15]. Similarly, the continuum body force $\mathbf{f}^e$, body couple $\mathbf{c}^e$, and energy supply rate r^e are computed by volume averaging the Lorentz forces (and accompanying couples and energies) acting on the charged particles. To summarize, if the solution of the microscopic problem is known, then the continuum coupling terms $\mathbf{f}^e$, $\mathbf{c}^e$, and r^e can be *deduced* using statistical averaging techniques.

In practice, however, the atomic detail (e.g., position, velocity, and charge of each discrete particle) required to generate the solution of the microscopic-scale problem is unavailable. Hence, the continuum-scale body force $\mathbf{f}^e$, body couple $\mathbf{c}^e$, and energy supply rate r^e reflecting the effect of the atomic-scale forces, couples, and energies induced by moving charges must be *postulated*. These postulates are generally motivated by either atomic physics or empiricism. One such model (for a general polarizable, magnetizable, deformable continuum) is coined the Maxwell-Minkowski

formulation [34]:

$$\rho\mathbf{f}^e \;=\; \sigma^*\mathbf{e}^* \,+\, \mathbf{j}^*\times\mathbf{b}^* \,+\, (\operatorname{grad}\mathbf{e}^*)^{\mathrm{T}}\,\mathbf{p}^* \,+\, \mu_o\,(\operatorname{grad}\mathbf{h}^*)^{\mathrm{T}}\,\mathbf{m}^* \,+\, \mathring{\mathbf{d}}^*\times\mathbf{b}^* \,+\, \mathbf{d}^*\times\mathring{\mathbf{b}}^*, \tag{2.21}$$

$$\rho\boldsymbol{\Gamma}^e \;=\; (\mathbf{e}^*\otimes\mathbf{p}^* \,-\, \mathbf{p}^*\otimes\mathbf{e}^*) \,+\, \mu_o\,(\mathbf{h}^*\otimes\mathbf{m}^* \,-\, \mathbf{m}^*\otimes\mathbf{h}^*)\,, \tag{2.22}$$

$$\rho r^e \,=\, \mathbf{j}^*\cdot\mathbf{e}^* \,+\, \rho\mathbf{e}^*\cdot\overline{\left(\frac{\dot{\mathbf{p}}^*}{\rho}\right)} \,+\, \rho\mu_o\mathbf{h}^*\cdot\overline{\left(\frac{\dot{\mathbf{m}}^*}{\rho}\right)}, \tag{2.23}$$

where

$$\mathring{\mathbf{u}} \;\stackrel{\text{def}}{=}\; \dot{\mathbf{u}} \,+\, \mathbf{u}\,(\operatorname{div}\mathbf{v}) \,-\, (\operatorname{grad}\mathbf{v})\mathbf{u} \;=\; \mathbf{u}' \,+\, \operatorname{curl}(\mathbf{u}\times\mathbf{v}) \,+\, \mathbf{v}\,(\operatorname{div}\mathbf{u}) \tag{2.24}$$

is a convected rate of an arbitrary vector $\mathbf{u} = \tilde{\mathbf{u}}(\mathbf{x}, t)$. This model is employed for the following reasons: Firstly, it has as special cases Maxwell's theory for polarizable solids and Brown's theory for magnetizable solids [7]. Secondly, as will be discussed in Section 3.3, the energy supply rate (2.23) contains electric and magnetic intensive-extensive conjugate pairs, consistent with the requirements of classical thermodynamics [9]. Use of (2.21)-(2.23) in the field equations (2.14)-(2.16) yields

$$\begin{aligned}\rho\dot{\mathbf{v}} \;=\; \rho\mathbf{f}^{ext} \,+\, \sigma^*\mathbf{e}^* \,+\, \mathbf{j}^*\times\mathbf{b}^* \,+\, (\operatorname{grad}\mathbf{e}^*)^{\mathrm{T}}\,\mathbf{p}^* \,+\, \mu_o\,(\operatorname{grad}\mathbf{h}^*)^{\mathrm{T}}\,\mathbf{m}^* \,+\, \mathring{\mathbf{d}}^*\times\mathbf{b}^* \\ +\, \mathbf{d}^*\times\mathring{\mathbf{b}}^* \,+\, \operatorname{div}\mathbf{T},\end{aligned} \tag{2.25}$$

$$\mathbf{T} \,-\, \mathbf{T}^{\mathrm{T}} \;=\; (\mathbf{p}^*\otimes\mathbf{e}^* \,-\, \mathbf{e}^*\otimes\mathbf{p}^*) \,+\, \mu_o\,(\mathbf{m}^*\otimes\mathbf{h}^* \,-\, \mathbf{h}^*\otimes\mathbf{m}^*)\,, \tag{2.26}$$

$$\dot{\varepsilon} \;=\; \frac{1}{\rho_R}\,\mathbf{P}\cdot\dot{\mathbf{F}} \,+\, \mathbf{e}^*\cdot\overline{\left(\frac{\dot{\mathbf{p}}^*}{\rho}\right)} \,+\, \mu_o\,\mathbf{h}^*\cdot\overline{\left(\frac{\dot{\mathbf{m}}^*}{\rho}\right)} \,+\, r^{ext} \,+\, \frac{1}{\rho}\,\mathbf{j}^*\cdot\mathbf{e}^* \,-\, \frac{1}{\rho}\operatorname{div}\mathbf{q}, \tag{2.27}$$

where ρ_R is the uniform reference density and

$$\mathbf{p}^* \;=\; \mathbf{d}^* \,-\, \epsilon_o\mathbf{e}^*, \qquad \mathbf{m}^* \;=\; \frac{1}{\mu_o}\,\mathbf{b}^* \,-\, \mathbf{h}^*, \qquad \mathbf{P} \;=\; J\mathbf{T}\mathbf{F}^{-\mathrm{T}} \tag{2.28}$$

are the effective electric polarization, effective magnetization, and first Piola-Kirchhoff stress, respectively.

Equations (2.25)-(2.27) can be formulated in an alternative way by defining an *effective stress tensor* $\boldsymbol{\tau} = \mathbf{T} + \mathbf{T}^e$, which consists of contributions from the Cauchy stress tensor $\mathbf{T}$ and the electromagnetic Maxwell stress tensor $\mathbf{T}^e$. The electromagnetic stress tensor $\mathbf{T}^e$ corresponding to the Maxwell-Minkowski formulation is $\mathbf{T}^e = \mathbf{e}^* \otimes \mathbf{p}^* + \mu_o \, \mathbf{h}^* \otimes \mathbf{m}^* - \frac{1}{2} \left(\mathbf{e}^* \cdot \mathbf{e}^* + \mathbf{h}^* \cdot \mathbf{h}^* \right)$ [34]. $\mathbf{T}^e$ is defined so that its skew symmetric part is $\boldsymbol{\Gamma}^e$ and its divergence is $\mathbf{f}^e$. By formulating the governing equations and the constitutive equations in terms of the effective stress tensor $\boldsymbol{\tau}$, instead of the Cauchy stress tensor $\mathbf{T}$, the coupling between the electromagnetic fields and the thermomechanical fields is eliminated from Eqs. (2.25) and (2.26), and is instead accounted for in the constitutive equations for $\boldsymbol{\tau}$.

2.4 Thermo-Electro-Magneto-Mechanical Processes

In this section, fully coupled TEMM processes and the different kinds of materials that undergo these processes are explored with the aid of multi physics interaction diagrams [49].

Linear, Reversible Processes

In this section, a brief description of processes characterized as linear, reversible thermo-electro-magneto-mechanical (TEMM) processes is presented and along with a few examples. In order to describe the wealth of phenomena that can be classified as coupled TEMM processes, multiphysics interaction diagrams are used for a comprehensive and concise description (Fig. 2.1).

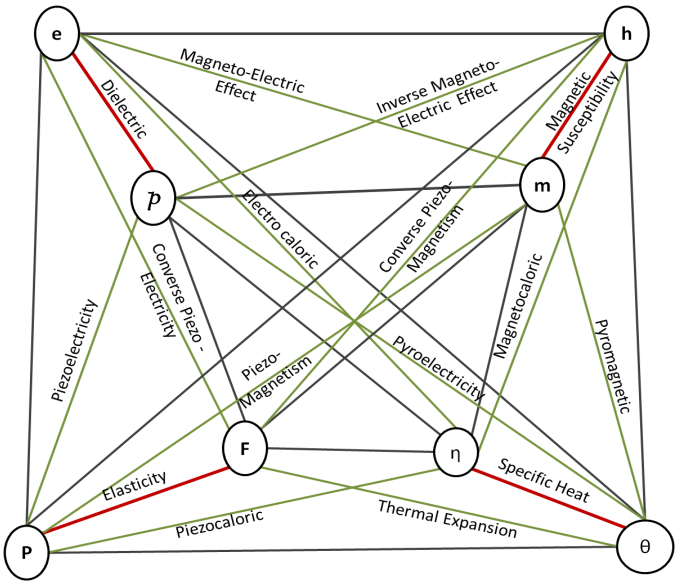

Figure 2.1: Multi-Physics Interaction Diagram (MPID) demonstrating Thermo-Electro-Magneto-Mechanical Effects

Mechanical, thermal, electrical and magnetic effects and the mutual coupling between these effects is described in this diagram. Each physical effect is defined by its corresponding extensive and intensive variables, marked at the inner and outer quadrilateral corners of the MPID respectively.

The diagonal edges (red lines) joining these two quadrilaterals signify the uncoupled processes e.g., elasticity, polarization, magnetization and heat capacity. In order to delineate the coupling effects, the diagram is divided into six subset panels, which relates any two of the four physical effects. Specifically, the coupling effect that relates intensive parameter corresponding to one physical effect to extensive parameter corresponding to another is known as a cross-effect or a primary effect. Owing to the linear nature of the model under consideration, any coupled TEMM effect can be studied as

a superposition of these uncoupled and coupled primary effects. A superposition of two or more of these physical effects is called a secondary effect. Primary effects are direct or one-step processes that describe the coupling between each of the physical effects and secondary effects are multi-step processes that are a superposition of two or more primary effects. For e.g., a linear thermo-electro-mechanical process can be best described as a superposition of linear thermo-electric (pyroelectricity) and linear electro-mechanical (piezoelectricity) processes. The coefficients for the process above are defined in table 2.3.

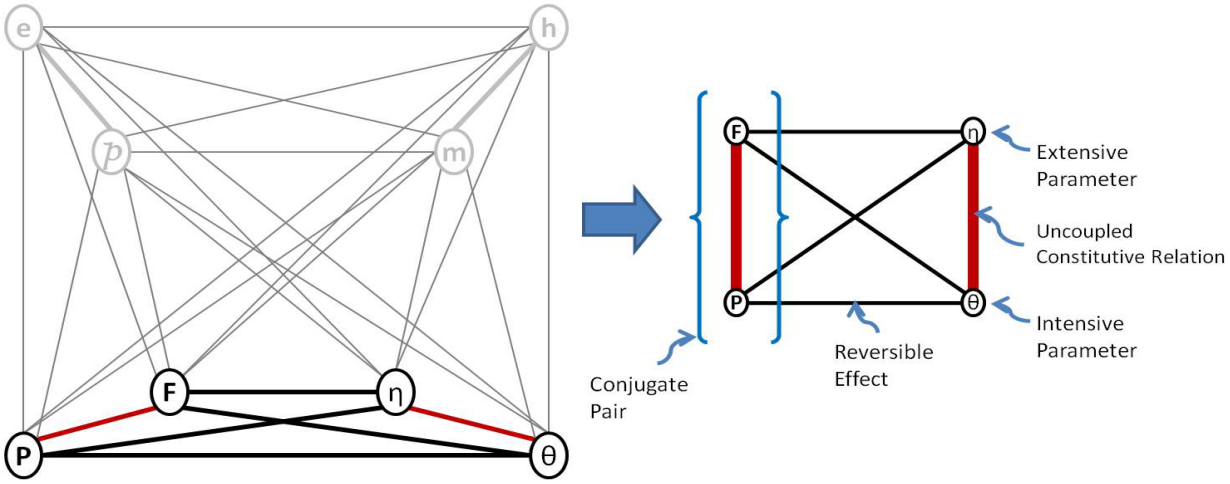

Figure 2.2: Description of the Subset Diagram

Transport Processes

Reversible processes are governed by near equilibrium thermodynamic state, i.e., there is no dependence on rates or gradients of physical quantities and the system is electrically neutral (net charge of the system is zero) [57, 34]. On the contrary, these

Table 2.2: Subset Diagrams of the Fully Coupled TEMM Multiphysics Interaction Diagram

Primary Effects	Subset Diagram
Direct and Inverse Piezoelectricity Ex: $BaTiO_3$, PZT	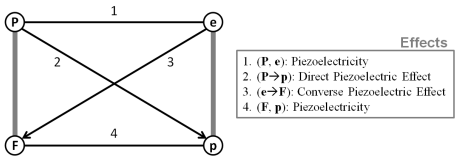
Thermal expansion, Piezocaloric effect Ex: *Crystal structures like Ferroics*	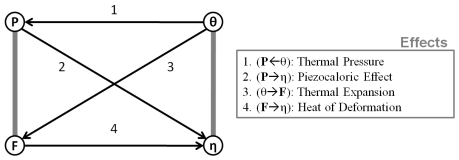
Pyromagnetic and Magnetocaloric effects Ex: *Gadolinium alloys* ($Gd_5Si_2Ge_2$), $PrNi_5$	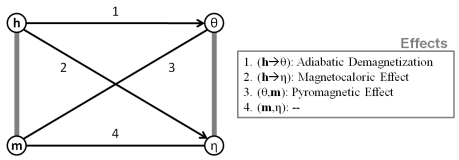
Magnetoelectric effects Ex: *Multiferroics*, Cr_2O_3	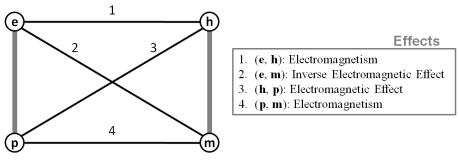
Pyroelectric and Electrocaloric effects Ex: *gallium nitride(GaN), caesium nitrate*($CsNO_3$)	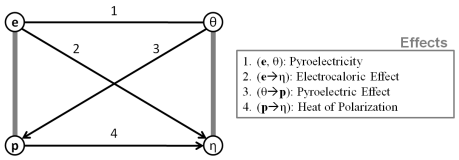
Piezomagnetic effect *Ex: Antiferromagnetics like FEMn, NiO*	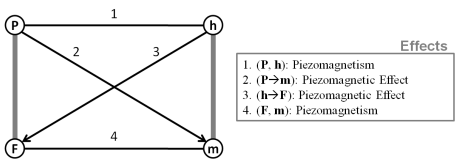

Table 2.3: Materials Constants and their Representations for Linear-Reversible Processes

Constant	**Representation**	**Constant**	**Representation**
Elasticity	$C^{o}_{ijkl} = \rho \dfrac{\partial^2 E^{F\theta pm}}{\partial C_{ij} \partial C_{kl}}$	Piezoelectric	$d^{e}_{ijk} = \rho \dfrac{\partial^2 E^{F\theta pm}}{\partial C_{ij} \partial p_{k}}$
Piezomagnetic	$d^{m}_{ijk} = \rho \dfrac{\partial^2 E^{F\theta pm}}{\partial C_{ij} \partial m_{k}}$	Thermal Stress	$\beta_{ij} = \rho \dfrac{\partial^2 E^{F\theta pm}}{\partial \theta \partial C_{ij}}$
Permittivity	$\chi^{e}_{ij} = \rho \dfrac{\partial^2 E^{F\theta pm}}{\partial p_{i} \partial p_{j}}$	Magneto-Electric	$\chi^{em}_{ij} = \rho \dfrac{\partial^2 E^{F\theta pm}}{\partial p_{i} \partial m_{j}}$
Pyroelectric	$L^{e}_{i} = \rho \dfrac{\partial^2 E^{F\theta pm}}{\partial p_{i} \partial \theta}$	Permeability	$\chi^{m}_{ij} = \rho \dfrac{\partial^2 E^{F\theta pm}}{\partial m_{i} \partial m_{j}}$
Pyromagnetic	$L^{m}_{i} = \rho \dfrac{\partial^2 E^{F\theta pm}}{\partial m_{i} \partial \theta}$	Specific Heat	$c = \rho \dfrac{\partial^2 E^{F\theta pm}}{\partial \theta^2}$

gradients and charges drive the transport processes and cannot be ignored. Transport processes are characterized by flow terms like, heat flow, energy flux and are far from equilibrium.

The MPID shown in Fig. 2.4 describes the Fourier's law of heat conduction and Ohm's law of electrical conduction [34]. This diagram also highlights thermoelectric effects like Seebeck effect, Peltier effects, Thomson heat as highlighted in the MPID [49]. These diagrams can also be used to describe thermomagnetic and galvenometric effects (Nerst or Ettinghausen effect) in magnetic materials, where magnetic fields arise due to time varying electric fields. A more detailed exposition on these effects and their modeling will be described in greater detail in Chapter 3.

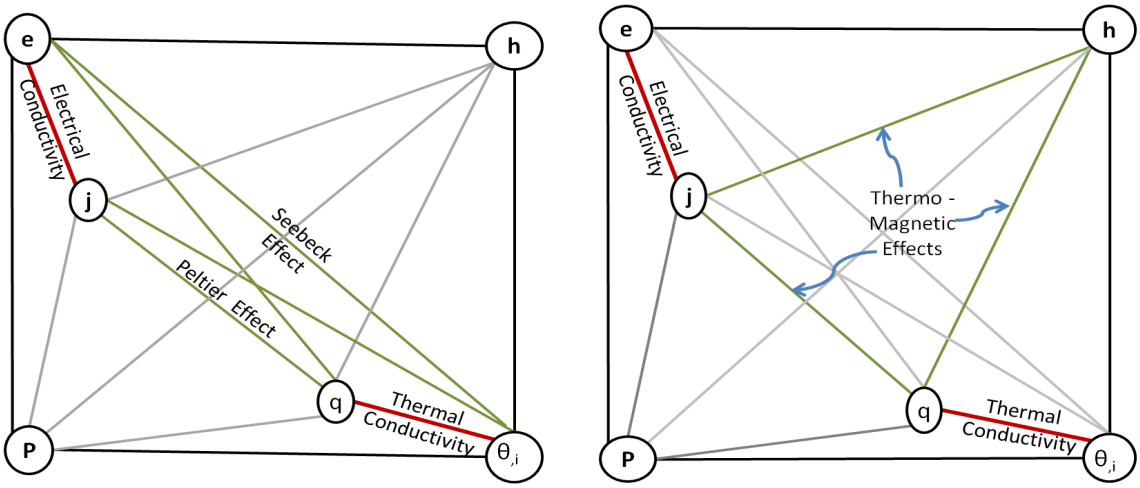

Figure 2.3: Multi-Physics Interaction Diagram (MPID) demonstrating Coupled Thermo-Electric Flow Processes

Hysteretic Processes

Transport processes are irreversible processes that are characterized by electric and thermal flux terms. Magnetic or mechanical irreversibilities observed in processes like magnetostriction, friction, plasticity are not accomodated in these flux terms. These processes are called dissipative processes where the dissipation is caused by microstructural changes in the material. Other frameworks like rational thermodynamics [3, 77], theory of internal variables [6, 67] were developed to characterize the dissipative processes. The free energy used to characterize these processes is assumed to be a function of an additional independent variable which is an internal variable describing its microstructural evolution. Internal variables are usually irreversible components of physical effects i.e., plastic strain, irreversible component of magnetization or polarization and have been used extensively for characterization

of dissipative materials like magnetostrictives, ferroic materials, and thermo-plastic materials [43, 72].

The free energies are predicted based on physics of the specific material rather than as a generic framework modeling hysteretic or irreversible effects. Unlike characterization of materials within linear, reversible regime, each material exhibiting hysteresis is characterized by a different form of Clausius-Duhem inequality. This makes it challenging to define a unifying framework that can describe the irreversible effects observed in these materials. In Chapter 3, a unique framework is developed unifying all these irreversible and reversible effects.

2.5 Conclusion

In this chapter continuum theory of electromagnetic solids in a deformable, polarizable, and magnetizable media is presented. The various electrodynamic continuum theories describing fully coupled TEMM behavior are explored, and a comparison of these theories is presented in detail. The first principles presented in this chapter will be subsequently used as the starting point to derive the unified theoretical framework in the following chapters. A brief description of fully coupled thermo-electro-magneto-mechanical processes is also presented with the aid of multiphysics interaction diagrams [49]. This background will be used in the following chapters for development of the unified TEMM framework.

Chapter 3: Unified Continuum Characterization of Fully Coupled Thermo-Electro-Magneto-Mechanical Processes

3.1 Introduction

The objective of the work presented in this chapter is to develop characterization techniques and modeling tools describing fully coupled thermo-electro-magneto-mechanical (TEMM) behavior. This framework is intended to enable design of novel multifunctional materials and intelligent systems. The customary practice in the smart materials community is to a priori specialize material models to a particular regime of behavior suitable for a particular set of operating conditions. For instance, dynamic electromagnetic fields, anisotropy, and material nonlinearity are often neglected (weak physical effects); material response is frequently confined to low-signal, small-deformation ranges of operation; or only a subset of the full TEMM coupling is accounted for. It is emphasized and acknowledged that these practices and the resulting models have proven successful at capturing the behavior a wide range of intelligent devices, systems, and structures in a wide range of operating environments. However, this specialized approach lacks the flexibility, breadth, and generality to facilitate modeling, characterization, design, and optimization of the next generation of

novel multifunctional materials. For instance, the customary quasi-static electromagnetic field approximation breaks down for multifunctional devices such as macrofiber composites, micro antenna devices, or load-bearing antennas that operate at higher frequencies (up to MHz-KHz). By ignoring some of the physics in its model, its design is limited.

To facilitate the design of novel multifunctional materials and their application in emerging technologies like the ones described above, fundamental advancements in the basic (continuum) modeling architecture are required, i.e., there is a need for mathematical modeling that captures or accounts for this new physics. This architecture must be broad enough to facilitate design and optimization of multifunctional materials and structures. In particular, a general 3-D multi-physics approach that accommodates fully coupled thermo-electro-magneto-mechanical behavior, finite deformations, nonlinear constitutive behavior, dynamic fields, etc. is needed.

The foundation for a general framework as envisioned in the aforementioned paragraph was laid out in the pioneering work of Hutter, Pao, etc. [34, 60, 19]. In these models, the first principles (i.e., Maxwell's equations, conservation of mass, balance of linear momentum, balance of angular momentum, and the first law of thermodynamics), boundary conditions, and coupling models were well-developed and studied extensively. The coupling models describe the electromagnetic interaction terms (namely, the electromagnetic body force, body couple, and energy supply) that couple the thermomechanical balance laws to Maxwell's equations. Some well known theories in literature that describe these electromagnetic interaction terms are Minkowski, Chu, Statistical. Further development of this work is needed, however, particularly in regards to aspects of constitutive modeling and material characterization:

(i) These models neither discuss nor explicitly identify the intensive-extensive conjugate pairs in the fundamental form of the first law of thermodynamics. They also do not discuss the notion of defining a fundamental energy potential (internal energy) or developing a fundamental formulation, as is customary in classical thermodynamics. *These concepts are essential ingredients, and in fact the starting points, for proceeding transparently and rigorously with the formalism of Legendre transformations and the axiomatic Coleman-Noll procedure.* Ambiguity in these identifications can lead to difficulty in reconciling with the formalism of classical thermodynamics.

(ii) The constitutive frameworks are not comprehensive in that they do not consider all possible combinations of independent variables, dependent variables, and thermodynamic potentials(or free energies). For example, [34] does not illustrate how to introduce enthalpy or Gibbs-like free energies (those that employ stress as an independent variable). A comprehensive framework would provide more flexibility in design and experimental characterization (the independent variables are controlled and the dependent variables are measured in an experiment).

(iii) These constitutive frameworks do not identify the concept of a secondary or auxiliary variable (i.e., a physical quantity that is not part of the aforementioned conjugate pairs, yet is accessible algebraically from them), neither do they illustrate how to rigorously introduce such a quantity as an independent variable.

For secondary variables to be an independent variable in a free energy, a mathematical transformation must be developed in a thermodynamically consistent manner to introduce it as such.

In this dissertation, these needs are addressed and the necessary first steps are taken towards creating a unified and comprehensive TEMM model for modeling, designing, and optimizing novel multifunctional materials. It is identified that the electromagnetic conjugate pairs follow from the choice of electromagnetic energy model. The electromagnetic energy contributes to the evolution of the internal energy, as quantified by the first law of thermodynamics. As there are numerous models for the electromagnetic energy in the literature, e.g., Minkowski, Chu, and so on, it is observed that the electromagnetic conjugate pairs differ from one model to another and, hence, are not unique.

A comprehensive catalogue of free energies, state variables (i.e., independent and dependent variables), and state equations that enables the characterization of fully coupled TEMM processes is developed, by addressing some of these issues. To generate this comprehensive catalogue, a complete combinatorial analysis of all possible combinations of thermal, electrical, magnetic, and mechanical independent variables is performed. Each of these combinations corresponds to a particular TEMM process, and each process, in turn, correlates with a set of experiments, the independent variables being controlled and the dependent variables being the measured responses. Each such experiment is characterized by a free energy and a set of state equations. New free energies are introduced through a battery of Legendre and Legendre-type transformations, many appearing in the literature for the first time. The breadth of

our catalogue is intended to provide engineers, applied physicists, and material scientists with optimal flexibility in their approach to characterizing and designing novel multifunctional materials: material properties can be deduced by working with a set of state equations that corresponds to a particular set of experiments, or energy and entropy landscapes can be constructed to achieve targeted performance properties expressed in terms of any set of TEMM quantities.

The material constitutive equations must further obey (i) invariance under an arbitrary superposed rigid body motion, (ii) satisfy the second law of thermodynamics and conservation of angular momentum, (iii) other material specific requirements like symmetry of the crystal structure.

In the second part of this chapter, invariance, angular momentum, and other material specific restrictions are imposed on these state equations to derive the material constitutive equations for three different classes of materials, i.e., (i) materials undergoing slow quasi-static processes and whose response can be approximated with linear, reversible response functions. Such processes can be characterized through principles of equilibrium thermodynamics where the material response is independent of rates, fluxes and there is no dissipation of energy (hence reversible). Some examples include, elastic materials, piezoelectric materials.(ii) materials that undergo transport processes and can be characterized using irreversible thermodynamics and the material response depends on thermal, electrical flux terms. Most of the thermoelectric materials exhibit transport processes like heat conduction, electric conduction, ettinghausen effect, nerst effect, (iii) materials that exhibit hysteresis and cannot be characterized by either of the above principles mentioned above. Some examples for this class of materials include magnetostrictives, ferroic materials, shape

memory alloys, e.t.c. This class of materials exhibit dissipation caused by changes in microstructure.

Constitutive behavior of materials specified in (i) and (ii) is consistent with the restrictions imposed by our statement of second law whereas dissipative materials (iii) do not necessarily obey these principles. In order to accommodate for their dissipative behavior, an order-parameter based thermodynamic framework originally developed by Gurtin and Fried [23] is utilized for characterization of ferroelectrics, ferromagnetic shape memory alloys by various authors. This framework uses a modified form of first law and reduced Clausius-Duhem inequality by assuming the existence of a internal forces called *micro-forces* that contribute to changes in the micro-structure and these forces act as work conjugate to changes in the corresponding order-parameter.

This chapter is structured as follows: In Section 3.2, the principles of classical thermodynamics are revisited and these concepts are used as a guideline to develop an analogous continuum thermodynamic framework. In Sections 3.3 - 3.5, a comprehensive catalogue of all possible state variables, thermodynamic potentials, and state equations that characterize TEMM processes are developed. According to classical thermodynamics [9], a *fundamental* energetic process involves specific internal energy as a function of *extensive* TEMM variables; the *conjugate intensive* quantities are the dependent variables. Thus, new free energies that utilize any or all of the conjugate intensive quantities as independent variables are introduced as Legendre transformations of the internal energy. In Section 3.4, energy potentials or free energies that utilize non-conjugate or auxiliary electromagnetic quantities as independent variables are introduced as Legendre-type transformations of the internal energy. In Section

3.5, the formalism of Sections 3.3 and 3.4 is extended to TEMM processes employing entropy rather than energy as the characterizing thermodynamic potential.

The second part of this chapter will focus on development of constitutive equations for various classes of materials and processes. In Section 3.6 invariance and angular momentum restrictions are applied to the state equations. The free energy is then expanded using Taylor series and this polynomial function is truncated after second order terms. This expression is then used to deduce a linear form for constitutive equations. The materials and the corresponding coupled effects that can be characterized with these equations are then cataloged in detail through the use of Multiphysics Interaction Diagrams (MPID) in Section 3.7. These interaction diagrams were developed to describe all of the linear thermo-electro-magneto-mechanical processes in [49]. These constitutive equations are further restricted in Section 3.7.1, by taking into account the material symmetry of crystal structure in thermodynamic equilibrium.

This framework is then extended to incorporate irreversible effects in Section 3.8. This procedure is not straight forward, unlike the analysis of linear processes, and requires additional independent variables characterizing additional effects. More specifically, two kinds of irreversible behavior are identified: (i) Transport Processes, (ii) Hysteretic Processes. In Section 3.8.1, general linearized equations are presented for materials exhibiting transport processes like conductivity, thermo-electric effects along with the corresponding MPIDs. In Section 3.9, an order-parameter based framework developed by Gurtin & Fried [23, 24] is extended to characterize fully coupled TEMM materials exhibiting hysteresis. As an example, the application of

this framework is demonstrated for ferroelectrics. To conclude the applications and consequences of this unified framework are discussed in Section 3.10.

3.2 Classical Thermodynamics for TEMM Materials: A Motivation for Characterization of Reversible Processes

This section presented a brief recap of the principles of classical thermodynamics, applicable to processes near equilibrium. This background is utilized to develop the continuum thermodynamic framework for fully coupled TEMM system by drawing appropriate analogies. In classical thermodynamics, internal energy U of a system in equilibrium, is described by conjugate pairs of intensive and extensive quantities. The first law of thermodynamics in differential form is given by

$$dU = \theta\, dS + \mathbf{T}\, d(\nabla \mathbf{u}) + \mathbf{e}\, d\mathbf{p}^e + \mu_o\, \mathbf{h}\, d\mathbf{m}^e \tag{3.1}$$

where, deformation $\nabla \mathbf{u}$, entropy S, electric dipole moment $\mathbf{p}^e$, and magnetic moment $\mathbf{m}^e$, are the *extensive variables* and they depend on the size or the amount of material in the system. The corresponding conjugate variables stress $\mathbf{T}$, temperature θ, electric field $\mathbf{e}$, and magnetic field $\mathbf{h}$ are the *intensive variables*, or properties of the system that are independent of its size or quantity.

To describe the thermodynamic state of this system, the internal energy U is posed as a function of the extensive variables, i.e.,

$$U = U((\nabla \mathbf{u})_{ij}, S, \mathbf{p}_i^e, \mathbf{m}_i^e) \tag{3.2}$$

Thermodynamic equilibrium defined by the minimum of internal energy, is described by the state equations that govern the relationship between the independent

(extensive) and dependent (intensive) variables.

$$\mathbf{T}_{ij} = \frac{\partial U}{\partial (\nabla \mathbf{u})_{ij}}, \quad \theta = \frac{\partial U}{\partial S}, \quad \mathbf{e}_i = \frac{\partial U}{\partial \mathbf{p}_i^e}, \quad \mu_o \mathbf{h} = \frac{\partial U}{\partial \mathbf{m}_i^e} \tag{3.3}$$

In other words, the fundamental thermodynamic relation 3.2 and the corresponding state equations describe the complete thermodynamic state of the system at equilibrium[4].

For an infinitesimal system of volume V and mass M, extensive functions like internal energy, dipole moment, mass, obey the additive property, i.e., they have values in a composite system equal to the sum of the values in each subsystem. For instance, $U(\nabla \mathbf{u}_{ij}, S, \mathbf{p}_i^e, \mathbf{m}_i^e)$ satisfies the following relation for a given scalar λ:

$$U(\lambda \nabla \mathbf{u}_{ij}, \lambda S, \lambda \mathbf{p}_i^e, \lambda \mathbf{m}_i^e) = \lambda U(\nabla \mathbf{u}_{ij}, S, \mathbf{p}_i^e, \mathbf{m}_i^e). \tag{3.4}$$

On the other hand, the intensive variables like temperature take the same values everywhere in a system at equilibrium i.e., uniform properties.

Alternative free eneries that utilize any or all of the conjugate intensive quantities as independent variables are introduced as Legendre transforms of the internal energy. A standard form of Legendre transform of internal energy U

$$U_{LT} = U - (\text{extensive quantity}).(\text{corresponding intensive quantity}) \tag{3.5}$$

For instance, temperature θ can be introduced as an independent variable by defining Helmholtz potential A as Legendre transform of internal energy, i.e.,

$$A = U - S.\theta \tag{3.6}$$

[4]In classical thermodynamics the mechanical conjugate pair is often described by volume(extensive) and pressure(intensive). Such a model provides a good description for fluids. For solids, the stress strain conjugate pairs describe the complete nature of deformation. For the special case of hydrostatic pressure, these variables reduce to pV description.

Substituting in (3.1), the corresponding thermodynamic relation is obtained

$$dA = -S\,d\theta + \mathbf{T}\,d(\nabla\mathbf{u}) + \mathbf{e}\,d\mathbf{p}^e + \mu_o\,\mathbf{h}\,d\mathbf{m}^e \tag{3.7}$$

These corresponding state equations can be used to describe quasi-static processes consisting of a sequence of states that are infinitesimally close to equilibrium (processes that are infinitely slow), in which case the process is typically reversible [10].

The classical thermodynamics framework outlined above describes a thermodynamic system of finite mass with uniform properties. On the other hand, our continuum balance laws (2.9)-(3.15) are defined for local (pointwise) quantities normalized per unit mass. Such a description is possible under the assumption that the TEMM fields involved are sufficiently smooth [27]. In this approach, also referred to as *continuum thermodynamics*, *specific* internal energy is posed as a function of *pointwise* quantities such as deformation, specific entropy, polarization and magnetization. These quantities are analogous to the extensive quantities described above, but are expressed on a per mass or specific unit to describe the quantity at a particular point (valid only for continuous systems). Drawing an analogy with classical thermodyanmics, a *specific extensive quantity* is defined from its corresponding extensive quantity by using its additive property, i.e., $\lambda = 1/\mathrm{M}$ is used in Eq.(3.4).

$$\frac{U}{M} = \varepsilon, \quad \frac{S}{M} = \eta \tag{3.8}$$

where ε and η are internal energy and entropy per unit mass respectively. Also, from the definition of polarization and magnetization vectors, it is observed that

$$\frac{\mathbf{p}_e}{M} = \frac{1}{\rho}\frac{\mathbf{p}_e}{V} = \frac{\mathbf{p}}{\rho}, \quad \frac{\mathbf{m}_e}{M} = \frac{1}{\rho}\frac{\mathbf{m}_e}{V} = \frac{\mathbf{m}}{\rho} \tag{3.9}$$

where $\mathbf{p}$ and $\mathbf{m}$ are the polarization and magnetization vectors respectively[5]. Owing to the homogeneity (additivity) of internal energy function, it can be deduced that for internal energy functional $U(\nabla \mathbf{u}_{ij}, S, \mathbf{p}_i^e, \mathbf{m}_i^e)$ defined in Eq.(3.2), an analogous form exists for specific internal energy functional given by:

$$\varepsilon = \frac{U}{M} = \tilde{\varepsilon}(\mathbf{F}, \eta, \frac{\mathbf{p}^*}{\rho}, \frac{\mathbf{m}^*}{\rho}) \tag{3.10}$$

Drawing a similar analogy, the appropriate form of Legendre transform of specific internal energy can now be defined as

$$\varepsilon_{LT} = \varepsilon - (\text{specific extensive quantity}).(\text{corresponding intensive quantity}) \tag{3.11}$$

This formalism is thus adopted to describe any general Legendre transform of internal energy in this work. Following the same guidelines as above, the intensive quantities are then introduced as independent variables through the use of Legendre transform of the form (3.11), e.g., specific Helmholtz free energy is defined as

$$E^{F\theta pm} = \varepsilon - \eta.\theta \tag{3.12}$$

Table 3.1 lists the possible extensive, intensive and specific extensive pairs.

3.3 State Equations Rendered by the Second Law of Thermodynamics: Energy Formulations

The pointwise field equations (2.9)-(2.13) and (2.25)-(2.27) constitute the first principles of our TEMM model. For the purposes of developing the state equations that complete the model, the fields appearing in the first-principle equations are

[5]The derivation of conjugate terms for mechanical variables in solids, i.e., Piola-Kirchhoff stress tensor ($\mathbf{P}$) (intensive), deformation gradient tensor ($\mathbf{F}$) (specific extensive), are described by Landau and Lifshitz [42].

Table 3.1: Extensive, Intensive and Specific Extensive Variables (extensive per unit mass) of a Equilibrium TEMM process

Intensive	**Extensive**	**Specific Extensive**
Temperature (θ)	Entropy (S)	Specific Entropy (η)
Electric Field ($\mathbf{e}$)	Dipole Moment ($\mathbf{p}_e$)	Specific Dipole ($\mathbf{p}/\rho$)
Magnetic Field ($\mathbf{h}$)	Magnetic Moment ($\mathbf{m}_e$)	Specific Magnetic Moment ($\mu_0\,\mathbf{m}/\rho$)
Stress ($\mathbf{P}$)	Deformation ($\delta\mathbf{x}$)	Strain ($\mathbf{F}$)

conceptually divided into three groups, e.g.,

$$\{\mathbf{x}, \eta, \mathbf{p}^*, \mathbf{m}^*\}, \quad \{\mathbf{P}, \theta, \mathbf{e}^*, \mathbf{h}^*, \varepsilon, \mathbf{q}, \mathbf{j}^*\}, \quad \{\rho, \mathbf{f}^{ext}, r^{ext}, \sigma^*\}. \tag{3.13}$$

The elements of the first group are regarded as the independent variables, and the elements of the second group are regarded as the dependent variables[6]. This nomenclature applied to division (3.13) indicates that the fields $\mathbf{P}$, θ, $\mathbf{e}^*$, $\mathbf{h}^*$, ε, $\mathbf{q}$, and $\mathbf{j}^*$ are determined from *material response functions* that, in general, depend on the history of the motion $\mathbf{x}$, specific entropy η, effective electric polarization $\mathbf{p}^*$, and effective magnetization $\mathbf{m}^*$, and possibly their rates or gradients. The elements of the third set are identified as balancing terms. A group of quantities $\mathbf{x}$, η, $\mathbf{p}^*$, $\mathbf{m}^*$, $\mathbf{P}$, θ, $\mathbf{e}^*$, $\mathbf{h}^*$, ε, $\mathbf{q}$, $\mathbf{j}^*$, ρ, $\mathbf{f}^{ext}$, r^{ext}, and σ^* which satisfy the governing equations (2.9)-(2.13) and (2.25)-(2.27) for all space and time in the domain of interest describes a *thermo-electro-magneto-mechanical (TEMM) process.*

[6]In this division, $\mathbf{b}^*$, $\mathbf{d}^*$, and $\mathbf{T}$ are relegated to *secondary* dependent variables, i.e., variables that can be calculated from the independent and *primary* dependent variables in (3.13) using the algebraic relationships (4.12).

Following the formalism of Coleman and Noll [14, 13], the second law of thermodynamics is imposed for all such TEMM processes. The particular statement of second law adopted in this work is the Clausius-Duhem inequality[7]

$$\frac{d}{dt}\int_{\mathcal{V}} \rho\eta \, dv \;\; \geq \;\; \int_{\mathcal{V}} \rho \frac{r^{ext}}{\theta} dv \;\; - \;\; \int_{\partial\mathcal{V}} \frac{h}{\theta} \, da, \tag{3.14}$$

whose pointwise progeny is

$$\rho\dot{\eta} \; - \; \rho \, \frac{r^{ext}}{\theta} \; + \; \operatorname{div}\left(\frac{\mathbf{q}}{\theta}\right) \;\; \geq \;\; 0, \tag{3.15}$$

where θ is the absolute temperature, η is the specific entropy, and $h = \mathbf{q} \cdot \mathbf{n}$. Inequality (3.15) is algebraically combined with the first law of thermodynamics (2.27) to produce the reduced Clausius-Duhem inequality

$$-\dot{\varepsilon} + \frac{1}{\rho_R} \mathbf{P} \cdot \dot{\mathbf{F}} + \theta\dot{\eta} + \mathbf{e}^* \cdot \overline{\left(\frac{\dot{\mathbf{p}}^*}{\rho}\right)} + \mu_o \, \mathbf{h}^* \cdot \overline{\left(\frac{\dot{\mathbf{m}}^*}{\rho}\right)} + \frac{1}{\rho} \, \mathbf{j}^* \cdot \mathbf{e}^* - \frac{1}{\rho\theta} \, \mathbf{q} \cdot \operatorname{grad} \theta \;\; \geq \;\; 0. \tag{3.16}$$

Note that the balancing term r^{ext} was eliminated, rendering inequality (3.16) a restriction on the response functions for $\mathbf{P}$, θ, $\mathbf{e}^*$, $\mathbf{h}^*$, ε, $\mathbf{q}$, and $\mathbf{j}^*$.

It is assumed that the response of the material is path independent, reversible (excluding thermal flux and Joule heating), and rate insensitive. This implies that the material is non-dissipative and free of hysteresis, and the deformation – although it may be large – is elastic and fully recoverable. In terms of the division (3.13), these assumptions imply that the dependence of the response on the motion $\mathbf{x}$ is only through the deformation gradient $\mathbf{F} = \operatorname{Grad} \mathbf{x}$ evaluated at the present time t. Dependence of the response on the remaining independent variables η, $\mathbf{p}^*$, and $\mathbf{m}^*$ is only through their values at the present time t, not their histories, rates, or gradients.

[7] Alternative statements of the second law have been presented and investigated by numerous authors. For instance, an approach championed by Green and Naghdi [25] involves a separation of the Clausius-Duhem inequality into an entropy balance law and isolated statements of second law inequalities.

3.3.1 The fundamental formulation

The special case of a quasi-static process is imposed here, i.e., a process that can be completely described through equilibrium thermodynamics. Analogous to classical thermodynamics[9], (i) the *thermodynamic potential* is the specific internal energy ε, and (ii) the *fundamental* statement (3.16) of the second law consists of contributions from *conjugate pairs* of thermal, electrical, magnetic, and mechanical quantities. Each conjugate pair is the product (or inner product) of an *extensive* quantity in rate form and an *intensive* quantity in non-rate form.[8] The natural independent variables are those appearing as rates, i.e., the extensive quantities $\mathbf{F}$, η, $\mathbf{p}^*/\rho$, and $\mathbf{m}^*/\rho$, and the natural dependent variables are the intensive quantities $\mathbf{P}$, θ, $\mathbf{e}^*$, and $\mathbf{h}^*$. (These are consistent with the assumptions on material response discussed above.)

$$\mathbf{P} = \breve{\mathbf{P}}\left(\mathbf{F}, \eta, \frac{\mathbf{p}^*}{\rho}, \frac{\mathbf{m}^*}{\rho}\right), \quad \theta = \breve{\theta}\left(\mathbf{F}, \eta, \frac{\mathbf{p}^*}{\rho}, \frac{\mathbf{m}^*}{\rho}\right), \quad \mathbf{e}^* = \breve{\mathbf{e}}^*\left(\mathbf{F}, \eta, \frac{\mathbf{p}^*}{\rho}, \frac{\mathbf{m}^*}{\rho}\right),$$

$$\mathbf{h}^* = \breve{\mathbf{h}}^*\left(\mathbf{F}, \eta, \frac{\mathbf{p}^*}{\rho}, \frac{\mathbf{m}^*}{\rho}\right), \quad \varepsilon = \breve{\varepsilon}\left(\mathbf{F}, \eta, \frac{\mathbf{p}^*}{\rho}, \frac{\mathbf{m}^*}{\rho}\right), \tag{3.17}$$

where the superscript breve is used to distinguish a function from its value.

In what follows, it is demonstrated how restrictions imposed by the second law of thermodynamics yield a set of *state equations* [56, 9] that provide the dependent variables $\mathbf{P}$, θ, $\mathbf{e}^*$, and $\mathbf{h}^*$ as partial derivatives of the specific internal energy ε (the thermodynamic potential or free energy) with respect to the independent variables $\mathbf{F}$, η, $\mathbf{p}^*/\rho$, and $\mathbf{m}^*/\rho$, respectively. In order to obtain the *constitutive functions* that characterize a particular TEMM material, the state equations are modified to satisfy invariance, angular momentum, stability, and material symmetry requirements, and

[8] In so doing, the extensive quantities are differentiated per unit mass such as specific entropy, which are *formally* intensive, from *fundamentally* intensive quantities such as temperature.

the material constants are determined experimentally. Use of chain rule on $\varepsilon = \breve{\varepsilon}\,(\mathbf{F}, \eta, \mathbf{p}^*/\rho, \mathbf{m}^*/\rho)$ gives

$$\dot{\varepsilon} \;=\; \frac{\partial \breve{\varepsilon}}{\partial \mathbf{F}} \cdot \dot{\mathbf{F}} \;+\; \frac{\partial \breve{\varepsilon}}{\partial \eta}\,\dot{\eta} \;+\; \frac{\partial \breve{\varepsilon}}{\partial \left(\frac{\mathbf{p}^*}{\rho}\right)} \cdot \overline{\left(\frac{\mathbf{p}^*}{\rho}\right)^{\cdot}} \;+\; \frac{\partial \breve{\varepsilon}}{\partial \left(\frac{\mathbf{m}^*}{\rho}\right)} \cdot \overline{\left(\frac{\mathbf{m}^*}{\rho}\right)^{\cdot}}, \tag{3.18}$$

and substitution of this result into the second law (3.16) leads to

$$\begin{aligned} &\left(\frac{1}{\rho_R}\,\mathbf{P} \;-\; \frac{\partial \breve{\varepsilon}}{\partial \mathbf{F}}\right) \cdot \dot{\mathbf{F}} \;+\; \left(\theta - \frac{\partial \breve{\varepsilon}}{\partial \eta}\right)\dot{\eta} \;+\; \left(\frac{1}{\rho}\,\mathbf{e}^* - \frac{\partial \breve{\varepsilon}}{\partial \left(\frac{\mathbf{p}^*}{\rho}\right)}\right) \cdot \overline{\left(\frac{\mathbf{p}^*}{\rho}\right)^{\cdot}} \\ &+\; \left(\frac{\mu_o}{\rho}\,\mathbf{h}^* - \frac{\partial \breve{\varepsilon}}{\partial \left(\frac{\mathbf{m}^*}{\rho}\right)}\right) \cdot \overline{\left(\frac{\mathbf{m}^*}{\rho}\right)^{\cdot}} \;+\; \frac{1}{\rho}\,\mathbf{j}^* \cdot \mathbf{e}^* \;-\; \frac{1}{\rho\theta}\,\mathbf{q} \cdot \operatorname{grad}\theta \;\geq\; 0. \end{aligned} \tag{3.19}$$

Since the coefficients of the rate terms (e.g., $\dot{\mathbf{F}}$, $\dot{\eta}$) in inequality (3.19) may be varied independently and are arbitrary, it follows that the coefficients vanish, i.e.,

$$\mathbf{P} \;=\; \rho_R\,\frac{\partial \breve{\varepsilon}}{\partial \mathbf{F}}, \qquad \theta \;=\; \frac{\partial \breve{\varepsilon}}{\partial \eta}, \qquad \mathbf{e}^* \;=\; \rho\,\frac{\partial \breve{\varepsilon}}{\partial \left(\frac{\mathbf{p}^*}{\rho}\right)}, \qquad \mathbf{h}^* \;=\; \frac{\rho}{\mu_o}\,\frac{\partial \breve{\varepsilon}}{\partial \left(\frac{\mathbf{m}^*}{\rho}\right)}. \tag{3.20}$$

What remains of inequality (3.19), i.e., $\mathbf{j}^* \cdot \mathbf{e}^* - \frac{1}{\theta}\,\mathbf{q} \cdot \operatorname{grad}\theta \;\geq\; 0$, is called the *residual inequality*.[9] The independent variables $\mathbf{F}$, η, $\mathbf{p}^*/\rho$, $\mathbf{m}^*/\rho$, the thermodynamic energy potential $\varepsilon = \breve{\varepsilon}\,(\mathbf{F}, \eta, \mathbf{p}^*/\rho, \mathbf{m}^*/\rho)$, and the state equations (3.20) are collectively coined the *fundamental formulation*.

3.3.2 The modified fundamental formulation

In order to use the more conventional quantities electric polarization $\mathbf{p}^*$ and magnetization $\mathbf{m}^*$ as the electromagnetic independent variables (rather than $\mathbf{p}^*/\rho$ and

[9]The residual inequality quantifies irreversibilities in a TEMM process, in this case Joule heating and heat flux [9, 34]. Accordingly, unlike the other dependent variables (see Eq. (3.20)), $\mathbf{j}^*$ and $\mathbf{q}$ are not derivable from the free energy, i.e., they are not state variables.

$\mathbf{m}^*/\rho$), the chain rule

$$\overline{\left(\frac{\mathbf{p}^*}{\rho}\right)^{\cdot}} \;=\; \frac{1}{\rho}\,\dot{\mathbf{p}}^* \;+\; \frac{1}{\rho}\left(\mathbf{F}^{-\mathrm{T}}\cdot\dot{\mathbf{F}}\right)\mathbf{p}^*, \qquad \overline{\left(\frac{\mathbf{m}^*}{\rho}\right)^{\cdot}} \;=\; \frac{1}{\rho}\,\dot{\mathbf{m}}^* \;+\; \frac{1}{\rho}\left(\mathbf{F}^{-\mathrm{T}}\cdot\dot{\mathbf{F}}\right)\mathbf{m}^* \tag{3.21}$$

is used to rewrite the fundamental form (3.16) of the Clausius-Duhem inequality[10]

$$\begin{aligned} &-\dot{\varepsilon} \;+\; \left[\frac{1}{\rho_R}\,\mathbf{P} \;+\; \frac{1}{\rho}\left(\mathbf{e}^*\cdot\mathbf{p}^* \;+\; \mu_o\,\mathbf{h}^*\cdot\mathbf{m}^*\right)\mathbf{F}^{-\mathrm{T}}\right]\cdot\dot{\mathbf{F}} \;+\; \theta\dot{\eta} \\ &+\; \frac{1}{\rho}\,\mathbf{e}^*\cdot\dot{\mathbf{p}}^* \;+\; \frac{\mu_o}{\rho}\,\mathbf{h}^*\cdot\dot{\mathbf{m}}^* \;+\; \frac{1}{\rho}\,\mathbf{j}^*\cdot\mathbf{e}^* \;-\; \frac{1}{\rho\theta}\,\mathbf{q}\cdot\operatorname{grad}\theta \;\geq\; 0, \end{aligned} \tag{3.22}$$

where

$$\overline{\left(\frac{1}{\rho}\right)^{\cdot}} \;=\; \frac{1}{\rho}\operatorname{div}\mathbf{v}, \qquad \operatorname{div}\mathbf{v} \;=\; \operatorname{tr}\mathbf{L} \;=\; \operatorname{tr}\left(\dot{\mathbf{F}}\mathbf{F}^{-1}\right) \;=\; \mathbf{F}^{-\mathrm{T}}\cdot\dot{\mathbf{F}}. \tag{3.23}$$

In the modified form of the second law (3.22), the thermodynamic potential ε is a function of the independent variables $\mathbf{F}$, η, $\mathbf{p}^*$, and $\mathbf{m}^*$, i.e., $\varepsilon = \bar{\varepsilon}\left(\mathbf{F}, \eta, \mathbf{p}^*, \mathbf{m}^*\right)$, and polarization $\mathbf{p}^*$ and magnetization $\mathbf{m}^*$ appear as rates. A superscript bar is used instead of a superscript breve to signify a different internal energy function with the same value (cf. with $(3.17)_5$). Use of the chain rule gives

$$\dot{\varepsilon} \;=\; \frac{\partial\bar{\varepsilon}}{\partial\mathbf{F}}\cdot\dot{\mathbf{F}} \;+\; \frac{\partial\bar{\varepsilon}}{\partial\eta}\,\dot{\eta} \;+\; \frac{\partial\bar{\varepsilon}}{\partial\mathbf{p}^*}\cdot\dot{\mathbf{p}}^* \;+\; \frac{\partial\bar{\varepsilon}}{\partial\mathbf{m}^*}\cdot\dot{\mathbf{m}}^*, \tag{3.24}$$

and substitution of this result into (3.22) leads to

$$\begin{aligned} &\left(\frac{1}{\rho_R}\,\mathbf{P} \;+\; \frac{1}{\rho}\left(\mathbf{e}^*\cdot\mathbf{p}^* \;+\; \mu_o\,\mathbf{h}^*\cdot\mathbf{m}^*\right)\mathbf{F}^{-\mathrm{T}} - \frac{\partial\bar{\varepsilon}}{\partial\mathbf{F}}\right)\cdot\dot{\mathbf{F}} \;+\; \left(\theta - \frac{\partial\bar{\varepsilon}}{\partial\eta}\right)\dot{\eta} \\ &+\; \left(\frac{1}{\rho}\,\mathbf{e}^* - \frac{\partial\bar{\varepsilon}}{\partial\mathbf{p}^*}\right)\cdot\dot{\mathbf{p}}^* \;+\; \left(\frac{\mu_o}{\rho}\,\mathbf{h}^* - \frac{\partial\bar{\varepsilon}}{\partial\mathbf{m}^*}\right)\cdot\dot{\mathbf{m}}^* \;+\; \frac{1}{\rho}\,\mathbf{j}^*\cdot\mathbf{e}^* \;-\; \frac{1}{\rho\theta}\,\mathbf{q}\cdot\operatorname{grad}\theta \;\geq\; 0. \end{aligned} \tag{3.25}$$

[10] As a result of this operation, the conjugate of $\mathbf{F}$ is now a linear combination of the first Piola-Kirchhoff stress and a pair of electro-magneto-mechanical terms.

Since the coefficients of $\dot{\mathbf{F}}$, $\dot{\eta}$, $\dot{\mathbf{p}}^*$, and $\dot{\mathbf{m}}^*$ in inequality (3.25) are independent of the rates, and the rates may be varied independently and are arbitrary, it follows that the coefficients vanish, i.e.,

$$\mathbf{P} \;=\; \rho_R \frac{\partial \bar{\varepsilon}}{\partial \mathbf{F}} \;-\; J\left(\mathbf{e}^* \cdot \mathbf{p}^* + \mu_o\, \mathbf{h}^* \cdot \mathbf{m}^*\right) \mathbf{F}^{-\mathrm{T}}, \qquad \theta \;=\; \frac{\partial \bar{\varepsilon}}{\partial \eta},$$

$$\mathbf{e}^* \;=\; \rho \frac{\partial \bar{\varepsilon}}{\partial \mathbf{p}^*}, \qquad \mathbf{h}^* \;=\; \frac{\rho}{\mu_o} \frac{\partial \bar{\varepsilon}}{\partial \mathbf{m}^*}. \tag{3.26}$$

The independent variables $\mathbf{F}$, η, $\mathbf{p}^*$, $\mathbf{m}^*$, the thermodynamic energy potential $\varepsilon = \bar{\varepsilon}\left(\mathbf{F}, \eta, \mathbf{p}^*, \mathbf{m}^*\right)$, and the state equations (3.26) are collectively coined the *modified fundamental formulation*.

3.3.3 Other energetic formulations

In principle, knowledge of the internal energy function $\varepsilon = \breve{\varepsilon}\left(\mathbf{F}, \eta, \mathbf{p}^*/\rho, \mathbf{m}^*/\rho\right)$ or $\varepsilon = \bar{\varepsilon}\left(\mathbf{F}, \eta, \mathbf{p}^*, \mathbf{m}^*\right)$ is necessary and sufficient to characterize any general TEMM process. (Said differently, specification of the internal energy alone determines $\mathbf{P}$, θ, $\mathbf{e}^*$, and $\mathbf{h}^*$; refer to the state equations (3.20) and (3.26).) However, process characterization is more straightforwardly accomplished when the choice of independent and dependent variables synchronizes with those one wishes to control and measure, respectively. To change any or all of the independent variables, a new thermodynamic potential function or free energy is defined through a Legendre transformation of the internal energy. With this in mind, and the fundamental formulation as a template, Other formulations characterized by alternative sets of independent variables and thermodynamic free energies are systematically investigated. In particular, all possible Legendre transforms $E^{(a)(b)(c)(d)}$ of the internal energy are studied, where the superscript letters (a), (b), (c), and (d) are placeholders for an appropriate mechanical, thermal, electrical, and magnetic independent variable, respectively. This

compact notation denotes that the free energy or the Legendre-transformed energy potential $E^{F\theta pm}$, for instance, is a function of deformation, temperature, effective electric polarization, and effective magnetization.[11]

As shown in Table 3.2, the free energies are categorized into four families, each employing a common set of thermomechanical independent variables: Family 1, deformation and specific entropy, both extensive; Family 2, deformation (extensive) and temperature (intensive); Family 3, stress (intensive) and specific entropy (extensive); and Family 4, stress and temperature, both intensive. Either effective electric field intensity or effective electric polarization, and either effective magnetic field intensity or effective magnetization, complete the set of independent variables. Thus, within each family, there are four different energy potentials, each associated with one of the four possible sets of independent variables.

Table 3.2: Free Energies and Associated Independent Variables

Family 1	Family 2	Family 3	Family 4
ε	$\mathrm{E}^{F\theta pm}$	$\mathrm{E}^{P\eta pm}$	$\mathrm{E}^{P\theta pm}$
$\mathrm{E}^{F\eta em}$	$\mathrm{E}^{F\theta em}$	$\mathrm{E}^{P\eta em}$	$\mathrm{E}^{P\theta em}$
$\mathrm{E}^{F\eta ph}$	$\mathrm{E}^{F\theta ph}$	$\mathrm{E}^{P\eta ph}$	$\mathrm{E}^{P\theta ph}$
$\mathrm{E}^{F\eta eh}$	$\mathrm{E}^{F\theta eh}$	$\mathrm{E}^{P\eta eh}$	$\mathrm{E}^{P\theta eh}$

In the sections that follow, the state equations associated with some of the free energies listed in Table 3.2 are derived. These representative cases are intended to provide the reader with a sufficient blueprint to reproduce the full set of state equations catalogued in Appendix A.

[11]The superscripts p and m in $E^{F\theta pm}$ are understood to represent the *effective* quantities $\mathbf{p}^*$ and $\mathbf{m}^*$.

Family 1: Entropy-Deformation Family

In Family 1, the common thermomechanical independent variables are deformation $\mathbf{F}$ and specific entropy η, both extensive quantities. Free energies that use deformation, entropy, and either or both of the intensive electromagnetic quantities as independent variables are introduced as Legendre transformations of the internal energy $\varepsilon = \bar{\varepsilon}\,(\mathbf{F}, \eta, \mathbf{p}^*, \mathbf{m}^*)$. In the formulation that follows, the intensive electromagnetic quantities $\mathbf{e}^*$ and $\mathbf{h}^*$ are promoted to independent variables, and concomitantly relegate $\mathbf{p}^*$ and $\mathbf{m}^*$ to dependent variables.

Entropy-Deformation-Electric Field-Magnetic Field Formulation

In this formulation, $\{\mathbf{F}, \eta, \mathbf{e}^*, \mathbf{h}^*\}$ is the set of independent variables. The free energy $E^{F\eta eh}$ is defined as the Legendre transformation of internal energy $\varepsilon = \bar{\varepsilon}\,(\mathbf{F}, \eta, \mathbf{p}^*, \mathbf{m}^*)$ with respect to the electromagnetic variables, from $\mathbf{p}^*$ to $\mathbf{e}^*$ and $\mathbf{m}^*$ to $\mathbf{h}^*$,

$$E^{F\eta eh} \;=\; \varepsilon \;-\; \frac{1}{\rho}\,\mathbf{e}^* \cdot \mathbf{p}^* \;-\; \frac{\mu_o}{\rho}\,\mathbf{h}^* \cdot \mathbf{m}^*, \tag{3.27}$$

from which

$$\begin{aligned} \dot{E}^{F\eta eh} \;=\; \dot{\varepsilon} \;-\; \frac{1}{\rho}\Big[(\mathbf{e}^* \cdot \mathbf{p}^*)\,\mathbf{F}^{-\mathrm{T}} \cdot \dot{\mathbf{F}} \;+\; \mathbf{e}^* \cdot \dot{\mathbf{p}}^* \;+\; \mathbf{p}^* \cdot \dot{\mathbf{e}}^*\Big] \\ -\; \frac{\mu_o}{\rho}\Big[(\mathbf{h}^* \cdot \mathbf{m}^*)\,\mathbf{F}^{-\mathrm{T}} \cdot \dot{\mathbf{F}} \;+\; \mathbf{h}^* \cdot \dot{\mathbf{m}}^* \;+\; \mathbf{m}^* \cdot \dot{\mathbf{h}}^*\Big] \end{aligned} \tag{3.28}$$

follows, where Eq. (3.23) is used. Substituting (3.28) into (3.22) leads to

$$-\dot{E}^{F\eta eh} + \frac{1}{\rho_R}\mathbf{P}\cdot\dot{\mathbf{F}} + \theta\dot{\eta} - \frac{1}{\rho}\,\mathbf{p}^*\cdot\dot{\mathbf{e}}^* - \frac{\mu_o}{\rho}\,\mathbf{m}^*\cdot\dot{\mathbf{h}}^* + \frac{1}{\rho}\,\mathbf{j}^*\cdot\mathbf{e}^* - \frac{1}{\rho\theta}\,\mathbf{q}\cdot\mathrm{grad}\,\theta \;\geq\; 0, \tag{3.29}$$

a statement of the second law of thermodynamics for this formulation.[12] Via the chain rule,

$$\dot{E}^{F\eta eh} \;=\; \frac{\partial E^{F\eta eh}}{\partial \mathbf{F}} \cdot \dot{\mathbf{F}} \;+\; \frac{\partial E^{F\eta eh}}{\partial \eta}\, \dot{\eta} \;+\; \frac{\partial E^{F\eta eh}}{\partial \mathbf{e}^*} \cdot \dot{\mathbf{e}}^* \;+\; \frac{\partial E^{F\eta eh}}{\partial \mathbf{h}^*} \cdot \dot{\mathbf{h}}^*, \tag{3.30}$$

and subsequent use of (3.30) in (3.29), it follows that

$$\begin{aligned} &\left(\frac{1}{\rho_R}\,\mathbf{P} \;-\; \frac{\partial E^{F\eta eh}}{\partial \mathbf{F}}\right) \cdot \dot{\mathbf{F}} \;+\; \left(\theta \;-\; \frac{\partial E^{F\eta eh}}{\partial \eta}\right) \dot{\eta} \;-\; \left(\frac{\mathbf{p}^*}{\rho} \;+\; \frac{\partial E^{F\eta eh}}{\partial \mathbf{e}^*}\right) \cdot \dot{\mathbf{e}}^* \\ &-\left(\frac{\mu_o}{\rho}\,\mathbf{m}^* \;+\; \frac{\partial E^{F\eta eh}}{\partial \mathbf{h}^*}\right) \cdot \dot{\mathbf{h}}^* \;+\; \frac{1}{\rho}\,\mathbf{j}^* \cdot \mathbf{e}^* \;-\; \frac{1}{\rho\theta}\,\mathbf{q} \cdot \operatorname{grad}\theta \;\;\geq\;\; 0. \end{aligned} \tag{3.31}$$

Since the coefficients of $\dot{\mathbf{F}}$, $\dot{\eta}$, $\dot{\mathbf{e}}^*$, and $\dot{\mathbf{h}}^*$ are independent of the rates, and the rates may be varied independently and are arbitrary, it follows that the coefficients vanish, i.e.,

$$\mathbf{P} \;=\; \rho_R\, \frac{\partial E^{F\eta eh}}{\partial \mathbf{F}}, \quad \theta \;=\; \frac{\partial E^{F\eta eh}}{\partial \eta}, \quad \mathbf{p}^* \;=\; -\,\rho\, \frac{\partial E^{F\eta eh}}{\partial \mathbf{e}^*}, \quad \mathbf{m}^* \;=\; -\,\frac{\rho}{\mu_o}\, \frac{\partial E^{F\eta eh}}{\partial \mathbf{h}^*}, \tag{3.32}$$

with $\mathbf{j}^* \cdot \mathbf{e}^* - \frac{1}{\theta}\,\mathbf{q} \cdot \operatorname{grad}\theta \;\geq\; 0$ the residual inequality.

Family 2: Temperature-Deformation Family

In Family 2, Legendre-transformed free energy that use temperature (intensive quantity) rather than specific entropy (extensive quantity) as the thermal independent variable are introduced.

Temperature-Deformation-Electric Field-Magnetization Formulation

In this formulation, $\mathbf{F}$, θ, $\mathbf{e}^*$, and $\mathbf{m}^*$ are the independent variables. The free energy $E^{F\theta em}$ is defined as the Legendre transformation of internal energy $\varepsilon = \bar{\varepsilon}\,(\mathbf{F}, \eta, \mathbf{p}^*, \mathbf{m}^*)$

[12] All formulations presented in this work have a corresponding second law statement.

with respect to the thermal and electrical variables, from η to θ and $\mathbf{p}^*$ to $\mathbf{e}^*$,

$$E^{F\theta em} \;=\; \varepsilon \;-\; \theta\eta \;-\; \frac{1}{\rho}\,\mathbf{e}^*\cdot\mathbf{p}^*, \tag{3.33}$$

whose rate form

$$\dot{E}^{F\theta em} \;=\; \dot{\varepsilon} \;-\; \theta\dot{\eta} \;-\; \eta\dot{\theta} \;-\; \frac{1}{\rho}\left[\left(\mathbf{e}^*\cdot\mathbf{p}^*\right)\mathbf{F}^{-\mathrm{T}}\cdot\dot{\mathbf{F}} \;+\; \mathbf{e}^*\cdot\dot{\mathbf{p}}^* \;+\; \mathbf{p}^*\cdot\dot{\mathbf{e}}^*\right], \tag{3.34}$$

when inserted in (3.22), yields the second law statement

$$\begin{aligned} &-\;\dot{E}^{F\theta em} \;+\; \left[\frac{1}{\rho_R}\,\mathbf{P} \;+\; \frac{\mu_o}{\rho}\,\left(\mathbf{h}^*\cdot\mathbf{m}^*\right)\mathbf{F}^{-\mathrm{T}}\right]\cdot\dot{\mathbf{F}} \;-\; \eta\dot{\theta} \;-\; \frac{1}{\rho}\,\mathbf{p}^*\cdot\dot{\mathbf{e}}^* \\ &+\; \frac{\mu_o}{\rho}\,\mathbf{h}^*\cdot\dot{\mathbf{m}}^* \;+\; \frac{1}{\rho}\,\mathbf{j}^*\cdot\mathbf{e}^* \;-\; \frac{1}{\rho\theta}\,\mathbf{q}\cdot\operatorname{grad}\theta \;\geq\; 0. \end{aligned} \tag{3.35}$$

Use of the chain rule on $\dot{E}^{\,F\theta em}$ leads to the state equations

$$\begin{aligned} &\mathbf{P} \;=\; \rho_R\,\frac{\partial E^{F\theta em}}{\partial\mathbf{F}} \;-\; \mu_o\,J\,\left(\mathbf{h}^*\cdot\mathbf{m}^*\right)\mathbf{F}^{-\mathrm{T}}, \qquad \eta \;=\; -\,\frac{\partial E^{F\theta em}}{\partial\theta}, \\ &\mathbf{p}^* \;=\; -\rho\,\frac{\partial E^{F\theta em}}{\partial\mathbf{e}^*}, \qquad \mathbf{h}^* \;=\; \frac{\rho}{\mu_o}\,\frac{\partial E^{F\theta em}}{\partial\mathbf{m}^*}. \end{aligned} \tag{3.36}$$

Family 3: Entropy-Stress Family

In Family 3, free energies that utilize the intensive quantity $\mathbf{P}$, rather than the extensive quantity $\mathbf{F}$, as the mechanical independent variable are introduced. Sets of state equations are constructed using the fundamental form of the Clausius-Duhem inequality (3.16), where $\mathbf{P}$ and $\mathbf{F}$ form an intensive-extensive conjugate pair and $\varepsilon = \breve{\varepsilon}\left(\mathbf{F},\eta,\mathbf{p}^*/\rho,\mathbf{m}^*/\rho\right)$.[13] In the formulation that follows, the intensive quantities $\mathbf{P}$ and $\mathbf{h}^*$ are promoted to independent variables, and concomitantly the extensive quantities $\mathbf{F}$ and $\mathbf{m}^*/\rho$ are relegated to dependent variables.

[13]Note that $\mathbf{P}$ and $\mathbf{F}$ are not conjugate variables in the modified form of the Clausius-Duhem inequality (3.22), where $\varepsilon = \bar{\varepsilon}\left(\mathbf{F},\eta,\mathbf{p}^*,\mathbf{m}^*\right)$, necessitating our use of the fundamental form (3.16).

Entropy-Stress-Polarization-Magnetic Field Formulation

In this formulation, the independent variables are $\mathbf{P}$, η, $\mathbf{p}^*/\rho$, and $\mathbf{h}^*$. $E^{P\eta ph}$, the corresponding free energy is defined as the Legendre transformation of internal energy $\varepsilon = \breve{\varepsilon}\,(\mathbf{F}, \eta, \mathbf{p}^*/\rho, \mathbf{m}^*/\rho)$ with respect to the mechanical and magnetic variables, from $\mathbf{F}$ to $\mathbf{P}$ and $\mathbf{m}^*/\rho$ to $\mathbf{h}^*$,

$$E^{P\eta ph} \;=\; \varepsilon \;-\; \frac{1}{\rho_R}\,\mathbf{P}\cdot\mathbf{F} \;-\; \mu_o\,\mathbf{h}^*\cdot\frac{\mathbf{m}^*}{\rho}, \tag{3.37}$$

or, in rate form,

$$\dot{E}^{P\eta ph} \;=\; \dot{\varepsilon} \;-\; \frac{1}{\rho_R}\,\mathbf{P}\cdot\dot{\mathbf{F}} \;-\; \frac{1}{\rho_R}\,\mathbf{F}\cdot\dot{\mathbf{P}} \;-\; \mu_o\,\frac{\mathbf{m}^*}{\rho}\cdot\dot{\mathbf{h}}^* \;-\; \mu_o\,\mathbf{h}^*\cdot\overset{\cdot}{\overline{\left(\frac{\mathbf{m}^*}{\rho}\right)}}. \tag{3.38}$$

Inserting (3.38) in (3.16) yields the second law statement

$$-\dot{E}^{P\eta ph} - \frac{1}{\rho_R}\,\mathbf{F}\cdot\dot{\mathbf{P}} + \theta\dot{\eta} + \mathbf{e}^*\cdot\overset{\cdot}{\overline{\left(\frac{\mathbf{p}^*}{\rho}\right)}} - \mu_o\,\frac{\mathbf{m}^*}{\rho}\cdot\dot{\mathbf{h}}^* + \frac{1}{\rho}\,\mathbf{j}^*\cdot\mathbf{e}^* - \frac{1}{\rho\theta}\,\mathbf{q}\cdot\operatorname{grad}\theta \;\geq\; 0, \tag{3.39}$$

and application of the chain rule to $\dot{E}^{P\eta ph}$ leads to

$$\begin{aligned} &-\;\left(\frac{1}{\rho_R}\,\mathbf{F} \;+\; \frac{\partial E^{P\eta ph}}{\partial \mathbf{P}}\right)\cdot\dot{\mathbf{P}} \;+\; \left(\theta - \frac{\partial E^{P\eta ph}}{\partial \eta}\right)\dot{\eta} \;+\; \left(\mathbf{e}^* \;-\; \frac{\partial E^{P\eta ph}}{\partial\left(\frac{\mathbf{p}^*}{\rho}\right)}\right)\cdot\overset{\cdot}{\overline{\left(\frac{\mathbf{p}^*}{\rho}\right)}} \\ &-\;\left(\frac{\mu_o}{\rho}\,\mathbf{m}^* \;+\; \frac{\partial E^{P\eta ph}}{\partial \mathbf{h}^*}\right)\cdot\dot{\mathbf{h}}^* \;+\; \frac{1}{\rho}\,\mathbf{j}^*\cdot\mathbf{e}^* \;-\; \frac{1}{\rho\theta}\,\mathbf{q}\cdot\operatorname{grad}\theta \quad\geq\quad 0, \end{aligned} \tag{3.40}$$

from which the state equations

$$\mathbf{F} \;=\; -\rho_R\,\frac{\partial E^{P\eta ph}}{\partial \mathbf{P}}, \quad \theta \;=\; \frac{\partial E^{P\eta ph}}{\partial \eta}, \quad \mathbf{e}^* \;=\; \frac{\partial E^{P\eta ph}}{\partial\left(\frac{\mathbf{p}^*}{\rho}\right)}, \quad \mathbf{m}^* \;=\; -\frac{\rho}{\mu_o}\,\frac{\partial E^{P\eta ph}}{\partial \mathbf{h}^*} \tag{3.41}$$

follow.

Family 4: Temperature-Stress Family

In Family 4, Legendre-transformed energy potentials or free energies that use the intensive quantities stress and temperature, rather than the extensive quantities

deformation and entropy, as the thermomechanical independent variables are introduced.

Temperature-Stress-Electric Field-Magnetic Field Formulation

The set of independent variables for this formulation is $\{\mathbf{P}, \theta, \mathbf{e}^*, \mathbf{h}^*\}$. The corresponding thermodynamic energy potential $E^{P\theta eh}$ is defined as the Legendre transformation of internal energy $\varepsilon = \breve{\varepsilon}\,(\mathbf{F}, \eta, \mathbf{p}^*/\rho, \mathbf{m}^*/\rho)$ with respect to the mechanical, thermal, electrical, and magnetic variables, from $\mathbf{F}$ to $\mathbf{P}$, η to θ, $\mathbf{p}^*/\rho$ to $\mathbf{e}^*$, and $\mathbf{m}^*/\rho$ to $\mathbf{h}^*$,

$$E^{\,P\theta eh} \;=\; \varepsilon \;-\; \frac{1}{\rho_R}\mathbf{P}\cdot\mathbf{F} \;-\; \theta\eta \;-\; \mathbf{e}^*\cdot\frac{\mathbf{p}^*}{\rho} \;-\; \mu_o\,\mathbf{h}^*\cdot\frac{\mathbf{m}^*}{\rho}. \tag{3.42}$$

Taking the rate of (3.42) gives

$$\begin{aligned}\dot{E}^{P\theta eh} \;=\; \dot{\varepsilon} \;-\; \frac{1}{\rho_R}\mathbf{P}\cdot\dot{\mathbf{F}} \;-\; \frac{1}{\rho_R}\mathbf{F}\cdot\dot{\mathbf{P}} \;-\; \theta\dot{\eta} \;-\; \eta\dot{\theta} \;-\; \mathbf{e}^*\cdot\overset{\cdot}{\overline{\left(\frac{\mathbf{p}^*}{\rho}\right)}} \\ -\; \frac{\mathbf{p}^*}{\rho}\cdot\dot{\mathbf{e}}^* \;-\; \mu_o\,\mathbf{h}^*\cdot\overset{\cdot}{\overline{\left(\frac{\mathbf{m}^*}{\rho}\right)}} \;-\; \mu_o\,\frac{\mathbf{m}^*}{\rho}\cdot\dot{\mathbf{h}}^*,\end{aligned} \tag{3.43}$$

and substitution of this result into (3.16) yields

$$-\dot{E}^{P\theta eh} - \frac{1}{\rho_R}\mathbf{F}\cdot\dot{\mathbf{P}} - \eta\dot{\theta} - \frac{\mathbf{p}^*}{\rho}\cdot\dot{\mathbf{e}}^* - \mu_o\,\frac{\mathbf{m}^*}{\rho}\cdot\dot{\mathbf{h}}^* + \frac{1}{\rho}\,\mathbf{j}^*\cdot\mathbf{e}^* - \frac{1}{\rho\theta}\,\mathbf{q}\cdot\operatorname{grad}\theta \;\geq\; 0. \tag{3.44}$$

Use of the chain rule on $\dot{E}^{\,P\theta eh}$ leads to the state equations

$$\mathbf{F} \;=\; -\rho_R\frac{\partial E^{\,P\theta eh}}{\partial \mathbf{P}}, \quad \eta \;=\; -\frac{\partial E^{\,P\theta eh}}{\partial \theta}, \quad \mathbf{p}^* \;=\; -\,\rho\,\frac{\partial E^{\,P\theta eh}}{\partial \mathbf{e}^*}, \quad \mathbf{m}^* \;=\; -\frac{\rho}{\mu_o}\,\frac{\partial E^{\,P\theta eh}}{\partial \mathbf{h}^*}. \tag{3.45}$$

3.4 Energy Formulations with Non-Conjugate Independent Variables

Recall from Section 3.3 that the internal energy $\varepsilon = \breve{\varepsilon}\,(\mathbf{F}, \eta, \mathbf{p}^*/\rho, \mathbf{m}^*/\rho)$ is a function of the *extensive* quantities $\mathbf{F}$, η, $\mathbf{p}^*/\rho$, and $\mathbf{m}^*/\rho$. In Families 3 and 4, free energies

employing one or more of the *intensive* quantities $\mathbf{P}$, θ, $\mathbf{e}^*$, and $\mathbf{h}^*$ as an independent variable are introduced as Legendre transformations of $\varepsilon = \breve{\varepsilon}\,(\mathbf{F}, \eta, \mathbf{p}^*/\rho, \mathbf{m}^*/\rho)$. It is emphasized that these intensive quantities must appear in one of the thermal, mechanical, electrical, or magnetic intensive-extensive conjugate pairs in the fundamental Clausius-Duhem inequality (3.16).[14] As an example, the free energy $E^{P\eta pm}$ is the Legendre transformation of the internal energy $\varepsilon = \breve{\varepsilon}\,(\mathbf{F}, \eta, \mathbf{p}^*/\rho, \mathbf{m}^*/\rho)$ with respect to the mechanical variable, from $\mathbf{P}$ to $\mathbf{F}$, where $\mathbf{P}$ and $\mathbf{F}$ form an intensive-extensive conjugate pair in (3.16). In this case, the Legendre transformation promotes the intensive quantity $\mathbf{P}$ to an independent variable and relegates the conjugate extensive quantity $\mathbf{F}$ to a dependent variable.

3.4.1 Electric displacement and magnetic induction

In this section, $\mathbf{F}$, η, $\mathbf{d}^*$, and $\mathbf{b}^*$ are selected as the independent variables. The effective electric displacement $\mathbf{d}^*$ and the effective magnetic induction $\mathbf{b}^*$, however, are not part of a conjugate pair in either the fundamental statement (3.16) or the modified statement (3.22) of the second law. As a result, these *non-conjugate* or *auxiliary* quantities cannot be introduced as independent variables through a conventional Legendre transformation of the internal energy. This is circumvented by

[14]Similar logic holds for the modified second law statement (3.22) and the corresponding internal energy $\varepsilon = \bar{\varepsilon}\,(\mathbf{F}, \eta, \mathbf{p}^*, \mathbf{m}^*)$ used to obtain the Legendre-transformed energy potentials in Families 1 and 2.

positing a Legendre-type transformation of $\varepsilon = \bar{\varepsilon}\,(\mathbf{F}, \eta, \mathbf{p}^*, \mathbf{m}^*)$, i.e.,[15]

$$E^{F\eta db} \;=\; \varepsilon \;+\; \frac{\epsilon_o}{2\rho}\,\mathbf{e}^*\cdot\mathbf{e}^* \;+\; \frac{\mu_o}{2\rho}\,\mathbf{h}^*\cdot\mathbf{h}^*, \tag{3.46}$$

whose rate form is

$$\dot{E}^{F\eta db} \;=\; \dot{\varepsilon} \;+\; \frac{1}{2\rho}\left(\epsilon_o\mathbf{e}^*\cdot\mathbf{e}^* + \mu_o\mathbf{h}^*\cdot\mathbf{h}^*\right)\mathbf{F}^{-\mathrm{T}}\cdot\dot{\mathbf{F}} \;+\; \frac{1}{\rho}\left(\epsilon_o\mathbf{e}^*\cdot\dot{\mathbf{e}}^* + \mu_o\mathbf{h}^*\cdot\dot{\mathbf{h}}^*\right), \tag{3.47}$$

where (3.23) is used. Substitution of (3.47) into (3.22), and subsequent use of the algebraic relationships in (4.12), leads to

$$\begin{aligned} &-\;\dot{E}^{F\eta db} \;+\; \left[\frac{1}{\rho_R}\,\mathbf{P} \;+\; \frac{1}{\rho}\left(\mathbf{e}^*\cdot\mathbf{d}^* + \mathbf{h}^*\cdot\mathbf{b}^* - \frac{1}{2}\,\epsilon_o\,\mathbf{e}^*\cdot\mathbf{e}^* - \frac{1}{2}\,\mu_o\,\mathbf{h}^*\cdot\mathbf{h}^*\right)\mathbf{F}^{-\mathrm{T}}\right]\cdot\dot{\mathbf{F}} \\ &+\;\theta\dot{\eta} \;+\; \frac{1}{\rho}\,\mathbf{e}^*\cdot\dot{\mathbf{d}}^* \;+\; \frac{1}{\rho}\,\mathbf{h}^*\cdot\dot{\mathbf{b}}^* \;+\; \frac{1}{\rho}\,\mathbf{j}^*\cdot\mathbf{e}^* \;-\; \frac{1}{\rho\theta}\,\mathbf{q}\cdot\operatorname{grad}\theta \;\geq\; 0, \end{aligned} \tag{3.48}$$

the second law statement for this formulation. Note that $\mathbf{d}$ and $\mathbf{b}$ appear as rates in inequality (3.48), i.e., as independent variables. Use of the chain rule on $\dot{E}^{F\eta db}$ leads to

$$\begin{aligned} &\left[\frac{1}{\rho_R}\,\mathbf{P} - \frac{\partial E^{F\eta db}}{\partial\mathbf{F}} + \frac{1}{\rho}\left(\mathbf{e}^*\cdot\mathbf{d}^* + \mathbf{h}^*\cdot\mathbf{b}^* - \frac{1}{2}\,\epsilon_o\,\mathbf{e}^*\cdot\mathbf{e}^* - \frac{1}{2}\,\mu_o\,\mathbf{h}^*\cdot\mathbf{h}^*\right)\mathbf{F}^{-\mathrm{T}}\right]\cdot\dot{\mathbf{F}} \\ &+\;\left(\theta - \frac{\partial E^{F\eta db}}{\partial\eta}\right)\dot{\eta} \;+\; \left(\frac{1}{\rho}\,\mathbf{e}^* - \frac{\partial E^{F\eta db}}{\partial\mathbf{d}^*}\right)\cdot\dot{\mathbf{d}}^* \;+\; \left(\frac{1}{\rho}\,\mathbf{h}^* - \frac{\partial E^{F\eta db}}{\partial\mathbf{b}^*}\right)\cdot\dot{\mathbf{b}}^* \\ &+\;\frac{1}{\rho}\,\mathbf{j}^*\cdot\mathbf{e}^* \;-\; \frac{1}{\rho\theta}\,\mathbf{q}\cdot\operatorname{grad}\theta \;\geq\; 0, \end{aligned} \tag{3.49}$$

from which the state equations

$$\begin{aligned} &\mathbf{P} \;=\; \rho_R\frac{\partial E^{F\eta db}}{\partial\mathbf{F}} \;-\; J\left(\mathbf{e}^*\cdot\mathbf{d}^* + \mathbf{h}^*\cdot\mathbf{b}^* - \frac{1}{2}\,\epsilon_o\,\mathbf{e}^*\cdot\mathbf{e}^* - \frac{1}{2}\,\mu_o\,\mathbf{h}^*\cdot\mathbf{h}^*\right)\mathbf{F}^{-\mathrm{T}}, \\ &\theta \;=\; \frac{\partial E^{F\eta db}}{\partial\eta}, \qquad \mathbf{e}^* \;=\; \rho\frac{\partial E^{F\eta db}}{\partial\mathbf{d}^*}, \qquad \mathbf{h}^* \;=\; \rho\frac{\partial E^{F\eta db}}{\partial\mathbf{b}^*} \end{aligned} \tag{3.50}$$

[15]This formulation makes contact with a formulation presented by Green & Naghdi in [26]. This contact, however, is unexpected as the two formulations were developed from different perspectives. In particular, it turns out that the terms from the energy supply rate r^e that Green & Naghdi "transferred to be included in the internal energy" (p. 184), although not explicitly identified by the authors, are precisely the last two terms on the right-hand side of our Legendre-type transformation (3.46). Green & Naghdi's "augmented" internal energy (although not symbolically differentiated from their original internal energy) is thus equivalent to our free energy $E^{F\eta db}$ defined in (3.46).

follow. State equations for other formulations that employ either of the non-conjugate electromagnetic quantities $\mathbf{d}^*$ or $\mathbf{b}^*$ as an independent variable are catalogued in Appendix A.

3.5 Entropy as a Characterizing Thermodynamic Potential

In Sections 3.3 and 3.4, a comprehensive thermodynamic framework is developed that uses energetic potentials to characterize fully coupled TEMM processes. In this section, an alternative thermodynamic framework is presented, wherein entropy and Legendre transforms of entropy are used as the characterizing potentials. The *fundamental* form of the Clausius-Duhem inequality is rewritten as:

$$\dot{\eta} + \frac{1}{\rho_R}\frac{\mathbf{P}}{\theta}\cdot\dot{\mathbf{F}} - \frac{1}{\theta}\dot{\varepsilon} + \frac{\mathbf{e}^*}{\theta}\cdot\overset{\cdot}{\left(\frac{\mathbf{p}^*}{\rho}\right)} + \mu_o\frac{\mathbf{h}^*}{\theta}\cdot\overset{\cdot}{\left(\frac{\mathbf{m}^*}{\rho}\right)} + \frac{1}{\rho\theta}\mathbf{j}^*\cdot\mathbf{e}^* - \frac{1}{\rho\theta^2}\mathbf{q}\cdot\operatorname{grad}\theta \;\geq\; 0. \tag{3.51}$$

With entropy η as the thermodynamic potential, the natural independent variables, i.e., the extensive quantities, are the rate terms $\mathbf{F}$, ε, $\mathbf{p}^*/\rho$, and $\mathbf{m}^*/\rho$. The corresponding dependent variables, i.e., the conjugate intensive quantities, are identified as the coefficients of these rate terms, namely $\mathbf{P}/\theta$, $1/\theta$, $\mathbf{e}^*/\theta$, and $\mathbf{h}^*/\theta$. Thus, the *fundamental entropic relationship* [9], i.e., entropy as a function of *extensive variables,* is

$$\eta \;=\; \breve{\eta}\left(\mathbf{F}, \varepsilon, \frac{\mathbf{p}^*}{\rho}, \frac{\mathbf{m}^*}{\rho}\right). \tag{3.52}$$

In order to use polarization $\mathbf{p}^*$ and magnetization $\mathbf{m}^*$ as the electromagnetic independent variables instead of the extensive quantities $\mathbf{p}^*/\rho$ and $\mathbf{m}^*/\rho$, the Clausius-Duhem

inequality (3.51) is rewritten using the chain rule (3.21) and the relations (3.23)

$$\dot{\eta} + \frac{1}{\rho_R \theta}\left[\mathbf{P} + J\,(\mathbf{e}^* \cdot \mathbf{p}^* + \mu_o\,\mathbf{h}^* \cdot \mathbf{m}^*)\,\mathbf{F}^{-\mathrm{T}}\right] \cdot \dot{\mathbf{F}} - \frac{1}{\theta}\,\dot{\varepsilon} + \frac{1}{\rho\theta}\,\mathbf{e}^* \cdot \dot{\mathbf{p}}^* + \frac{\mu_o}{\rho\theta}\,\mathbf{h}^* \cdot \dot{\mathbf{m}}^* + \frac{1}{\rho\theta}\,\mathbf{j}^* \cdot \mathbf{e}^* - \frac{1}{\rho\theta^2}\,\mathbf{q} \cdot \operatorname{grad}\theta \;\geq\; 0. \tag{3.53}$$

Use of the chain rule on the thermodynamic potential $\eta = \bar{\eta}\,(\mathbf{F}, \varepsilon, \mathbf{p}^*, \mathbf{m}^*)$ gives

$$\dot{\eta} \;=\; \frac{\partial \bar{\eta}}{\partial \mathbf{F}} \cdot \dot{\mathbf{F}} + \frac{\partial \bar{\eta}}{\partial \varepsilon}\,\dot{\varepsilon} + \frac{\partial \bar{\eta}}{\partial \mathbf{p}^*} \cdot \dot{\mathbf{p}}^* + \frac{\partial \bar{\eta}}{\partial \mathbf{m}^*} \cdot \dot{\mathbf{m}}^*. \tag{3.54}$$

Substitution of this result into inequality (3.53) leads to the state equations corresponding to this formulation, i.e.,

$$\mathbf{P} = -\,\rho_R \theta\,\frac{\partial \bar{\eta}}{\partial \mathbf{F}} - J\,(\mathbf{e}^* \cdot \mathbf{p}^* + \mu_o\,\mathbf{h}^* \cdot \mathbf{m}^*)\,\mathbf{F}^{-\mathrm{T}}, \qquad \frac{1}{\theta} = \frac{\partial \bar{\eta}}{\partial \varepsilon}\,,$$
$$\mathbf{e}^* \;=\; -\,\rho\theta\,\frac{\partial \bar{\eta}}{\partial \mathbf{p}^*}, \qquad \mathbf{h}^* \;=\; -\,\frac{\rho\theta}{\mu_o}\,\frac{\partial \bar{\eta}}{\partial \mathbf{m}^*}. \tag{3.55}$$

The independent variables $\mathbf{F}$, ε, $\mathbf{p}^*$, $\mathbf{m}^*$, the thermodynamic energy potential $\eta = \bar{\eta}\,(\mathbf{F}, \varepsilon, \mathbf{p}^*, \mathbf{m}^*)$, and the state equations (3.55) are collectively coined the *internal energy-deformation-polarization-magnetization formulation.*

With this formulation as a template, other formulations involving alternative sets of independent variables is investigated. Similar to the energetic formulations presented in Section 3.3 (refer to Table 3.2 and Appendix A), the entropic formulations are categorized into four families, each with a common set of thermomechanical independent variables: Family 1, $\mathbf{F}$ and ε, both extensive; Family 2, $\mathbf{F}$ (extensive) and θ (intensive); Family 3, $\mathbf{P}/\theta$ (intensive) and ε (extensive); and Family 4, $\mathbf{P}/\theta$ and θ, both intensive. Either $\mathbf{e}^*/\theta$ (intensive) or $\mathbf{p}^*/\rho$ (extensive), and either $\mathbf{h}^*/\theta$ (intensive) or $\mathbf{m}^*/\rho$ (extensive), are selected as the electrical and magnetic independent variables, respectively. Thus, within each family, there are four different formulations,

each associated with one of the four possible sets of independent variables. Also associated with each of these formulations is an entropy potential $\eta^{(a)(b)(c)(d)}$, where the superscripts (a), (b), (c), and (d) are placeholders for an appropriate mechanical, thermal, electrical, or magnetic independent variable (refer to Table 3.3).

It is observed that the intensive variables $\mathbf{P}/\theta$, $\mathbf{e}^*/\theta$, and $\mathbf{h}^*/\theta$ discussed above depend on temperature and are thus not purely mechanical, electrical, and magnetic, respectively. It is later shown that this temperature dependence can be eliminated for certain sets of independent variables.

Table 3.3: Entropic Potentials and Associated Independent Variables

Family 1	Family 2	Family 3	Family 4
η	$\eta^{F\theta pm}$	$\eta^{P\varepsilon pm}$	$\eta^{P\theta pm}$
$\eta^{F\varepsilon em}$	$\eta^{F\theta em}$	$\eta^{P\varepsilon em}$	$\eta^{P\theta em}$
$\eta^{F\varepsilon ph}$	$\eta^{F\theta ph}$	$\eta^{P\varepsilon ph}$	$\eta^{P\theta ph}$
$\eta^{F\varepsilon eh}$	$\eta^{F\theta eh}$	$\eta^{P\varepsilon eh}$	$\eta^{P\theta eh}$

3.5.1 Legendre-Transformed Entropic Potentials

Legendre-transformed entropic potentials for a purely thermomechanical process are known as *Massieu-Planck functions*[16] [9, 68]. In our framework, the Massieu-Planck functions are extended to a fully coupled thermo-electro-magneto-mechanical process for the first time. Recall that for the fundamental entropic relationship, the extensive quantities $\mathbf{F}$, ε, $\mathbf{p}^*/\rho$, and $\mathbf{m}^*/\rho$ are the independent variables, and the conjugate intensive quantities $\mathbf{P}/\theta$, $1/\theta$, $\mathbf{e}^*/\theta$, and $\mathbf{h}^*/\theta$ are the dependent variables.

[16]Legendre transforms of entropy are known as free entropies, a concept first introduced by Francois Massieu to characterize fluids [51, 50]. Free entropies appear frequently in statistical thermodynamics [41].

The first-order Legendre transformations required to change any of the extensive thermal, electrical, magnetic, or mechanical independent variables to their intensive counterparts are listed in Table 3.4. In fact, any potential listed in Table 3.3 can be constructed from a combination of the first-order Legendre transformations listed in Table 3.4, and the corresponding state equations can be derived from second law restrictions.

Table 3.4: First-Order Legendre Transformations

IVs	Transformation Equations
$\varepsilon \Rightarrow \dfrac{1}{\theta}$	$\eta^{F\theta pm} = \eta - \varepsilon \dfrac{1}{\theta}$
$\mathbf{F} \Rightarrow \dfrac{\mathbf{P}}{\theta}$	$\eta^{P\varepsilon pm} = \eta + \dfrac{\mathbf{F}}{\rho_R} \cdot \dfrac{\mathbf{P}}{\theta}$
$\dfrac{\mathbf{p}^*}{\rho} \Rightarrow \dfrac{\mathbf{e}^*}{\theta}$	$\eta^{F\varepsilon em} = \eta + \dfrac{\mathbf{p}^*}{\rho} \cdot \dfrac{\mathbf{e}^*}{\theta}$
$\dfrac{\mathbf{m}^*}{\rho} \Rightarrow \dfrac{\mathbf{h}^*}{\theta}$	$\eta^{F\varepsilon ph} = \eta + \mu_o \dfrac{\mathbf{m}^*}{\rho} \cdot \dfrac{\mathbf{h}^*}{\theta}$

3.5.2 State Equations

In this section, the derivation of the state equations is demonstrated for some of the entropic potentials listed in Table 3.3. The full set of Legendre transformations and state equations are catalogued in Appendix A.

Internal Energy-Deformation-Electric Field-Magnetization Formulation

In this formulation, the independent variables are $\mathbf{F}$, ε, $\mathbf{e}^*/\theta$, and $\mathbf{m}^*$. The potential $\eta^{F\varepsilon em}$ is introduced as the Legendre transform of entropy $\eta = \breve{\eta}\left(\mathbf{F}, \varepsilon, \mathbf{p}^*/\rho, \mathbf{m}^*/\rho\right)$

with respect to the electrical variable, i.e.,

$$\eta^{F\varepsilon em} \;=\; \breve{\eta} \;+\; \frac{\mathbf{p}^*}{\rho}\cdot\frac{\mathbf{e}^*}{\theta}, \tag{3.56}$$

as shown in Table 3.4, whose rate form is

$$\dot{\eta}^{\,F\varepsilon em} \;=\; \dot{\breve{\eta}} \;+\; \left(\frac{\mathbf{e}^*}{\theta}\right)\cdot\overline{\left(\frac{\dot{\mathbf{p}}^*}{\rho}\right)} \;+\; \left(\frac{\mathbf{p}^*}{\rho}\right)\cdot\overline{\left(\frac{\dot{\mathbf{e}}^*}{\theta}\right)}. \tag{3.57}$$

Upon substituting the rate form (3.57) into inequality (3.51) and eliminating $\dot{\eta}$, the second-law inequality for this formulation becomes

$$\dot{\eta}^{\,F\varepsilon em} + \frac{1}{\rho_R}\,\frac{\mathbf{P}}{\theta}\cdot\dot{\mathbf{F}} - \frac{1}{\theta}\,\dot{\varepsilon} - \left(\frac{\mathbf{p}^*}{\rho}\right)\cdot\overline{\left(\frac{\dot{\mathbf{e}}^*}{\theta}\right)} + \mu_o\,\frac{\mathbf{h}^*}{\theta}\cdot\overline{\left(\frac{\dot{\mathbf{m}}^*}{\rho}\right)} + \frac{1}{\rho\theta}\,\mathbf{j}^*\cdot\mathbf{e}^* - \frac{1}{\rho\theta^2}\,\mathbf{q}\cdot\operatorname{grad}\theta \;\geq\; 0. \tag{3.58}$$

Inequality (3.58) is rewritten by applying the chain rule to the magnetization rate term and subsequently using the chain rule (3.21) and (3.23), i.e.,

$$\begin{aligned}\dot{\eta}^{\,F\varepsilon em} \;+\; \frac{1}{\rho_R\theta}\,\left[\mathbf{P} \;+\; \mu_o J\,(\mathbf{h}^*\cdot\mathbf{m}^*)\,\mathbf{F}^{-\mathrm{T}}\right]\cdot\dot{\mathbf{F}} \;-\; \frac{1}{\theta}\,\dot{\varepsilon} \;-\; \left(\frac{\mathbf{p}^*}{\rho}\right)\cdot\overline{\left(\frac{\dot{\mathbf{e}}^*}{\theta}\right)} \;+\; \frac{\mu_o}{\rho\theta}\,\mathbf{h}^*\cdot\dot{\mathbf{m}}^* \\ +\; \frac{1}{\rho\theta}\,\mathbf{j}^*\cdot\mathbf{e}^* \;-\; \frac{1}{\rho\theta^2}\,\mathbf{q}\cdot\operatorname{grad}\theta \;\geq\; 0.\end{aligned} \tag{3.59}$$

Using the chain rule

$$\dot{\eta}^{\,F\varepsilon em} \;=\; \frac{\partial\eta^{F\varepsilon em}}{\partial\mathbf{F}}\cdot\dot{\mathbf{F}} \;+\; \frac{\partial\eta^{F\varepsilon em}}{\partial\varepsilon}\,\dot{\varepsilon} \;+\; \frac{\partial\eta^{F\varepsilon em}}{\partial\left(\frac{\mathbf{e}^*}{\theta}\right)}\cdot\overline{\left(\frac{\dot{\mathbf{e}}^*}{\theta}\right)} \;+\; \frac{\partial\eta^{F\varepsilon em}}{\partial\mathbf{m}^*}\cdot\dot{\mathbf{m}}^* \tag{3.60}$$

in inequality (3.59) leads to the state equations

$$\begin{aligned}&\mathbf{P} \;=\; -\,\rho_R\theta\,\frac{\partial\eta^{F\varepsilon em}}{\partial\mathbf{F}} \;-\; \mu_o J\,(\mathbf{h}^*\cdot\mathbf{m}^*)\,\mathbf{F}^{-\mathrm{T}}, \qquad \frac{1}{\theta} \;=\; \frac{\partial\eta^{F\varepsilon em}}{\partial\varepsilon}, \\ &\mathbf{p}^* \;=\; \rho\,\frac{\partial\eta^{F\varepsilon em}}{\partial\left(\frac{\mathbf{e}^*}{\theta}\right)}, \qquad \mathbf{h}^* \;=\; -\frac{\rho\theta}{\mu_o}\,\frac{\partial\eta^{F\varepsilon em}}{\partial\mathbf{m}^*}\,.\end{aligned} \tag{3.61}$$

For this particular formulation, the electrical independent variable $\mathbf{e}^*/\theta$ is dependent on temperature. This dependence cannot be eliminated for $\eta^{\,F\varepsilon em}$ or any of the

other potentials belonging to Families 1 and 3. However, for the potentials belonging to Families 2 and 4, where the thermal independent variable is θ, it is possible to eliminate this dependence, as is demonstrated in the following example.

Temperature-Stress-Electric Field-Magnetic Field Formulation

In this formulation, the independent variables are all intensive quantities. The entropic potential $\eta^{P\theta eh}$ is defined as the Legendre transform of entropy $\eta = \breve{\eta}\,(\mathbf{F}, \varepsilon, \mathbf{p}^*/\rho, \mathbf{m}^*/\rho)$ with respect to all four independent variables, from extensive to intensive ($\mathbf{F}$ to $\mathbf{P}/\theta$, ε to $1/\theta$, $\mathbf{p}^*/\rho$ to $\mathbf{e}^*/\theta$, and $\mathbf{m}^*/\rho$ to $\mathbf{h}^*/\theta$), i.e.,

$$\eta^{P\theta eh} \;=\; \breve{\eta} \;-\; \varepsilon\,\frac{1}{\theta} \;+\; \frac{1}{\rho_R}\,\mathbf{F}\cdot\frac{\mathbf{P}}{\theta} \;+\; \frac{\mathbf{p}^*}{\rho}\cdot\frac{\mathbf{e}^*}{\theta} \;+\; \mu_o\,\frac{\mathbf{m}^*}{\rho}\cdot\frac{\mathbf{h}^*}{\theta}, \tag{3.62}$$

following Table 3.4. The rate form of this equation is

$$\begin{aligned}\dot{\eta}^{P\theta eh} \;=\; \dot{\breve{\eta}} \;-\; \frac{1}{\theta}\,\dot{\varepsilon} \;-\; \varepsilon\,\overline{\left(\frac{1}{\theta}\right)^{\cdot}} \;+\; \frac{1}{\rho_R}\left(\frac{\mathbf{P}}{\theta}\right)\cdot\dot{\mathbf{F}} \;+\; \frac{1}{\rho_R}\,\mathbf{F}\cdot\overline{\left(\frac{\mathbf{P}}{\theta}\right)^{\cdot}} \;+\; \left(\frac{\mathbf{e}^*}{\theta}\right)\cdot\overline{\left(\frac{\mathbf{p}^*}{\rho}\right)^{\cdot}} \\ +\; \mu_o\left(\frac{\mathbf{h}^*}{\theta}\right)\cdot\overline{\left(\frac{\mathbf{m}^*}{\rho}\right)^{\cdot}} \;+\; \mu_o\left(\frac{\mathbf{m}^*}{\rho}\right)\cdot\overline{\left(\frac{\mathbf{h}^*}{\theta}\right)^{\cdot}}.\end{aligned} \tag{3.63}$$

The second law corresponding to this formulation is obtained by substituting the rate form (3.63) into inequality (3.51), i.e.,

$$\begin{aligned}\dot{\eta}^{P\theta eh} \;-\; \frac{1}{\rho_R}\,\mathbf{F}\cdot\overline{\left(\frac{\mathbf{P}}{\theta}\right)^{\cdot}} \;+\; \varepsilon\,\overline{\left(\frac{1}{\theta}\right)^{\cdot}} \;-\; \frac{\mathbf{p}^*}{\rho}\cdot\overline{\left(\frac{\mathbf{e}^*}{\theta}\right)^{\cdot}} \;-\; \mu_o\,\frac{\mathbf{m}^*}{\rho}\cdot\overline{\left(\frac{\mathbf{h}^*}{\theta}\right)^{\cdot}} \\ +\; \frac{1}{\rho\theta}\,\mathbf{j}^*\cdot\mathbf{e}^* \;-\; \frac{1}{\rho\theta^2}\,\mathbf{q}\cdot\operatorname{grad}\theta \;\geq\; 0.\end{aligned} \tag{3.64}$$

The rate terms in inequality (3.64) are rewritten as

$$\overline{\left(\frac{\mathbf{P}}{\theta}\right)^{\cdot}} \;=\; \frac{1}{\theta}\,\dot{\mathbf{P}} \;-\; \frac{\dot{\theta}}{\theta^2}\,\mathbf{P}, \quad \overline{\left(\frac{\mathbf{e}^*}{\theta}\right)^{\cdot}} \;=\; \frac{1}{\theta}\,\dot{\mathbf{e}}^* \;-\; \frac{\dot{\theta}}{\theta^2}\,\mathbf{e}^*, \quad \overline{\left(\frac{\mathbf{h}^*}{\theta}\right)^{\cdot}} \;=\; \frac{1}{\theta}\,\dot{\mathbf{h}}^* \;-\; \frac{\dot{\theta}}{\theta^2}\,\mathbf{h}^*, \tag{3.65}$$

which leads to

$$\dot{\eta}^{P\theta eh} - \frac{1}{\rho_R\theta}\,\mathbf{F}\cdot\dot{\mathbf{P}} - \frac{1}{\theta^2}\left(\varepsilon - \frac{1}{\rho_R}\,\mathbf{P}\cdot\mathbf{F} - \frac{1}{\rho}\,\mathbf{e}^*\cdot\mathbf{p}^* - \frac{1}{\rho}\,\mathbf{h}^*\cdot\mathbf{m}^*\right)\dot{\theta}$$
$$- \frac{1}{\rho\theta}\,\mathbf{p}^*\cdot\dot{\mathbf{e}}^* - \frac{\mu_o}{\rho\theta}\,\mathbf{m}^*\cdot\dot{\mathbf{h}}^* + \frac{1}{\rho\theta}\,\mathbf{j}^*\cdot\mathbf{e}^* - \frac{1}{\rho\theta^2}\,\mathbf{q}\cdot\operatorname{grad}\theta \;\geq\; 0, \tag{3.66}$$

enabling the use of $\mathbf{P}$, θ, $\mathbf{e}^*$, and $\mathbf{h}^*$ as independent variables. The chain rule

$$\dot{\eta}^{P\theta eh} = \frac{\partial\eta^{P\theta eh}}{\partial\mathbf{P}}\cdot\dot{\mathbf{P}} + \frac{\partial\eta^{P\theta eh}}{\partial\theta}\,\dot{\theta} + \frac{\partial\eta^{P\theta eh}}{\partial\mathbf{e}^*}\cdot\dot{\mathbf{e}}^* + \frac{\partial\eta^{P\theta eh}}{\partial\mathbf{h}^*}\cdot\dot{\mathbf{h}}^* \tag{3.67}$$

is then used in inequality (3.66) to derive the state equations

$$\varepsilon = \theta^2\,\frac{\partial\eta^{P\theta eh}}{\partial\theta} + \frac{1}{\rho_R}\,\mathbf{P}\cdot\mathbf{F} + \frac{1}{\rho}\,\mathbf{e}^*\cdot\mathbf{p}^* + \frac{\mu_o}{\rho}\,\mathbf{m}^*\cdot\mathbf{h}^*,$$
$$\mathbf{F} = \rho_R\theta\,\frac{\partial\eta^{P\theta eh}}{\partial\mathbf{P}}, \qquad \mathbf{p}^* = \rho\,\theta\,\frac{\partial\eta^{P\theta eh}}{\partial\mathbf{e}^*}, \qquad \mathbf{m}^* = \frac{\rho\,\theta}{\mu_o}\,\frac{\partial\eta^{P\theta eh}}{\partial\mathbf{h}^*}. \tag{3.68}$$

It is emphasized that the operation (3.65) allowed the state equations (3.68) to be written in terms of the purely mechanical ($\mathbf{P}$), thermal (θ), electrical ($\mathbf{e}^*$), and magnetic ($\mathbf{h}^*$) independent variables, which are more favorable for characterization than $\mathbf{P}/\theta$, $1/\theta$, $\mathbf{e}^*/\theta$, and $\mathbf{h}^*/\theta$. This formalism can be applied to all potentials belonging to Families 2 and 4 (i.e., potentials with temperature θ as the thermal independent variable) in order to eliminate the temperature dependence of the mechanical, electrical, and magnetic independent variables.

3.6 Derivation of Constitutive Equations for a Fully Coupled Linear, Reversible TEMM Process

The state equations derived above are the restrictions imposed by second-law of thermodynamics and are applicable to quasi-static or reversible TEMM processes. These restrictions describe the thermodynamic state of a particular process but do not contain any specific material information to be used as a constitutive equation. In

addition to satisfying the second-law restrictions, constitutive equations must satisfy *conservation of angular momentum, invariance* and *material symmetry requirements*. Thus the state equations need to be modified to accommodate these requirements. In the following section these equations are modified to satisfy the restrictions imposed by invariance and angular momentum equation.

3.6.1 Invariance of Constitutive Equations

As stated earlier, in order to derive the constitutive behavior of material the constitutive equations need to satisfy invariance requirements. A particular notion of invariance called invariance under *superimposed rigid body motion* (SRMBs) is emphasized in this work. Invariance under SRMBs demands that if two motions of a body composed of the same material differ only by a SRMB (i.e., translation and rotation), for the proposed constitutive equation of the material to be physical, the constitutive response generated in the two motions must be the same apart from the orientation. For a more detailed presentation on invariance see [27]. State equations derived in previous sections are modified to satisfy the invariance requirements. In order to satisfy invariance requirements, the potential function is redefined as a function of objective variables, i.e., the independent variables used are modified to satisfy objectivity. For the fully coupled TEMM process, the corresponding objective tensors satisfying invariance and angular momentum have been defined in [61]. These objective vectors and tensors are utilized for our analysis as follows:

$$E^{F\theta pm}\left(\mathbf{F},\theta,\mathbf{e}^{*},\mathbf{h}^{*}\right) \;=\; E^{F\theta pm}\left(\mathbf{C},\theta,\mathbf{e}_{e},\mathbf{h}_{e}\right) \tag{3.69}$$

where,

$$\mathbf{C} = \mathbf{F}^{\mathrm{T}}\mathbf{F}, \qquad \mathbf{e}_e = \frac{1}{\rho}\mathbf{F}^{\mathrm{T}}\mathbf{e}^*, \qquad \mathbf{h}_e = \frac{\mu_o}{\rho}\mathbf{F}^{\mathrm{T}}\mathbf{h}^* \tag{3.70}$$

are the objective quantities corresponding to strain tensor, electric and magnetic field vectors respectively.

The constitutive equations are now modified by substituting (3.69) into the state equations corresponding to the potential $E^{F\theta pm}$. Using chain rule it is deduced that:

$$\begin{aligned}
\mathbf{e}^* &= \rho\frac{\partial E^{F\theta pm}}{\partial \mathbf{p}} = \rho\frac{\partial E^{F\theta pm}}{\partial \mathbf{p}_e}\frac{\partial \mathbf{p}_e}{\partial \mathbf{p}} = \frac{\partial E^{F\theta pm}}{\partial \mathbf{p}_e}\mathbf{F}^{\mathrm{T}} \\
\mathbf{h}^* &= \frac{\rho}{\mu_o}\frac{\partial E^{F\theta pm}}{\partial \mathbf{m}^*} = \frac{\rho}{\mu_o}\frac{\partial E^{F\theta pm}}{\partial \mathbf{m}_e}\frac{\partial \mathbf{m}_e}{\partial \mathbf{m}^*} = \frac{\partial E^{F\theta pm}}{\partial \mathbf{m}_e}\mathbf{F}^{\mathrm{T}}\ \text{sgn J}
\end{aligned} \tag{3.71}$$

similarly,

$$\begin{aligned}
\mathbf{T} &= \rho\frac{\partial E^{F\theta pm}}{\partial \mathbf{F}}\mathbf{F}^{\mathrm{T}} - (\mathbf{e}^*\cdot\mathbf{p} + \mu_o\mathbf{h}^*\cdot\mathbf{m}^*)\,\mathbf{I} \\
&= \rho\left(\frac{\partial E^{F\theta pm}}{\partial \mathbf{C}}\frac{\partial \mathbf{C}}{\partial \mathbf{F}} + \frac{\partial E^{F\theta pm}}{\partial \mathbf{p}_e}\frac{\partial \mathbf{p}_e}{\partial \mathbf{F}} + \frac{\partial E^{F\theta pm}}{\partial \mathbf{m}_e}\frac{\partial \mathbf{m}_e}{\partial \mathbf{F}}\right)\mathbf{F}^{\mathrm{T}} - (\mathbf{e}^*\cdot\mathbf{p} + \mu_o\mathbf{h}^*\cdot\mathbf{m}^*)\,\mathbf{I} \\
&= \rho\mathbf{F}\frac{\partial E^{F\theta pm}}{\partial \mathbf{C}}\mathbf{F}^{\mathrm{T}} + \mathbf{p}\otimes\mathbf{e}^* + \mu_o\mathbf{m}^*\otimes\mathbf{h}^* - (\mathbf{p}\cdot\mathbf{e}^* + \mu_o\mathbf{m}^*\cdot\mathbf{h}^*)\,\mathbf{I}
\end{aligned} \tag{3.72}$$

Thus, equations (3.71) - (3.72) are the frame invariant form of the state equations. It can also be verified that the equation (3.72) satisfies the angular momentum restriction (2.15).

3.6.2 Taylor Series Expansion of Potential Function in Terms of Independent Variables

Now that a general form of constitutive equations satisfying invariance and angular momentum are developed, further material specific restrictions are imposed on the constitutive equations to derive an integrable closed form for free energy function. Various techniques have been used in literature to specify the free energies corresponding to a process [72].

- Truncating the power series expansion and choosing coefficients to ensure observed physical phenomena. This method is phenomenological.

- Statistical mechanics principles in combination with mean field approximations.

- Piecewise quadratic approximations to the globally defined models derived using (a) and (b) above.

In this section the form of energy potential is derived using (a) for the special case of linear processes. Taylor series expansion upto second order terms is demonstrated for a potential function corresponding to a particular process. This polynomial function is truncated after second order terms and is used to deduce a linear form for constitutive equations. It is observed that the coefficients arising in this expansion are unknown and need to determined from appropriate experimental data.

$$
\begin{aligned}
E^{F\theta pm}\left(\mathbf{C},\theta,\mathbf{p}_e,\mathbf{m}_e\right) \;=\; & E^{F\theta pm}\left(\mathbf{x}_o\right) \;+\; \frac{1}{2}\frac{\partial^2 E^{F\theta pm}}{\partial C_{ij}\partial C_{kl}}\left(\mathbf{x}_o\right)\hat{C}_{ij}\hat{C}_{kl} \;+\; \frac{1}{2}\frac{\partial^2 E^{F\theta pm}}{\partial p_i \partial p_j}\left(\mathbf{x}_o\right)\hat{p}_i\hat{p}_j \\
& + \frac{1}{2}\frac{\partial^2 E^{F\theta pm}}{\partial m_i \partial m_j}\left(\mathbf{x}_o\right)\hat{m}_i\hat{m}_j \;+\frac{1}{2}\frac{\partial^2 E^{F\theta pm}}{\partial \theta^2}\left(\mathbf{x}_o\right)\hat{\theta}^2 \;+\; \frac{\partial^2 E^{F\theta pm}}{\partial C_{ij}\partial p_k}\left(\mathbf{x}_o\right)\hat{C}_{ij}\hat{p}_k \\
& + \frac{\partial^2 E^{F\theta pm}}{\partial C_{ij}\partial m_k}\left(\mathbf{x}_o\right)\hat{C}_{ij}\hat{m}_k \;+\; \frac{\partial^2 E^{F\theta pm}}{\partial p_i \partial m_j}\left(\mathbf{x}_o\right)\hat{p}_i\hat{m}_j \;+\; \frac{\partial^2 E^{F\theta pm}}{\partial \theta \partial C_{ij}}\left(\mathbf{x}_o\right)\hat{\theta}\,\hat{C}_{ij} \\
& + \frac{\partial^2 E^{F\theta pm}}{\partial \theta \partial p_i}\left(\mathbf{x}_o\right)\hat{\theta}\,\hat{p}_i \;+\; \frac{\partial^2 E^{F\theta pm}}{\partial \theta \partial m_i}\left(\mathbf{x}_o\right)\hat{\theta}\,\hat{m}_i \;+ \text{higher order terms}
\end{aligned}
\tag{3.73}
$$

This expression is now substituted in equations (3.71) - (3.72) to derive the linear form of constitutive relations by ignoring the higher-order terms.

$$\hat{S}_{ij} \;=\; \rho\frac{\partial^2 E^{F\theta pm}}{\partial C_{ij}\partial C_{kl}}\left(\mathbf{x}_o\right)\hat{C}_{kl} \;+\; \frac{\partial^2 E^{F\theta pm}}{\partial C_{ij}\partial p_k}\left(\mathbf{x}_o\right)\hat{p}_k \;+\; \frac{\partial^2 E^{F\theta pm}}{\partial C_{ij}\partial m_k}\left(\mathbf{x}_o\right)\hat{m}_k \;+\; \frac{\partial^2 E^{F\theta pm}}{\partial\theta\partial C_{ij}}\left(\mathbf{x}_o\right)\hat{\theta} \tag{3.74}$$

$$\hat{e}^*_k \;=\; \rho\frac{\partial^2 E^{F\theta pm}}{\partial C_{ij}\partial p_k}\left(\mathbf{x}_o\right)\hat{C}_{ij} \;+\; \frac{\partial^2 E^{F\theta pm}}{\partial p_i\partial p_k}\left(\mathbf{x}_o\right)\hat{p}_i \;+\; \frac{\partial^2 E^{F\theta pm}}{\partial p_k\partial m_i}\left(\mathbf{x}_o\right)\hat{m}_i \;+\; \frac{\partial^2 E^{F\theta pm}}{\partial\theta\partial p_k}\left(\mathbf{x}_o\right)\hat{\theta} \tag{3.75}$$

$$\hat{h}^*_k \;=\; \rho\frac{\partial^2 E^{F\theta pm}}{\partial C_{ij}\partial m_k}\left(\mathbf{x}_o\right)\hat{C}_{ij} \;+\; \frac{\partial^2 E^{F\theta pm}}{\partial m_k\partial p_i}\left(\mathbf{x}_o\right)\hat{p}_i \;+\; \frac{\partial^2 E^{F\theta pm}}{\partial m_i\partial m_k}\left(\mathbf{x}_o\right)\hat{m}_i \;+\; \frac{\partial^2 E^{F\theta pm}}{\partial\theta\partial m_k}\left(\mathbf{x}_o\right)\hat{\theta} \tag{3.76}$$

$$\hat{\eta} \;=\; \rho\frac{\partial^2 E^{F\theta pm}}{\partial C_{ij}\partial\theta}\left(\mathbf{x}_o\right)\hat{C}_{ij} \;+\; \frac{\partial^2 E^{F\theta pm}}{\partial p_i\partial\theta}\left(\mathbf{x}_o\right)\hat{p}_i \;+\; \frac{\partial^2 E^{F\theta pm}}{\partial\theta\partial m_i}\left(\mathbf{x}_o\right)\hat{m}_i \;+\; \frac{\partial^2 E^{F\theta pm}}{\partial\theta^2}\left(\mathbf{x}_o\right)\hat{\theta} \tag{3.77}$$

where,

$$\mathbf{S} = \mathbf{F}^{-1}\left[\mathbf{T} - \left(\mathbf{p}\otimes\mathbf{e}^* \;+\; \mathbf{m}^*\otimes\mathbf{h}^*\right) \;-\; \left(\mathbf{p}\cdot\mathbf{e}^* \;+\; \mathbf{m}^*\cdot\mathbf{h}^*\right)\mathbf{I}\right]\mathbf{F}^{-\mathrm{T}}$$

3.7 Linear-Reversible Processes

The unknown coefficients that arise in the linearized set of equations are to be determined from experimental procedure. The class of materials and the processes that can be modeled from this framework can be described better through the Multi-Physics Interaction Diagram (MPID) that highlights all reversible TEMM processes (Refer to Chapter 2), giving a physical meaning to these constants and describing the underlying physics.

Mechanical, thermal, electrical and magnetic effects and the mutual coupling between these effects is described in this diagram. Each physical effect is defined by its corresponding extensive and intensive variables, marked at the inner and outer

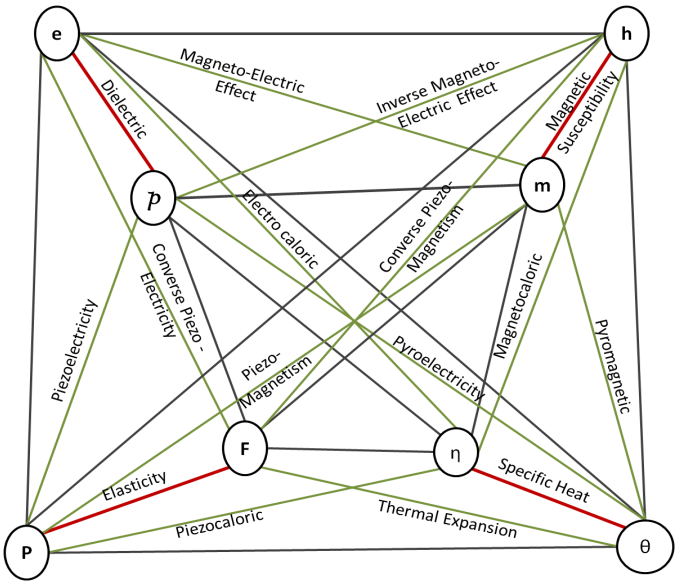

Figure 3.1: Multi-Physics Interaction Diagram (MPID) demonstrating Thermo-Electro-Magneto-Mechanical Effects

quadrilateral corners of the MPID respectively. The extensive and intensive variables corresponding to each of these physical effects is described in Table 3.5.

The diagonal edges (red lines) joining these two quadrilaterals signify the uncoupled processes e.g., elasticity, polarization, magnetization and heat capacity. In order to delineate the coupling effects, the diagram is divided into six subset panels, which relates any two of the four physical effects. All these physical effects are described in detail in Chapter 2.

Here, an attempt to characterize the unknown coefficients in equations (3.74) - (3.77) is made, for the special case of linear reversible processes and the corresponding form of energy potential is deduced. The coefficients for the process above are defined in Table 3.5.

Table 3.5: Materials Constants and their Representations for Linear-Reversible Processes

Constant	**Representation**	**Constant**	**Representation**
Elasticity	$C^o_{ijkl} = \rho \dfrac{\partial^2 E^{F\theta pm}}{\partial C_{ij} \partial C_{kl}}$	Piezoelectric	$d^e_{ijk} = \rho \dfrac{\partial^2 E^{F\theta pm}}{\partial C_{ij} \partial p_k}$
Piezomagnetic	$d^m_{ijk} = \rho \dfrac{\partial^2 E^{F\theta pm}}{\partial C_{ij} \partial m_k}$	Thermal Stress	$\beta_{ij} = \rho \dfrac{\partial^2 E^{F\theta pm}}{\partial \theta \partial C_{ij}}$
Permittivity	$\chi^e_{ij} = \rho \dfrac{\partial^2 E^{F\theta pm}}{\partial p_i \partial p_j}$	Magneto-Electric	$\chi^{em}_{ij} = \rho \dfrac{\partial^2 E^{F\theta pm}}{\partial p_i \partial m_j}$
Pyroelectric	$L^e_i = \rho \dfrac{\partial^2 E^{F\theta pm}}{\partial p_i \partial \theta}$	Permeability	$\chi^m_{ij} = \rho \dfrac{\partial^2 E^{F\theta pm}}{\partial m_i \partial m_j}$
Pyromagnetic	$L^m_i = \rho \dfrac{\partial^2 E^{F\theta pm}}{\partial m_i \partial \theta}$	Specific Heat	$c = \rho \dfrac{\partial^2 E^{F\theta pm}}{\partial \theta^2}$

The form of potential for this process is given by:

$$E^{F\theta pm} = \frac{1}{2} C^o_{ijkl} C_{ij} C_{kl} + \frac{1}{2} \chi^e_{ij} p_i p_j + \frac{1}{2} \chi^m_{ij} m_i m_j + \frac{1}{2} c \theta^2 + d^e_{ijk} C_{ij} p_k + d^m_{ijk} C_{ij} m_k + \beta_{ij} C_{ij} \theta + \chi^{em}_{ij} p_i m_k + L^e_i \theta p_i + L^m_i \theta m_i \quad (3.78)$$

3.7.1 Symmetry Restrictions on the Crystal Structure

Now that the linearized set of constitutive equations are obtained, the number of unknown material constants are reduced using material symmetry arguments. Every polycrystalline material has a crystal structure that corresponds to a symmetry element. Materials that undergo one or more of the linear thermo-electro-mechanical processes in the MPID (e.g. piezoelectricity, pyroelectricity, elasticity etc.), can be classified into 32 crystallographic symmetry groups. These groups are based on rotation, reflection and inversion symmetry. The material properties corresponding to these crystal classes are polar tensors ranging from rank zero to four. A detailed description of all the symmetry groups and derivation of relationship between material

constants using symmetry arguments for each of these crystal classes are discussed in detail in Newnham [59].

Time inversal is a nonspatial symmetry operation that reverses the direction of current flow, reversing the direction of magnetization. For magnetic structures, the concept of time inversion symmetry becomes an additional consideration, which increases the total number of possible symmetry groups to 122 (90 magnetic and 32 crystallographic point groups). For material exhibiting magnetization (coupled with electric, mechanical or thermal effects), the material constants are axial tensors ranging from rank zero to four.

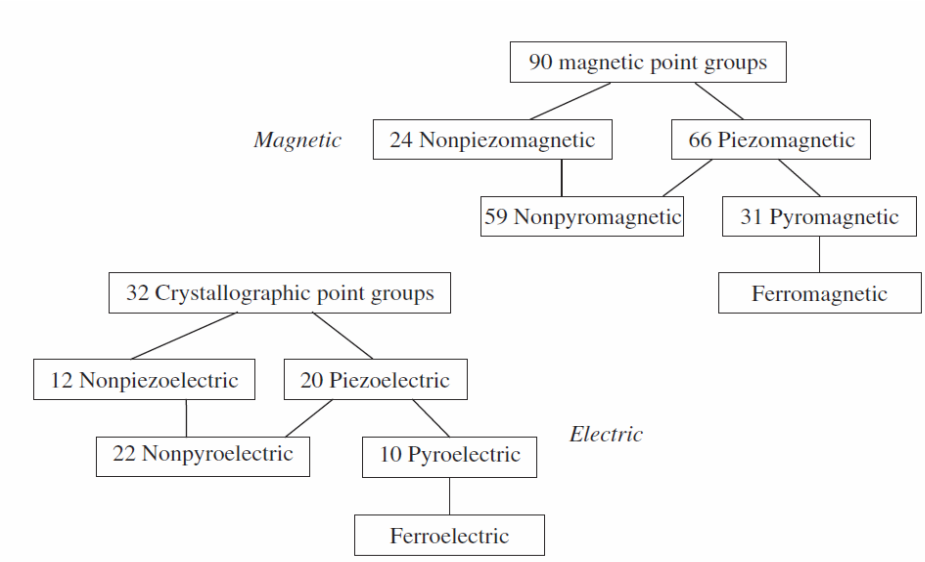

Figure 3.2: Magnetic and Crystallographic Symmetry Groups Exhibiting Coupled Effects

Depending on the symmetry group corresponding to the material, its constants like elasticity constant, piezoelectric constant have a particular form. Symmetry

groups of all possible combinations of thermal, electrical, magnetic and mechanical interactions have been derived and discussed in detail in [59]. Let us now look into an example of a material that exhibits a fully coupled TEMM behavior and belongs to hexagonal group; its constitutive relationship will have the form:

$$
\begin{bmatrix}
\sigma_{11} \\ \sigma_{22} \\ \sigma_{33} \\ \sigma_{23} \\ \sigma_{31} \\ \sigma_{12} \\ \hline
D_1 \\ D_2 \\ D_3 \\ \hline
B_1 \\ B_2 \\ B_3 \\ \hline
\delta S
\end{bmatrix}
=
\left[\begin{array}{cccccc|ccc|ccc|c}
C_{11} & C_{12} & C_{13} & 0 & 0 & 0 & 0 & 0 & d_{31} & 0 & 0 & b_{31} & \alpha_{11} \\
C_{12} & C_{11} & C_{13} & 0 & 0 & 0 & 0 & 0 & d_{31} & 0 & 0 & b_{31} & \alpha_{11} \\
C_{13} & C_{13} & C_{33} & 0 & 0 & 0 & 0 & 0 & d_{33} & 0 & 0 & b_{33} & \alpha_{33} \\
0 & 0 & 0 & C_{44} & 0 & 0 & d_{14} & d_{15} & 0 & 0 & b_{15} & 0 & 0 \\
0 & 0 & 0 & 0 & C_{44} & 0 & d_{15} & -d_{14} & 0 & b_{15} & 0 & 0 & 0 \\
0 & 0 & 0 & 0 & 0 & C_{66} & 0 & 0 & 0 & 0 & 0 & 0 & 0 \\ \hline
0 & 0 & 0 & d_{14} & d_{15} & 0 & \varepsilon_{11} & 0 & 0 & q_{11} & 0 & 0 & 0 \\
0 & 0 & 0 & d_{15} & -d_{14} & 0 & 0 & \varepsilon_{11} & 0 & 0 & q_{11} & 0 & 0 \\
d_{31} & d_{31} & d_{33} & 0 & 0 & 0 & 0 & 0 & \varepsilon_{33} & 0 & 0 & q_{33} & Q_3^{(e)} \\ \hline
0 & 0 & 0 & 0 & b_{15} & 0 & q_{11} & 0 & 0 & \mu_{11} & 0 & 0 & 0 \\
0 & 0 & 0 & b_{15} & 0 & 0 & 0 & q_{11} & 0 & 0 & \mu_{11} & 0 & 0 \\
b_{31} & b_{31} & b_{33} & 0 & 0 & 0 & 0 & 0 & q_{33} & 0 & 0 & \mu_{33} & Q_3^{(m)} \\ \hline
\alpha_{11} & \alpha_{11} & \alpha_{33} & 0 & 0 & 0 & 0 & 0 & Q_3^{(e)} & 0 & 0 & Q_3^{(m)} & c
\end{array}\right]
\begin{bmatrix}
\epsilon_{11} \\ \epsilon_{22} \\ \epsilon_{33} \\ \epsilon_{23} \\ \epsilon_{31} \\ \epsilon_{12} \\ \hline
E_1 \\ E_2 \\ E_3 \\ \hline
H_1 \\ H_2 \\ H_3 \\ \hline
\delta T
\end{bmatrix}
$$

where $C_{66} = 1/2(C_{11} - C_{12})$

As it can be observed, the use of crystal symmetry greatly reduces the number of unknowns in the material characterization and in turn reduces the number of experiments needed to complete the characterization.

3.8 Non-equilibrium Thermodynamics

The work presented in earlier sections describes the characterization of materials that exhibit linear, reversible behavior. This framework is concerned with ideal processes taking place at infinitely slow rate, approximated with a sequence of equilibrium states. For more realistic processes far from equilibrium, i.e., processes involving finite velocities, fluxes, dissipative effects, or inhomogeneous effects, this framework is not valid and can only compare the initial and final equilibrium states.

Thus there is a need to extend this framework to systems with non-linear, irreversible material behavior. Irreversible processes are catergorized into (i) transport

processes [9], i.e., processes like heat conduction, electrical conduction that are characterized by flux terms (ii) dissipative processes, i.e., processes like friction, viscous effects (observed in viscoplastic, viscoelastic materials), hysteresis (observed in ferroic materials), dielectric losses which are characterized by dissipation of energy. In the following sections, constitutive models are developed for both transport and dissipative processes observed in materials.

3.8.1 Characterization of Transport Processes

As stated earlier, in our constitutive models presented in previous sections, it is assumed that the processes are close to equilibrium. This assumption is invalid for transport processes, which are characterized by flow terms like, heat flow, energy flux and are far from equilibrium. In order to characterize these processes, additional constitutive equations are required to describe current density $\mathbf{j}^*$ and heat flux vector $\mathbf{q}$. The Clausius-Duhem inequality is now revisited:

$$-\dot{\varepsilon} + \frac{1}{\rho_R}\,\mathbf{P}\cdot\dot{\mathbf{F}} + \theta\dot{\eta} + \mathbf{e}^*\cdot\widehat{\left(\frac{\mathbf{p}^*}{\rho}\right)} + \mu_o\,\mathbf{h}^*\cdot\widehat{\left(\frac{\mathbf{m}^*}{\rho}\right)} + \frac{1}{\rho}\,\mathbf{j}^*\cdot\mathbf{e}^* - \frac{1}{\rho\theta}\,\mathbf{q}\cdot\mathrm{grad}\,\theta \;\geq\; 0. \quad (3.79)$$

In order to characterize the transport processes, in addition to free energy function, there is a need to develop constitutive equations for $\mathbf{j}^*$ and $\mathbf{q}$. Two new independent variables are introduced that characterize the flow in transport processes, namely charge density σ^* and temperature gradient $\nabla\theta$[17]. The response functions corresponding to this process are of the form:

$$\psi \;=\; \tilde{\psi}(\mathbf{F}, \mathbf{e}^*, \mathbf{h}^*, \theta, \nabla\theta, \sigma^*), \quad \mathbf{q} \;=\; \tilde{\mathbf{q}}(\mathbf{F}, \mathbf{e}^*, \mathbf{h}^*, \theta, \nabla\theta, \sigma^*), \quad \mathbf{j}^* \;=\; \tilde{\mathbf{j}}(\mathbf{F}, \mathbf{e}^*, \mathbf{b}, \theta, \nabla\theta, \sigma^*) \quad (3.80)$$

[17]It is noted that in a near equilibrium state the system is homogeneous i.e., there is no dependence on rates or gradients of physical quantities and the system is electrically neutral (net charge of the system is zero) [57, 34]. On the contrary, these gradients and charges drive the transport processes and cannot be ignored.

Applying the chain rule on free energy function

$$\dot{\psi} = \frac{\partial \psi}{\partial \mathbf{F}} \cdot \dot{\mathbf{F}} + \frac{\partial \psi}{\partial \mathbf{e}} \cdot \dot{\mathbf{e}} + \frac{\partial \psi}{\partial \mathbf{h}} \cdot \dot{\mathbf{h}} + \frac{\partial \psi}{\partial \theta} \cdot \dot{\theta} + \frac{\partial \psi}{\partial \nabla\theta} \cdot \nabla\dot{\theta} + \frac{\partial \psi}{\partial \sigma} \cdot \dot{\sigma}, \tag{3.81}$$

substituting in the Clausius-Duhem inequality and applying the same arguments as before, the restrictions are deduced

$$\mathbf{P} \;=\; \rho_R \frac{\partial \psi}{\partial \mathbf{F}}, \qquad \eta \;=\; -\frac{\partial \psi}{\partial \theta}, \qquad \mathbf{p}^* \;=\; -\,\rho\, \frac{\partial \psi}{\partial \mathbf{e}^*}, \qquad \mathbf{m}^* \;=\; -\frac{\rho}{\mu_o}\, \frac{\partial \psi}{\partial \mathbf{h}^*}. \tag{3.82}$$

$$\frac{\partial \psi}{\partial \sigma} = 0, \qquad \frac{\partial \psi}{\partial \nabla\theta} = 0 \tag{3.83}$$

along with the residual inequality,

$$\mathbf{j}^* \cdot \mathbf{e}^* \;-\; \frac{1}{\theta}\, \mathbf{q} \cdot \operatorname{grad} \theta \;\geq\; 0. \tag{3.84}$$

It is evident from Eq. (3.83) that internal energy is independent of charge density σ and temperature gradient $\nabla\theta$. Thus, the constitutive equations describing $\mathbf{j}^*$ and $\mathbf{q}$ are developed from the restrictions imposed by the residual inequality (3.84). For the restriction (3.84) to hold, a possible solution is

$$\mathbf{q} \;=\; \tilde{\mathbf{K}}(\mathbf{h}, \theta, \sigma^*) \cdot \nabla\theta \;+\; \tilde{\mathbf{L}}^e(\mathbf{h}, \theta, \sigma^*) \cdot \mathbf{e}^* \tag{3.85}$$

$$\mathbf{j}^* \;=\; \tilde{\mathbf{L}}^t(\mathbf{h}, \theta, \sigma^*) \cdot \nabla\theta \;+\; \tilde{\mathbf{R}}(\mathbf{h}, \theta, \sigma^*) \cdot \mathbf{e}^* \tag{3.86}$$

where the coefficients are defined such that it satisfies (3.84) for all values of σ and $\nabla\theta$.

In order to satisfy invariance, $\mathbf{q}_e$ and $\mathbf{j}_e^*$ are rewritten as functions of frame invariant vectors, tensors (refer to section. 3).

$$\mathbf{q}_e \;=\; \mathbf{F}^T\, \hat{\mathbf{q}}(\mathbf{C}, \mathbf{e}_e, \mathbf{h}_e, \theta, \nabla_X\theta, \sigma^*), \quad \mathbf{j}_e^* \;=\; \mathbf{F}^T\, \hat{\mathbf{j}}(\mathbf{C}, \mathbf{e}_e, \mathbf{h}_e, \theta, \nabla_X\theta, \sigma^*) \tag{3.87}$$

For small deformations, invariance requirements can be ignored as $F_{ij} \approx \delta_{ij}$ (and the effect of superimposed rigid body motion on the physical quantities is ignored).

By restricting the equations to small deformations and assuming small deviations from thermostatic equilibrium, the system is linearized as demonstrated in the earlier section.

$$\mathbf{q} \;=\; -\tilde{\mathbf{K}}(\mathbf{h},\theta,\sigma^*)\cdot\nabla\theta \;+\; \tilde{\mathbf{L}}(\mathbf{h},\theta,\sigma^*)\cdot\mathbf{e}^* \tag{3.88}$$

$$\mathbf{j}^* \;=\; \tilde{\mathbf{L}}^T(\mathbf{h},\theta,\sigma^*)\cdot\frac{\nabla\theta}{\theta} \;+\; \tilde{\mathbf{R}}(\mathbf{h},\theta,\sigma^*)\cdot\mathbf{e}^* \tag{3.89}$$

such that $\mathbf{K}$, $\mathbf{R}$ are positive definite tensors.

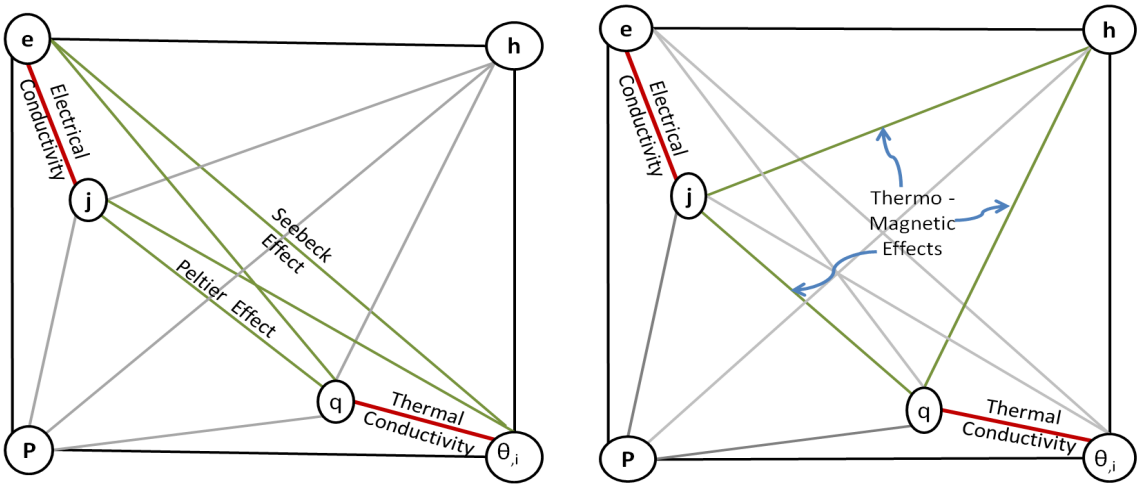

Figure 3.3: Multi-Physics Interaction Diagram (MPID) demonstrating Coupled Thermo-Electric Flow Processes

The equations derived above describe the Fourier's law of heat conduction and Ohm's law of electrical conduction [34, 49]. The coupling coefficients describe various thermoelectric effects like Seebeck effect, Peltier effects, Thomson heat as highlighted in the MPID (Fig. 3.3) [49].These equations can also be used to describe thermomagnetic and galvenometric effects (Nerst or Ettinghausen effect) in magnetic materials,

where magnetic fields arise due to time varying electric fields. A more detailed exposition on these effects and their modeling has been described by Pipkin and Rivlin [62]. In the following section, models are developed for materials exhibiting the other kind of irreversibility, i.e., irreversibility caused by dissipation.

3.9 Characterization of Hysteretic, Frictional Effects

The modeling presented in Section 3.8.1 allows only description of transport processes that are characterized by electric and thermal flux terms. Magnetic or mechanical irreversibilities observed in processes like magnetostriction, friction, plasticity cannot be modeled using these flux terms. These processes are called dissipative processes where the dissipation is caused by microstructural changes in the material.

The framework developed in Sections 3.6 - 3.8.1 cannot be utilized to model these materials. Other frameworks like rational thermodynamics[3, 77], theory of internal variables [6, 67] were developed to characterize the dissipative processes. The free energy here is assumed to be a function of an additional independent variable which is an internal variable describing the microstructural evolution of hysteretic materials. Internal variables are usually irreversible components of physical effects i.e., plastic strain, irreversible component of magnetization or polarization and have been used extensively for characterization of dissipative materials like magnetostrictives, ferroic materials, and thermo-plastic materials [43, 72].

The free energies are predicted based on physics of the specific material rather than as a generic framework modeling hysteretic or irreversible effects. Unlike characterization of materials within linear, reversible regime, each material exhibiting hysteresis is characterized by a different form of Clausius-Duhem inequality. This

makes it challenging to define a unifying framework that can describe the irreversible effects observed in these materials. In this work, an approach developed by Gurtin and Fried [23, 24] is extended to model the behavior of dissipative materials using internal variables. This approach differs from other internal variable theories as it uses a modified form of first and second law of thermodynamics, in addition to a modified free energy functional, thus accommodating for material microstructural changes in the balance laws and not just as a constitutive equation.

3.9.1 Characterization of Phase Transitions using Order Parameter

In this section a thermodynamic framework describing the dissipative, hysteretic behavior exhibited by smart materials like ferroics, shape memory alloys, magnetostrictives, viscoplastics is developed. Some preliminary assumptions are made on the system, to focus on the dissipative aspects of second law. An isothermal process is assumed to ignore the flow processes like heat transfer. The objective is to study the dissipation caused by rearrangement of crystal structures or evolution of domain walls [72, 75, 44]. Such a study of the microscopic behavior of the crystal structure of the material is known as a branch of mechanics called micromechanics.

Due to the inability of Clausius-Duhem inequality to predict the dissipative effects, Gurtin and Fried postulate the existence of a new set of internal forces called **micro-forces** that describe the dissipation due to microstructural changes like rearrangement of crystal cell structures or domain wall evolutions. The internal variable that describes the microstructural evolution is called an **order-parameter**. The micro-forces are assumed to be work-conjugates to order-parameters which can describe the power density expended by material internally due to the microstructural

changes. The order-parameter definition is slightly vauge and is more specific to the material in consideration. For instance, in shape memory materials these micro-forces describe the martensite twin structure evolution [44, 29], whereas in polarizable or magnetizable media these forces describe the evolution of magnetic or electric domains walls.

More specifically, during an evolution of the micro-structure the order parameter ϕ will be a vector-field associated with it at all times and with each such evolution a configurational-force system (micro-forces) is associated that acts in response to changes in the order-parameter. This force system consists of a micro-stress ζ, an internal force π, and an external force γ distributed over a micro-structural domain B. The contribution of these forces is now utilized to describe the microstructural evolution. For a control volume R which is a subset of B,

1. $\int_{\partial R} (\zeta.\mathbf{n})\, \dot{\phi}\, da$ represents power expended across ∂R by neighbouring configurations exterior to R,

2. $\int_R \pi\, \dot{\phi}\, dv$ represents power expended on the atoms of R by the lattice; for example in the reordering of atoms within or transport of atoms between units cells, and

3. $\int_R \gamma\, \dot{\phi}\, dv$ represents power expended on the atoms of R by sources external to R.

The action of these forces on the subsystem R will now allow the force balance

$$\int_{\partial R} (\boldsymbol{\zeta}.\mathbf{n})\, da \,+\, \int_R (\boldsymbol{\pi} \,+\, \boldsymbol{\gamma})\; dv = 0 \tag{3.90}$$

or equivalently,

$$div\boldsymbol{\zeta} \,+\, \boldsymbol{\pi} \,+\, \boldsymbol{\gamma} \,=\mathbf{0} \tag{3.91}$$

in pointwise form.

First law of thermodynamics needs to be modified to add the terms that describe the dissipation. This is accomplished by adding a new set of conjugate pairs that assert the assumption that configurational forces are a response to the change in order-parameter [24, 28]. The first law of thermodynamics for this system is

$$\begin{aligned}\frac{d}{dt}\int_{\mathcal{R}}\rho\left(\varepsilon+\frac{1}{2}\mathbf{v}\cdot\mathbf{v}\right)dv \;&=\; \int_{\mathcal{R}}\rho\left(\mathbf{f}^{ext}+\mathbf{f}^{e}\right)\cdot\mathbf{v}\,dv \;+\; \int_{\partial\mathcal{R}}\mathbf{t}\cdot\mathbf{v}\,da \\ &+\int_{\mathcal{R}}\rho\left(r^{ext}+r^{e}\right)dv \;+\; \int_{\mathcal{R}}\left\langle\boldsymbol{\gamma}\cdot\dot{\boldsymbol{\phi}}\right\rangle dv \;+\; \int_{\partial\mathcal{R}}\left\langle\boldsymbol{\zeta}\cdot\dot{\boldsymbol{\phi}}\right\rangle da - \int_{\partial\mathcal{V}}h\,da. \qquad (3.92)\end{aligned}$$

This is combined with the Clausius-Duhem inequality

$$\frac{d}{dt}\int_{\mathcal{R}}\rho\eta\,dv \;\geq\; \int_{\mathcal{R}}\rho\frac{r^{ext}}{\theta}dv \;-\; \int_{\partial\mathcal{R}}\frac{h}{\theta}\,da,$$

and the following restrictions are imposed: (i) Thermal effects are ignored, i.e., $\theta =$ constant and $\dot{\theta}=0,\ \nabla\theta=0$ (ii) The configurational forces dominate the transport processes the electrical conduction and heat conduction terms are ignored, i.e., $\mathbf{j}=\mathbf{0}$ and $\mathbf{q}=\mathbf{0}$. The reduced Clausius-Duhem inequality can be derived by eliminating r^{ext}, i.e.,

$$\begin{aligned}\frac{\partial}{\partial t}\int_{\mathcal{R}}\rho\left(E^{F\theta pm}+\frac{1}{2}\mathbf{v}\cdot\mathbf{v}\right)dv \leq \int_{\mathcal{R}}\rho\left(\mathbf{f}^{ext}+\mathbf{f}^{e}\right)\cdot\mathbf{v}dv+\int_{\mathcal{R}}\rho\,\mathbf{r}^{e}\,dv \;+\; \int_{\partial\mathcal{R}}\mathbf{t}\cdot\mathbf{v}\,da \\ +\int_{\mathcal{R}}\left\langle\boldsymbol{\gamma}\cdot\dot{\boldsymbol{\phi}}\right\rangle dv \;+\; \int_{\partial\mathcal{R}}\left\langle\boldsymbol{\zeta}\cdot\dot{\boldsymbol{\phi}}\right\rangle da \qquad (3.93)\end{aligned}$$

where, $E^{F\theta pm}=\varepsilon-\theta\eta$ is the Helmholtz potential defined in Eq.(3.12). The presentation of first and second laws of thermodynamics in this work are consistent with the framework developed by Gurtin and Fried [23, 24].

As expected, The internal forces π are not included in the dissipation inequality. In addition to the independent variables presented above, the dependence of free

energy on order-parameter, its gradient and its rate is posited. For the rest of the analysis the free-energy $\psi = E^{F\theta eh}$ is used and is defined in this work through the Legendre transform

$$\psi = E^{F\theta pm} - \frac{\mathbf{p}}{\rho} \cdot \mathbf{e} - \frac{\mathbf{m}}{\rho} \cdot \mathbf{h} \tag{3.94}$$

The dependence of this free-energy on the electro-magneto-mechanical variables and vector order-parameter and its derivatives is assumed, and as stated earlier, the thermal dependence is suppressed, i.e.,

$$\psi = \psi \left(\mathbf{F},\, \mathbf{e},\, \mathbf{h},\, \boldsymbol{\phi},\, \nabla\boldsymbol{\phi},\, \dot{\boldsymbol{\phi}} \right) \tag{3.95}$$

This form of free energy should satisfy the restrictions imposed by second law of thermodynamics (3.93). At this point, no assumptions are made on dependence of order-parameters on other independent variables. To make the general presentation more specific to a deformable, polarizable, and magnetizable material, order-parameters[18] are defined along with the corresponding configurational force systems:

1. **Deformation order parameter**: Second-order tensor called *free-strain* $\mathbf{F}^0$, is used to describe the possible martensite variants and is defined to be the strain state at zero stress but not necessarily zero micro-force or electromagnetic fields.

- micro-forces $\zeta_{kij}nk$ (surface), ν_{ij}(internal), and g_{ij}(external), do work on changes in order-parameter free-strain. The corresponding balance equation;

$$\zeta_{kji,k} + \nu_{ji} + g_{ji} = 0. \tag{3.96}$$

[18]The order-parameters defined for an electro-magneto-mechanical dissipative processes defined in this work are consistent with the work presented by Su and Landis [75] and Landis [44] for ferroelectric and ferromagnetic materials respectively

2. **Polarizable media order parameter**: Polarization **p**, wherein the micro-forces $\xi^e_{ji} n_j$ (surface), π^e_i(internal), and γ^e_i(external) act as work conjugates to the order parameter. This configurational force system, which accounts for energy dissipated due to re-ordering of atoms in the unit cells, follows the force balance

$$\xi^e_{ji,j} + \pi^e_i + \gamma^e_i = 0. \tag{3.97}$$

3. **Magnetizable media order parameter**: Magnetizable **m**, wherein the micro-forces $\xi^m_{ji} n_j$ (surface), π^m_i(internal), and γ^m_i(external) act as work conjugates to the order parameter. This configurational force system accounts for energy dissipated in the magnetizable media due to ordering of spin within the lattice [44]. In micromagnetics the fundamental law corresponds to the angular momentum balance, that relates magnetic torque to the rate of change of angular momentum, i.e.,

$$\epsilon_{kji} m_j \left(\xi^m_{ji,j} + \pi^m_i + \gamma^m_i\right) + \epsilon_{kji} m_{j,l} \xi^m_{li} = \frac{\mu_0}{\kappa_0} \dot{m}_k. \tag{3.98}$$

where $\kappa_0 = -2.214 \times 10^5 m/(As)$ is the the gyromagnetic ratio for an electron spin

A configurational micro-force system corresponding to an isothermal deformable, polarizable, magnetizable media is thus established and these forces are represented in a multi-physics interaction diagrams.

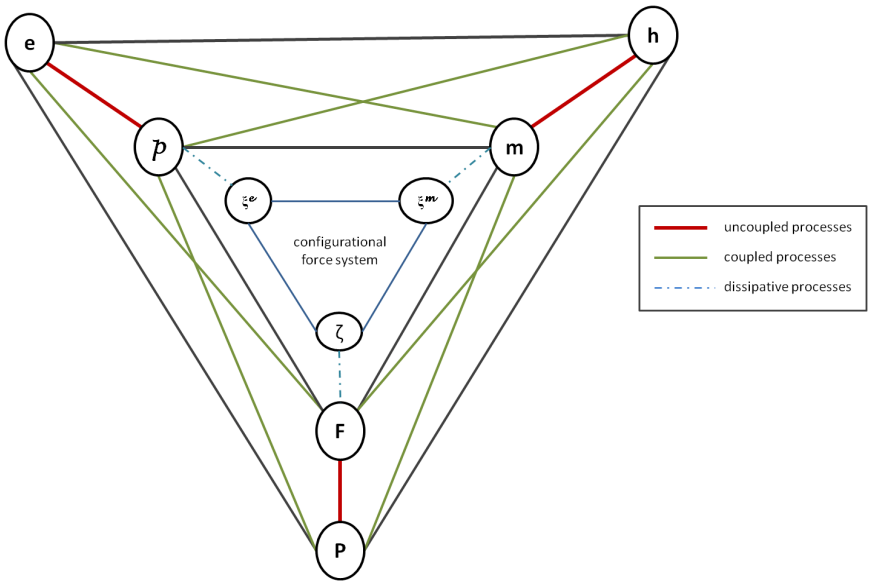

Figure 3.4: MPID demonstrating Electro-Magneto-Mechanical Dissipative Forces

The order-parameter and configurational forces described above are substituted into the dissipation inequality (3.93), i.e.,

$$\int_R \rho\,\dot{\psi}\,dv \leq \int_R \rho\,\left(\mathbf{f}_i^{ext} + \mathbf{f}_i^{e}\right)\mathbf{v}_i dv + \int_R \left(\mu_0 \mathbf{m}_i \dot{\mathbf{h}}_i \,+\, \mathbf{p}_i \dot{\mathbf{e}}_i\right)\,dv \,+\, \int_{\partial R} \mathbf{t}_i \mathbf{v}_i\,da$$
$$+ \int_R \left(\gamma_i^m \mathbf{m}_i \,+\, \gamma_i^e \mathbf{p}_i \,+\, \mathbf{g}_{ji}\mathbf{F}_{ij}^0\right)\,dv \,+\, \int_{\partial R} \left(\xi_{ij}^m n_j \mathbf{m}_i \,+\, \xi_{ij}^e n_j \mathbf{e}_i \,+\, \zeta_{kji} n_k \mathbf{F}_{ij}^0\right)\,da$$

which is equivalent to

$$\int_R \rho\,\dot{\psi}\,dv \leq \int_R \left(\frac{1}{\rho_R}\mathbf{P}_{ji}\dot{\mathbf{F}}_{ij}^0 \,+\, \mu_0 \mathbf{m}_i \dot{\mathbf{h}}_i \,+\, \mathbf{p}_i \dot{\mathbf{e}}_i \,+ \xi_{ji}^m \dot{\mathbf{m}}_{i,j} \,+\, \xi_{ji}^e \dot{\mathbf{p}}_{i,j} \,+\, \zeta_{kij}\dot{\mathbf{F}}_{ij,k}^0\right)$$
$$+ \int_R \left[\left(g_{ji} + \zeta_{kji,k}\right)\dot{\mathbf{F}}_{ij}^0 \,+\, \left(\gamma_i^m + \xi_{ji,j}^m\right)\dot{\mathbf{m}}_i \,+\, \left(\gamma_i^e + \xi_{ji,j}^e\right)\dot{\mathbf{p}}_i\right]\,dv. \quad (3.99)$$

The modified free energy depends on additional variables, namely, the electrical, magnetic and mechanical order parameters and their derivatives

$$\psi = \psi\left(\mathbf{F},\, \mathbf{e},\, \mathbf{h},\, \mathbf{F}^0,\, \nabla\mathbf{F}^0,\, \dot{\mathbf{F}}^0,\, \mathbf{m},\, \nabla\mathbf{m},\, \dot{\mathbf{m}},\, \mathbf{p},\, \nabla\mathbf{p},\, \dot{\mathbf{p}}\right). \quad (3.100)$$

Using the chain rule on free-energy and substituting this expression in Clausius-Duhem inequality,

$$\left(\frac{\partial\psi}{\partial\mathbf{F}_{ij}}-\frac{\mathbf{P}_{ij}}{\rho_R}\right)\dot{\mathbf{F}}_{ij}+\left(\frac{\partial\psi}{\partial\mathbf{h}_i}-\mu_0\mathbf{m}_i\right)\dot{\mathbf{h}}_i+\left(\frac{\partial\psi}{\partial\mathbf{e}_i}-\mathbf{p}_i\right)\dot{\mathbf{e}}_i+\left(\frac{\partial\psi}{\partial\mathbf{F}^0_{ij,k}}-\zeta_{kij}\right)\dot{\mathbf{F}}^0_{ij,k}$$
$$+\left(\frac{\partial\psi}{\partial\mathbf{m}_{i,j}}-\xi^m_{ji}\right)\dot{\mathbf{m}}_{i,j}+\left(\frac{\partial\psi}{\partial\mathbf{p}_{i,j}}-\xi^e_{ji}\right)\dot{\mathbf{p}}_{i,j}+\left(\frac{\partial\psi}{\partial\mathbf{F}^0_{ij}}+\nu_{ji}\right)\dot{\mathbf{F}}^0_{ij}+\left(\frac{\partial\psi}{\partial\mathbf{p}_i}+\pi^e_i\right)\dot{\mathbf{p}}_i$$
$$+\left(\frac{\partial\psi}{\partial\mathbf{m}_i}+\pi^m_i+\frac{\epsilon_{ijk}\epsilon_{jrs}}{\mathbf{m}^2}\mathbf{m}_{r,l}\xi_{ls}\mathbf{m}_k\right)\dot{\mathbf{m}}_i+\frac{\partial\psi}{\partial\dot{\mathbf{F}}^0_{ij}}\ddot{\mathbf{F}}^0_{ij}+\frac{\partial\psi}{\partial\dot{\mathbf{m}}_i}\ddot{\mathbf{m}}_i+\frac{\partial\psi}{\partial\dot{\mathbf{p}}_i}\ddot{\mathbf{p}}_i\leq 0 \quad (3.101)$$

The implicit assumption of equation (3.100) is that the dependent variables stress, magnetic field, electric field, micro-force tensors and internal forces are allowed to depend on variables presented in the argument. By following the approach presented in this work earlier, it can be deduced that free energy is independent of the rate terms $\dot{\mathbf{m}}$, $\dot{\mathbf{p}}$ and $\dot{\mathbf{P}}$, but the internal forces can still depend on the rate terms.

Following the Coleman and Noll approach [12, 13], in order for the independent variables to be controlled, their rates should be arbitrary and the only way the restrictions imposed by second law (3.101) are satisfied is when the following equations are satisfied

$$(1)\ \frac{\partial\psi}{\partial\dot{\mathbf{F}}^0_{ij}}=\frac{\partial\psi}{\partial\dot{\mathbf{p}}_i}=\frac{\partial\psi}{\partial\dot{\mathbf{m}}_i}=0\Rightarrow\psi=\psi\left(\mathbf{F},\,\mathbf{e},\,\mathbf{h},\,\mathbf{F}^0,\,\nabla\mathbf{F}^0,\,\mathbf{m},\,\nabla\mathbf{m},\,\mathbf{p},\,\nabla\mathbf{p}\right) \quad (3.102)$$

$$(2)\ \frac{\partial\psi}{\partial\mathbf{F}_{ij}}=\frac{1}{\rho_R}\mathbf{P}_{ij},\ \ \frac{\partial\psi}{\partial\mathbf{h}_i}=\mu_0\mathbf{m}_i,\ \ \frac{\partial\psi}{\partial\mathbf{e}_i}=\mathbf{p}_i, \quad (3.103)$$

$$(3)\ \frac{\partial\psi}{\partial\mathbf{F}^0_{ij,k}}=\zeta_{kij},\ \ \frac{\partial\psi}{\partial\mathbf{m}_{i,j}}=\xi^m_{ji},\ \ \frac{\partial\psi}{\partial\mathbf{p}_{i,j}}=\xi^e_{ji} \quad (3.104)$$

$$(4)\ \left(\frac{\partial\psi}{\partial\mathbf{F}^0_{ij}}+\nu_{ji}\right)\dot{\mathbf{F}}^0_{ij}+\left(\frac{\partial\psi}{\partial\mathbf{p}_i}+\pi^e_i\right)\dot{\mathbf{p}}_i+\left(\frac{\partial\psi}{\partial\mathbf{m}_i}+\pi^m_i+\frac{\epsilon_{ijk}\epsilon_{jrs}}{\mathbf{m}^2}\mathbf{m}_{r,l}\xi_{ls}\mathbf{m}_k\right)\dot{\mathbf{m}}_i\leq 0 \quad (3.105)$$

Defining the coefficients, i.e.,

$$k_i\equiv\frac{\partial\psi}{\partial\mathbf{m}_i},\quad a_i\equiv\frac{\partial\psi}{\partial\mathbf{p}_i},\quad c_{ij}\equiv\frac{\partial\psi}{\partial\mathbf{F}^0_{ij}}, \quad (3.106)$$

and noting the fact that the internal micro-forces need to satisfy the dissipation inequality (3.105), it is posited that these terms should take the form

$$\pi_i^m = -\frac{\epsilon_{ijk}\epsilon_{jrs}}{\mathbf{m}^2}\mathbf{m}_{r,l}\xi_{ls}\mathbf{m}_k - k_i - \beta_{ij}^{(1)}\dot{\mathbf{m}}_j - \alpha_{ij}^{(1)}\dot{\mathbf{p}}_j - \omega_{ikl}^{(1)}\dot{\mathbf{F}}_{kl}^0,$$
$$\pi_i^e = -a_i - \beta_{ij}^{(2)}\dot{\mathbf{m}}_j - \alpha_{ij}^{(2)}\dot{\mathbf{p}}_j - \omega_{ikl}^{(2)}\dot{\mathbf{F}}_{kl}^0, \quad \nu_{ij} = -c_{ij} - \beta_{ijk}^{(3)}\dot{\mathbf{m}}_k - \alpha_{ijk}^{(3)}\dot{\mathbf{p}}_k - \omega_{ijkl}^{(2)}\dot{\mathbf{F}}_{kl}^0 \tag{3.107}$$

such that the constants $\beta^{(i)}$, $\alpha^{(i)}$ and $\omega^{(i)}$ are positive definite and satisfy dissipation inequality.

If the existence of dissipation potential $\Omega(\dot{\mathbf{m}}, \dot{\mathbf{p}}, \dot{\mathbf{F}}^0)$ is assumed, these constants can be further derived as:

$$\beta_{ij}^{(1)} = \frac{\partial^2\Omega}{\partial\dot{\mathbf{m}}_i\dot{\mathbf{m}}_j}, \quad \alpha_{ij}^{(1)} = \beta_{ij}^{(2)} = \frac{\partial^2\Omega}{\partial\dot{\mathbf{p}}_i\dot{\mathbf{m}}_j}, \quad \alpha_{ij}^{(2)} = \frac{\partial^2\Omega}{\partial\dot{\mathbf{p}}_i\dot{\mathbf{p}}_j}, \quad \beta_{ijk}^{(3)} = \omega_{ijk}^{(1)} = \frac{\partial^2\Omega}{\partial\dot{\mathbf{m}}_i\dot{\mathbf{F}}_{jk}^0},$$
$$\alpha_{ijk}^{(3)} = \omega_{ijk}^{(2)} = \frac{\partial^2\Omega}{\partial\dot{\mathbf{p}}_i\dot{\mathbf{F}}_{jk}^0}, \quad \omega_{ijkl}^{(2)} = \frac{\partial^2\Omega}{\partial\dot{\mathbf{F}}_{ij}^0\dot{\mathbf{F}}_{kl}^0} \tag{3.108}$$

The unknown coefficients can be determined further by determining the specific material properties. As stated earlier, this theory has been used for characterization of ferroelectric and ferromagnetic shape memory alloys [75, 44, 46] , plasticity, viscoplasticity [29, 30]. A suitable form of free-energy describing the appropriate material behavior and consistent with restrictions imposed by second-law of thermodynamics has been presented for these materials. As an example, application of this framework for ferroelectrics is demonstrated below.

Example: Application to Ferroelectrics

For ferroelectric materials, the free energy dependence (3.102) is reduced to

$$\psi = \psi\left(\mathbf{F}_{ij},\, \mathbf{e}_i,\, \mathbf{p}_j,\, \mathbf{p}_{i,j}\right) \tag{3.109}$$

and the state equations (3.103) - (3.104) take the form

$$\frac{\partial \psi}{\partial \mathbf{F}_{ij}} = \frac{1}{\rho_R}\mathbf{P}_{ij}, \quad \frac{\partial \psi}{\partial \mathbf{e}_i} = \mathbf{p}_i, \quad \frac{\partial \psi}{\partial \mathbf{p}_{i,j}} = \xi^e_{ji} \tag{3.110}$$

along with the dissipation inequality

$$\left(\frac{\partial \psi}{\partial \mathbf{p}_i} + \pi^e_i\right)\dot{\mathbf{p}}_i \leq 0. \tag{3.111}$$

In order to satisfy the dissipation inequality, the internal force π^e takes the form

$$\pi^e_i = -a_i - \alpha^{(2)}_{ij}\dot{p}_j \tag{3.112}$$

such that the coefficient $\alpha^{(2)}_{ij} = \alpha^{(2)}_{ij}\left(\mathbf{F}_{ij}, \mathbf{e}_i, \mathbf{p}_i, \mathbf{p}_{i,j}, \dot{\mathbf{p}}_i\right)$ is positive definite.

Ginzburg-Landau Equation: Assuming that for high-temperature phase $\alpha^{(2)}_{ij}$ is constant and cubic, i.e., $\alpha^{(2)}_{ij} = \alpha^{(2)}\delta_{ij}$ and substituting equations (3.111) and $(3.110)_3$ into the electric micro-force balance (3.97), Ginzburg-Landau equation governing the evolution of the material polarization in a ferroelectric material is deduced.

$$\left(\frac{\partial \psi}{\partial \mathbf{p}_{i,j}}\right)_{,j} - \frac{\partial \psi}{\partial \mathbf{p}_i} + \gamma_i = \beta_{ij}\dot{\mathbf{p}}_j \tag{3.113}$$

Derivation of Free-Energy Function: The free energy introduced in equation (3.109) includes both the energy stored in the material and the energy stored in the free space occupied by the material and can be decomposed as

$$\psi\left(\mathbf{F}_{ij},\, \mathbf{e}_i,\, \mathbf{p}_j,\, \mathbf{p}_{i,j}\right) = \bar{\psi}\left(\mathbf{F}_{ij},\, \mathbf{p}_j,\, \mathbf{p}_{i,j}\right) + \frac{\kappa_0}{2}\mathbf{e}_i\mathbf{e}_i \tag{3.114}$$

Now in order to specify the general form of the free energy, it must contain a sufficient set of parameters such that for a given material these parameters can be fit to the spontaneous polarization, spontaneous strain, dielectric permittivity, piezoelectric coefficients and the elastic properties near the stress and electric field free spontaneous polarization and strain states. To accomplish this, the following form is introduced:

$$\psi = \frac{1}{2}C_{ijkl}\varepsilon_{ij}\varepsilon_{kl} + b_{ijkl}\varepsilon_{ij}\mathbf{p}_k\mathbf{p}_l + f_{ijklmn}\varepsilon_{ij}\varepsilon_{kl}\mathbf{p}_m\mathbf{p}_n + \frac{1}{2}a_{ijkl}\mathbf{p}_{i,j}\mathbf{p}_{k,l} + \frac{1}{2}\bar{a}_{ij}\mathbf{p}_i\mathbf{p}_j + g_{ijklmn}\varepsilon_{ij}\mathbf{p}_k\mathbf{p}_l\mathbf{p}_m\mathbf{p}_n + \frac{1}{4}\bar{\bar{a}}_{ijkl}\mathbf{p}_i\mathbf{p}_j\mathbf{p}_k\mathbf{p}_l + \frac{1}{6}\bar{\bar{\bar{a}}}_{ijklmn}\mathbf{p}_i\mathbf{p}_j\mathbf{p}_k\mathbf{p}_l\mathbf{p}_m\mathbf{p}_n + \frac{1}{8}\bar{\bar{\bar{\bar{a}}}}_{ijklmnrs}\mathbf{p}_i\mathbf{p}_j\mathbf{p}_k\mathbf{p}_l\mathbf{p}_m\mathbf{p}_n\mathbf{p}_r\mathbf{p}_s + +\frac{\kappa_0}{2}\,\mathbf{e}_i\mathbf{e}_i \tag{3.115}$$

In order to characterize the material, the unknown coefficients are determined by fitting the free energy function curve with the experimentally observed values.

3.10 Conclusion

A unified continuum framework has been developed and presented in this chapter. This framework is intended to enable modeling and characterizing thermo-electro-magneto-mechanical processes. This framework consists of two parts: (i) a comprehensive catalogue of state variables, thermodynamic potentials, and state equations, (ii) development of response functions for a broad range of deformable, polarizable, magnetizable materials. This framework was presented from a unified perspective integrating lexicon and concepts from continuum thermomechanics, classical electromagnetism, and classical thermodynamics. And, for the sake of generality, it was developed with minimal assumptions: it is three-dimensional, multiphysics, fully coupled, and capable of accommodating anisotropy, dynamic effects, strong electrical and magnetic fields, finite deformations, and other nonlinearities.

Central to the development of part (i) is the fundamental energetic process, which, *analogous to classical thermodynamics,* features extensive independent variables, intensive dependent variables, and specific internal energy as the characterizing thermodynamic potential. Collectively, the extensive independent variables, the specific

internal energy, and the set of state equations rendered by the second law of thermodynamics constitute the fundamental energetic formulation. *The fundamental energetic formulation was used as the thermodynamically consistent starting point from which all alternative energetic formulations were derived.* These alternative formulations were classified as either (i) those whose thermodynamic energy potentials use any or all of the conjugate intensive quantities as independent variables, or (ii) those whose energy potentials use one or more non-conjugate (auxiliary) electromagnetic quantities as independent variables. The former were introduced using Legendre transformations of the internal energy, the latter using novel Legendre-type transformations. This formalism was then extended to formulations that employ entropy rather than energy as the characterizing thermodynamic potential. Many of the thermodynamic potentials appearing in our catalogue, both energetic and entropic, were introduced for the first time.

Each of the TEMM processes catalogued in part (i) correlates with a set of experiments, the independent variables being controlled and the dependent variables being the measured responses. The breadth of this catalogue aims to provide experimentalists with optimal flexibility in their approach to designing and characterizing materials: energy or entropy landscapes can be constructed to achieve targeted performance properties expressed mathematically in the language of any set of TEMM quantities, or material properties can be deduced by working with a set of state equations that corresponds to a particular set of experiments. This catalogue also represents a starting point for characterizing constrained TEMM materials and processes; it is particularly compatible with modeling approaches that regard constraints (e.g., incompressibility) as constitutive limits, i.e., restrictions on the constitutive behavior

of the material as described by the thermodynamic potential[68]. Lastly, although our framework is restricted to equilibrium thermodynamics, which can only be applied to reversible quasi-static TEMM processes, through the use of internal variables or phenomenological modeling [13], this methodology can be straightforwardly extended to model irreversible processes (e.g., viscoplasticity, magnetic hysteresis).

This characterization was used to develop response functions for TEMM materials whose constitutive behavior can be approximated with linear, reversible response. Multiphysics interaction diagrams delineating coupled linear TEMM processes were presented. This framework was further extended to include non-equilibrium processes divided into two broad categories, i.e., (i) transport processes, (ii) hysteretic, frictional or dissipative processes.

Most of the thermoelectric materials exhibiting transport processes like heat conduction, electric conduction, ettinghausen effect, nerst effect etc., can be described using residual inequality corresponding to our statement of the second-law. These equations were supplemented with appropriate multiphysics interaction diagrams.

The second kind of irreversible processes are the ones that undergo microstructural phase changes. These materials often exhibit dissipative losses which causes hysteresis in material behavior. The constitutive equations derived from Clausius-Duhem inequality fails to predict this behavior. This framework was modified to include the microstructural changes, by defining a modified form of first and second law of thermodynamics. This theory was modified by assuming the existence of micro-forces that act as a conjugate to the order-parameter and contribute to changes in the micro-structure. To summarize, this chapter presents modeling and characterization techniques for multifunctional materials with coupled TEMM behavior. It is a unified

framework for a general deformable, polarizable, magnetizable medium applicable to multifunctional materials with expanded performance space and multifunctionality.

Chapter 4: Model-Based Optimization of Coupled Thermo-Electro-Magneto-Mechanical Behavior with Application to Load-Bearing Antennas

4.1 Introduction

This chapter details the systematic derivation of leading-order models for multifunctional materials and structures using nondimensionalization and perturbation theories. Earlier, in Chapters 2 & 3, a comprehensive theory governing the fully coupled thermo-electro-magneto-mechanical (TEMM) behavior was presented; this chapter presents the derivation of regime and structure specific models starting from the comprehensive TEMM theory, using nondimensionalization and perturbation techniques. The fully coupled TEMM theory presented in Chapter 2, based predominantly on first principles, employs the thermomechanical governing equations (2.13) - (2.16) coupled with Maxwell's equations (2.9) - (2.12), along with the macro-scale electromagnetic interaction terms (2.21) - (2.23). These equations are now utilized to deduce the complete set of nondimensionalized equations and the corresponding nondimensional quantities. Depending on the design of the structure and nature of the excitation, only a subset of fully coupled TEMM physical effects are dominant,

which dictates the appropriate computational model. The nondimensional quantities quantify the competition between various physical effects in the operation of the particular device, material, or structure. Assigning characteristic scales to all the physical quantities characterizes the particular process and provides a relative ordering of nondimensional quantities involved in the process [58]. This fixed relative ordering of all competing effects as quantified by nondimensional numbers, determines a "regime" of structure-environment interaction.

Perturbation techniques and asymptotic regime analysis can be used in two different ways; (i) Given a particular design and its operating regime, the leading order equations can be derived and solved for performance analysis, (ii) Given a set of targeted properties, the structure that gives the most optimal performance can be designed. In this chapter, both these formalisms are explored, especially with regards to design and analysis of Load-Bearing Antenna Structures. In this chapter, this formalism is illustrated for modeling and regime analysis of *Load-Bearing Antenna Structures*.

Load-bearing antennas structures are multifunctional devices with sensing and actuating capabilities integrated with a load-bearing structure. These antennas are appealing for military applications like Unmanned Aerial Vehicles (UAV), and have superior structural and electromagnetic radiation properties when compared to the conventional aircraft antennas due to their unique design that minimizes aerodynamic drag on the antenna structure. The load-bearing antenna structure is subjected to mechanical forces, temperature gradients, and electromagnetic fields, giving rise to highly-coupled nonlinear thermo-electro-magneto-mechanical (TEMM) behavior. In order to minimize the drag, the antenna is usually embedded in a load-bearing

composite structure 4.1. In order to improve its design, the nature of structural deformations and electromagnetic radiations of this design need to be optimized. This can be achieved by developing analytical techniques and computational tools for multi-scale, multi-physics modeling of composite load-bearing antennas.

The focus of this chapter is to develop mathematical models of load-bearing antennas for aerodynamic applications. Due to the complexity of this system, there is a limited literature available on analytical/computational modeling techniques for LBAs. Computational and analytical modeling techniques for single functional microstrip antennas in stationary media have been developed extensively in literature [47, 63, 39], but integration of antenna with mechanical structure interferes with its electrical performance and these models are no longer valid.

This chapter is structured as follows: In Section 4.2 the fully coupled TEMM model is revisited along with the coupling terms and interaction models. In Section 4.3, the equations presented in Section 4.2 are nondimensionalized and resulting nondimensional quantities are described. In Section 4.2, the design and working of load-bearing antenna is studied and the characteristic scales are assigned for the involved physical parameters. In Section 4.5, these characteristic scales are used to derive the operating regime and the leading order model for load-bearing antenna. The leading order model is solved analytically and the formalism is extended to a multilayer structure in Section 4.6. These analytical solutions are then utilized to calculate deflections and antenna gain for various materials and the results are compared. In Section 4.7, this formalism is extended to develop a two dimensional plate theory for linear coupled electro-magneto-mechanical behavior. The chapter is finally

concluded by summarizing the results and the contributions of this work in Section 4.11.

4.2 Fully Coupled 3-D Thermo-Electro-Magneto-Mechanical Problem

Coupled thermo-electro-magneto-mechanical behavior is governed by macroscopic continuum conservation laws and Maxwell's equations for deformable moving matter (in non-relativistic approximation). As discussed in Chapter 2, various formulations have been proposed in literature for coupled TEMM behavior in non-relativistic approximation [34] [60]. For consistency, the *Maxwell-Minkowski formulation* is used to derive all our mathematical frameworks throughout this dissertation. The fully coupled TEMM governing equations consisting of the electromagnetic Maxwell equations is revisited,

$$\nabla \cdot \mathbf{b} \;=\; \mathbf{0}, \tag{4.1}$$

$$\nabla \times \mathbf{e}^{*} \;=\; -\frac{\partial \mathbf{b}}{\partial t} \;-\; \nabla \times (\mathbf{b} \times \mathbf{v}), \tag{4.2}$$

$$\nabla \cdot \mathbf{d} \;=\; \sigma, \tag{4.3}$$

$$\nabla \times \mathbf{h}^{*} \;=\; \frac{\partial \mathbf{d}}{\partial t} \;+\; \nabla \times (\mathbf{d} \times \mathbf{v}) \;+\; \sigma \mathbf{v} \;+\; \mathbf{j}^{*}, \tag{4.4}$$

and the pointwise thermo-mechanical conservation laws, i.e.,

$$\dot{\rho} \;+\; \rho \nabla \cdot \mathbf{v} \;=\; 0, \tag{4.5}$$

$$\rho \dot{\mathbf{v}} \;=\; \rho \left(\mathbf{f}^{\mathbf{ext}} \;+\; \mathbf{f}^{\mathbf{e}} \right) \;+\; \nabla \cdot \mathbf{T}, \tag{4.6}$$

$$\mathbf{T}_{\mathbf{[ij]}} \;=\; \rho \mathbf{L}^{\mathbf{e}}_{\mathbf{ij}}, \tag{4.7}$$

$$\rho \dot{\varepsilon} \;=\; \rho r^{ext} \;+\; \rho r^{e} \;-\; \nabla \cdot \mathbf{q} \;+\; \mathbf{T} \cdot \mathbf{L}. \tag{4.8}$$

where, the primitive field quantities are: $\mathbf{e}$ - electric field intensity, $\mathbf{h}$ - magnetic field intensity, $\mathbf{d}$ - electric displacement, $\mathbf{b}$ - magnetic induction, $\mathbf{j}$ - surface current density and σ - charge density. The effective fields $\mathbf{e}^*$, $\mathbf{h}^*$, $\mathbf{j}^*$ are the fields and currents per area acting on the deformed body. $\mathbf{v}$ is velocity, ρ is density, $\mathbf{T}$ is Cauchy stress tensor, $\mathbf{q}$ is energy flux, ε is internal energy density and r^{ext} is external heat supply rate. These equations are coupled through electromagnetic and thermo-mechanical coupling terms given by body force $\mathbf{f}^e$, the couple $\mathbf{L}^e$, and heat supply rate r^e as discussed in Chapter 2.

$$\rho\mathbf{f}^e = \sigma\mathbf{e}^* + \mathbf{j}^* \times \mathbf{b} + \mathbf{p} \cdot \nabla\mathbf{e}^* + \mu_o\mathbf{m}^* \cdot \nabla\mathbf{h}^* + \mathring{\mathbf{d}} \times \mathbf{b} + \mathbf{d} \times \mathring{\mathbf{b}}, \tag{4.9}$$

$$\rho\mathbf{L}^e = \mathbf{p} \otimes \mathbf{e}^* - \mathbf{e}^* \otimes \mathbf{p} + \mu_o\mathbf{m}^* \otimes \mathbf{h}^* - \mu_o\mathbf{h}^* \otimes \mathbf{m}^*, \tag{4.10}$$

$$\rho r^e = \mathbf{j}^* \cdot \mathbf{e}^* + \rho\mathbf{e}^* \cdot \frac{d}{dt}(\frac{\mathbf{p}}{\rho}) + \rho\mu_o\mathbf{h}^* \cdot \frac{d}{dt}(\frac{\mathbf{m}^*}{\rho}). \tag{4.11}$$

where, the electromagnetic fields polarization vector $\mathbf{p}$ and magnetization vector $\mathbf{m}$ are given by:

$$\mathbf{p} = \mathbf{d} - \epsilon_o\mathbf{e}, \quad \mathbf{m} = \frac{1}{\mu_o}\mathbf{b} - \mathbf{h}. \tag{4.12}$$

and, the convected rate for an arbitrary vector $\mathbf{u} = \tilde{\mathbf{u}}(\mathbf{x}, t)$ is:

$$\mathring{\mathbf{u}} = \dot{\mathbf{u}} + \mathbf{u}\,(\operatorname{div}\mathbf{v}) - \mathbf{L}\mathbf{u} = \mathbf{u}' + \operatorname{curl}(\mathbf{u} \times \mathbf{v}) + \mathbf{v}\,(\operatorname{div}\mathbf{u}) \tag{4.13}$$

In Maxwell-Minkowski formulation, the effective fields $\mathbf{e}^*$, $\mathbf{h}^*$, $\mathbf{j}^*$, $\mathbf{m}^*$ are related to the primitive fields $\mathbf{e}$, $\mathbf{h}$, $\mathbf{j}$, $\mathbf{m}$ as demonstrated below [34]:

$$\mathbf{e}^* = \mathbf{e} + \mathbf{v} \times \mathbf{b}, \quad \mathbf{h}^* = \mathbf{h} - \mathbf{v} \times \mathbf{d}, \quad \mathbf{j}^* = \mathbf{j} - \sigma\mathbf{v}, \quad \mathbf{m}^* = \mathbf{m} + \mathbf{v} \times \mathbf{p}. \tag{4.14}$$

μ_o, ϵ_o are the permeability and permittivity in free space. The governing equations and coupling terms presented above are insufficient to solve the fully coupled system[19].

[19]In theory there are two ways to solve these set of equations. To solve the macroscopic equations directly with the aid of material constitutive laws or to solve the microscopic fields and deduce the

In order to close the mathematical model, further information on design and material choice of the structure is required. This will help in obtaining the material constitutive equations and boundary conditions that will complete the model. These will be addressed in the later sections after discussing further details of design and operation of load-bearing antenna structures. The nondimensionalization of the fully coupled TEMM theory is now presented.

4.3 Nondimensionalization of Governing Equations

The fully coupled multi-scale, multi-physics TEMM behavior is governed by the equations (4.1) - (4.7). Each TEMM physical quantity described in these equations corresponds to (i) a characteristic scale, which depends on the process and structure design, and (ii) the corresponding nondimensional quantity. For instance, the effective electric field $\mathbf{e}^*$ can be expressed as

$$\mathbf{e}^* = e_0 \, \tilde{\mathbf{e}}^* \tag{4.15}$$

where, e_0 represents the characteristic scale of effective electric field vector, and $\tilde{\mathbf{e}}^*$ represents the corresponding nondimensional quantity. The characteristic scale usually describes the order of magnitude of the physical quantity.

In the governing equations (4.1) - (4.7), a total of 110 scalar terms appear, with each term accounting for a particular physical effect. Some physical effects are dominant over others, and this produces a stratification of terms in every equation. This stratification can be deduced by presenting these equations in a nondimensional form,

macroscopic fields using statistical averaging over volume but such data at the microscopic level is unavailable and very much difficult to obtain.

by writing all the physical quantities involved in their nondimensional form (as demonstrated in (4.15)). The governing equations (4.1) - (4.7) in their nondimensional form are presented.

Electromagnetic Equations

$$\frac{\partial \tilde{b}_i}{\partial \tilde{x}_i} = 0 \tag{4.16}$$

$$A_0\,\epsilon_{ijk}\,\frac{\partial \tilde{e}_k^*}{\partial \tilde{x}_j} = -\frac{\partial \tilde{b}_i}{\partial \tilde{t}} - B_0\,\epsilon_{ijk}\epsilon_{klm}\,\frac{\partial \tilde{b}_l \tilde{v}_m}{\partial \tilde{x}_j} \tag{4.17}$$

$$\frac{\partial \tilde{d}_i}{\partial \tilde{x}_i} = D_0\,\tilde{\sigma} \tag{4.18}$$

$$E_0\,\epsilon_{ijk}\,\frac{\partial \tilde{h}_k^*}{\partial \tilde{x}_j} = \frac{\partial \tilde{d}_i}{\partial \tilde{t}} + B_0\,\epsilon_{ijk}\epsilon_{klm}\,\frac{\partial \tilde{d}_l \tilde{v}_m}{\partial \tilde{x}_j} + F_0\,\tilde{\sigma}\tilde{v}_i + G_0\,\tilde{j}_i \tag{4.19}$$

Thermomechanical Equations

$$\frac{\partial \tilde{\rho}}{\partial \tilde{t}} + S_0\left(\frac{\partial \tilde{\rho}}{\partial \tilde{x}_i}\,\tilde{v}_i + \tilde{\rho}\,\frac{\partial \tilde{v}_i}{\partial \tilde{x}_i}\right) = 0 \tag{4.20}$$

$$P_0\left(\tilde{\rho}\frac{\partial \tilde{v}_i}{\partial \tilde{t}} + \tilde{\rho}\,\frac{\partial \tilde{v}_k}{\partial \tilde{x}_k}\,v_i\right) = \tilde{\rho}\,\tilde{f}_i + Q_0\,\tilde{\rho}\,\tilde{f}_i^e + R_0\,\frac{\partial \tilde{T}_{ij}}{\partial \tilde{x}_j} \tag{4.21}$$

$$\tilde{T}_{ij} - \tilde{T}_{ij} = L_0\,\tilde{\rho}\tilde{L}^e, \tag{4.22}$$

$$\tilde{\rho}\frac{\partial \tilde{\varepsilon}}{\partial \tilde{t}} = I_0\,\tilde{\rho}\,\frac{\partial \tilde{v}_i}{\partial \tilde{x}_j}T_{ij} - K_0\,\frac{\partial \tilde{q}_i}{\partial \tilde{x}_i} + M_0\,\tilde{\rho}\,\tilde{r}^e + N_0\,\tilde{\rho}\,\tilde{r}^{ext} \tag{4.23}$$

All the field vectors and tensors with tilde represent the nondimensional quantities in this formulation. These quantities are presented in Table 4.1. Notations for characteristic scales of all the physical quantities are listed in Appendix A.

With these nondimensional quantities as a starting point, the operating regime and leading-order equations governing the electromagnetic and structural behavior of load-bearing antennas are derived. In the following section, a brief overview of design and working of load-bearing antennas is presented, to obtain the necessary data like constitutive equations and boundary conditions.

Table 4.1: Nondimensional Quantities Involved in Coupled TEMM Problem

Electromagnetic Non-Dimensional Quantities
$A_0 = \frac{e_0^* t_{e0}}{x_0 b_0}, \quad B_0 = \frac{v_0 t_{e0}}{x_o}, \quad D_0 = \frac{\sigma_0 x_0}{d_0}, \quad E_0 = \frac{h_0^* t_{e0}}{x_0 d_0}$ $F_0 = \frac{\sigma_0 t_{e0}}{d_0}, \quad G_0 = \frac{j_0 t_{e0}}{d_0}$
Thermomechanical Non-Dimensional Quantities
$S_0 = \frac{v_0 t_{m0}}{x_0}, \quad P_0 = \frac{v_0}{f_0 t_{m0}}, \quad Q_0 = \frac{f_0{}^e}{f_0}, \quad R_0 = \frac{T_0}{\rho_0 f_0 x_0}, \quad L_0 = \frac{\rho_0 L_0{}^e}{T_0}$ $I_0 = \frac{t_{m0} T_0 v_0}{\rho_0 x_0 \varepsilon_0}, \quad K_0 = \frac{q_0 t_{m0}}{x_0 \rho_0 \varepsilon_0}, \quad M_0 = \frac{r_0 t_{m0}}{\varepsilon_0}, \quad N_0 = \frac{r_0{}^e t_{m0}}{\varepsilon_0}$

4.4 Representative Design of Load-Bearing Antenna Structure

As described earlier, a load-bearing antenna is a multifunctional sensing and actuating device integrated with a load-bearing structure. This technology allows replacement of separate antenna and aircraft structures with one multi-functional structure.

An ideal design for load-bearing antenna, apart from meeting the electrical and mechanical design specifications for its application, should be able to minimize the spurious electromagnetic radiations and structural deflections caused by the external aerodynamic drag. This aerodynamic drag is dominant in smaller vehicles like UAVs, when aircraft antenna is designed with protruding aerials. This drag causes spurious deflections and affects the electrical performance of the antenna. In order to minimize the undesirable drag forces, load-bearing antennas are designed such that the

radiating component (antenna) is embedded in the aircraft structure without adding considerably to its weight [81].

Patch antennas have been widely used in the past due to their various operational advantages like conformability to planar and nonplanar surfaces, simple and inexpensive to manufacture, mechanically robust when mounted on rigid surfaces. The versatility in its design allows adjustment of electrical properties like resonant frequency, polarization, and impedance. Other than the various operational advantages stated above, they are usually fabricated as thin antennas with low weight, which allows easier integration with the mechanical structure to act as a Load-Bearing Antenna Structure [2].

Though features like compactness and conformability make patch antennas a good fit for our purpose, they also suffer from major disadvantages like low efficiency, low power, very narrow frequency bandwidth. Also, they are not designed to withstand the external mechanical and thermal loads. To overcome most of these difficulties, the single layer antenna is stacked with various layers designed to enhance the targeted properties. The designs proposed in You & Hwang consists of a patch antenna stacked with composite facesheets and honeycomb structures to enhance the mechanical properties and antenna gain [81]. These designs can be further improved by using different combination of materials. In this section, mathematical models predicting the comprehensive thermo-mechanical and electromagnetic behavior of load-bearing antennas are derived; these models are further used to optimize the antenna and structural performance.

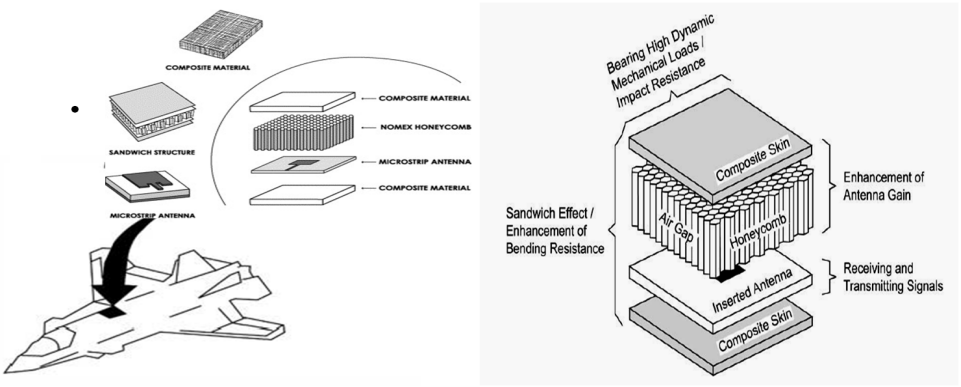

Figure 4.1: Load Bearing Antenna: Design and Working

Fig. 4.1 demonstrates one such design of a load-bearing antenna. The aim of this work is to optimize its performance by studying the coupled electro-magneto-mechanical process this antenna undergoes to perform the required functionalities. The antenna consists of a very thin ($t << \lambda_0$, where λ_0 is the free-space wavelength) metallic patch placed a small fraction of a wavelength ($h << \lambda_0$, usually $0.003\lambda_0 = h = 0.05\lambda_0$) above a ground plane (Fig. 4.2). In case of a rectangular patch, the length L of the element is usually $\lambda_0/3 < L < \lambda_0/2$. The patch and the ground plane are separated by a dielectric sheet, referred to as the substrate, as shown in Fig. 4.2. Dielectric materials with dielectric constants are usually in the range of $2.2 \leq \epsilon_r \leq 12$ can be used for this purpose. The patch is designed such that a large portion of the electromagnetic radiation is directed normal to the patch (broadside radiator). Thin substrates with higher dielectric constants minimize undesired radiation and coupling, and lead to smaller element sizes; however, because of their greater losses, they are less efficient and have relatively smaller bandwidths.

When a patch antenna is fed with a strip line or cable at any frequency, a charge distribution is established on the upper and lower surfaces of the patch, as well as on the surface of the ground plane. The interaction and movement of these charges creates current density on the patch, and consequently the electromagnetic fields under the patch. These fields are radiated through the 4 side walls. A single layer patch antenna usually resembles a dielectric cavity and has been traditionally modeled using these cavity models [47]. Using our perturbation analysis investigate the validity of this model for analysis of the multifunctional load-bearing antenna. In this section, the mathematical model for load-bearing antenna is developed using regime analysis and non dimensional characterization. The antenna designs described here are analyzed under static mechanical load distributions and high frequency electromagnetic fields for both structural and radiation properties.

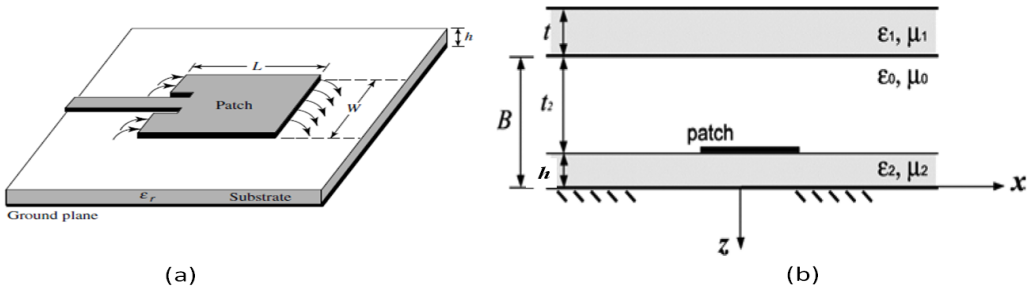

Figure 4.2: Microstrip Patch Antenna

Often times, dielectric materials exhibit low mechanical strengths, which leads to unwanted deflections of the antenna, which are not negligible for aerodynamic loads. In order to minimize these deflections and sustain the mechanical loads, honeycomb

structures can be added at both ends of the antenna. This adds to the mechanical strength of the antenna, without distorting its electromagnetic performance or increasing its weight considerably. In addition to this, very thin geometry of antenna is assumed, i.e., $h << L$. The objective of this work is to optimize this design by formulating an appropriate mathematical model that can predict the coupled TEMM behavior of this antenna. This model is then used to predict the radiation properties and transverse deflections of the antenna for four different substrate materials.

4.5 Formulation of Mathematical Model for Load-Bearing Antenna Structures

This section will focus on formulation of mathematical models to predict the behavior of load-bearing antennas using *nondimensional characterization* and *regime analysis*. It is recalled that a load-bearing antenna structure is subjected to mechanical forces, temperature gradients, and electromagnetic fields. Depending on the process and external conditions, some of these physical effects are dominant over others and these effects determine the leading-order theory/model. A fixed relative ordering among all competing effects describes the operating regime of the antenna; each regime is specified by positing all the nondimensional parameters (refer to Table 4.1) that arise in the nondimesionalized 3-D equations as some integer power of a fixed small number that characterizes the process. Utilizing the fact that patch antennas usually possess thin geometries, the small parameter assigned to this problem is its thickness ratio $\varepsilon = z_0/x_0$.

4.5.1 Characteristic Scales and The Operating Regime

In order to deduce the operating regime of the antenna, the characteristic scales need to be assigned to the physical parameters involved. The assumptions and restrictions on the process and design of the antenna are briefly discussed and the characteristic scales are assigned using this information. These characteristic scales will be subsequently used to derive the operating regime of load-bearing antenna structure. The antenna is excited with incident electric field with amplitude $10^6 V/m$ at a frequency of 200 GHz through the feedline, as a result of which current distributions are formed on the metallic patch.

The antenna structure is assumed to be subjected to static mechanical loads of the order of $10^2\, m/s^2$, consistent with aerodynamic loading under cruise mode. Also, it is assumed that the antenna installed on a moving vehicle, and can have a maximum speed of the order of $10^2\, m/s$.

The characteristic transverse length scales x_0 and y_0 are assigned to be the length and width of the patch, and z_0 as the thickness of the antenna. Thus using these assumptions and numbers from [47], [81, 82], the characteristic scales for length, velocity, force and electric field are assigned as:

$$x_0 = y_0 = 10^{-2} m; \quad z_0 = 10^{-3} m = x_0 \varepsilon; \quad v_0 = 10^2 m/s;$$

$$f_0 = 100 m/s^2; \quad e_0 = 10^6 V/m. \tag{4.24}$$

As observed from equation (4.24), the thickness ratio ϵ is of the order of 0.1.

Electromagnetic and mechanical time scales: The multi-scale coupled behavior of load-bearing antenna requires that the time scales are different for electromagnetic

and mechanical problems, since EM fields vary at much faster rates than mechanical fields. Time scales for electromagnetic and mechanical problems, t_{e0} and t_{m0} respectively, can be determined as follows

$$t_{e0} = \frac{1}{\omega_o} = 10^{-10}s; \qquad t_{m0} = \frac{x_0}{v_0} = 10^{-4}s \tag{4.25}$$

Other values of electromagnetic quantities are determined using the following characteristic scales

$$d_0 = \epsilon_o e_o = 10^{-5}A/m^2; \quad h_0 = \frac{e_0}{\omega_0 \mu_0 x_0} = 10^5 A/m; \quad b_0 = \mu_0 h_0 = 10^{-1}T$$
$$f_0 = 100m/s^2; \quad T_0 = \frac{f_0}{x_0 y_0} = 10^6 Pa \tag{4.26}$$

Also, density $\rho_0 = 10^3 kg/m^3$.

Thus with the characteristic scales assigned, the magnitudes of nondimensional numbers highlighted in Table 4.1 are now derived. The nondimensional numbers corresponding to the process can now be calculated and written as a power of thickness ratio ϵ.

Constitutive assumptions: For our present model linear constitutive relations for TEMM variables are considered. where, the strain field $\mathbf{S}$ is related to displacement

Electromagnetic	Mechanical
$\mathbf{d} = \epsilon \mathbf{e}^*, \quad \mathbf{b} = \mu \mathbf{h}^*, \quad \mathbf{j}^* = \sigma \mathbf{e}^*.$	$\mathbf{T} = \mathbf{C} \cdot \mathbf{S}.$

vector $\mathbf{u}$ as $\mathbf{S} = \frac{1}{2}(\nabla \mathbf{u} + (\nabla \mathbf{u})^T)$

For the choice of characteristic scales and constitutive assumptions presented above, magnitudes of nondimensional parameters are calculated and presented in

powers of thickness ratio ε in order to accomplish a complete ordering of all the terms in these equations.

$$A_0 = \tilde{A}_0\varepsilon^0,\ B_0 = \tilde{B}_0\varepsilon^3,\ E_0 = \tilde{E}_0\varepsilon^{-1},\ Q_0 = \tilde{Q}_0\varepsilon^2,\ R_0 = \tilde{R}_0\varepsilon^0,\ L_0 = \tilde{L}_0\varepsilon^3 \qquad (4.27)$$

where, $\varepsilon < \tilde{A}_0, \tilde{B}_0, \tilde{E}_0, \tilde{Q}_0, \tilde{R}_0, \tilde{L}_0 < \varepsilon^{-1}$

All the other nondimensional numbers in Table 4.1 are ignored for this system. For a given particular design, the regime is defined by equation (4.27). The mathematical model corresponding to this regime can now be derived with this knowledge.

4.5.2 Leading-Order Equations Governing Electromagnetic and Structural Behavior of Load-Bearing Antennas

In this section, derivation of the leading-order theory corresponding to the regime described in equation (4.27) is demonstrated. Using the nodimensionalized governing equations (4.1) - (4.7) as the starting point, along with constitutive equations and boundary conditions, regime analysis is used to deduce the most dominant physics of the problem.

Time harmonic electromagnetic fields are assumed

$$\mathbf{e}^*(x,y,z,t) = e_0\,\mathbf{e}(x,y,z)\,e^{j\omega t}; \qquad \mathbf{h}^*(x,y,z,t) = h_0\,\mathbf{h}(x,y,z)\,e^{j\omega t} \qquad (4.28)$$

and static mechanical fields.

The antenna is excited with incident electric field or potential difference along the thickness. The metallic patch and the ground plane are assumed to be perfect electric conductors, i.e., tangential component of electric field (x and y components) is assumed to be zero on both these surfaces. Thus, for small thickness ratios i.e., $z_0 << x_0, y_0$ it is assumed that the components of electric field along the x and y

directions are ignorable compared to the z-component. Thus the leading order value of electric field is contributed from its z-component; x, y components being of higher order, in particular,

$$\mathbf{e}(x,y,z) = e_0 \left(\varepsilon^2 \, \tilde{e}_x(x,y,z) \, \hat{\mathbf{i}} + \varepsilon^2 \, \tilde{e}_y(x,y,z) \, \hat{\mathbf{j}} + \tilde{e}_z(x,y,z) \, \hat{\mathbf{k}} \right) \tag{4.29}$$

For mechanical fields, simply supported boundary conditions are imposed on all the four corners, and a constant force distribution is assumed on the antenna-honeycomb structure (along -ve z-axis). Thus for the displacement field, it is posited that the deformation along z is dominant compared to the x, y components[20] i.e.,

$$\mathbf{u}(x,y,z) = u_0 \left(\varepsilon \, \tilde{u}_x(x,y,z) \, \hat{\mathbf{i}} + \varepsilon \, \tilde{u}_y(x,y,z) \, \hat{\mathbf{j}} + \tilde{u}_z(x,y,z) \, \hat{\mathbf{k}} \right) \tag{4.30}$$

For small values of ε, the following expansions are assumed for all the unknowns in the problem [55, 5]:

$$e_z = e_0 \sum_{n \geq 0}^{\infty} \varepsilon^n \, \tilde{e}_z^{(n)}, \quad e_x = e_0 \, \varepsilon^2 \sum_{n \geq 0}^{\infty} \varepsilon^n \, \tilde{e}_x^{(n)}, \quad e_y = e_0 \, \varepsilon^2 \sum_{n \geq 0}^{\infty} \varepsilon^n \, \tilde{e}_y^{(n)} \tag{4.31}$$

$$u_z = u_0 \sum_{n \geq 0}^{\infty} \varepsilon^n \, \tilde{u}_z^{(n)}, \quad u_x = u_0 \, \varepsilon \sum_{n \geq 0}^{\infty} \varepsilon^n \, \tilde{u}_x^{(n)}, \quad u_y = u_0 \, \varepsilon \sum_{n \geq 0}^{\infty} \varepsilon^n \, \tilde{u}_y^{(n)}. \tag{4.32}$$

For electric flux density $\mathbf{d}$, stress field $\mathbf{T}$, the constitutive relations described in Appendix are used to posit the expansion for these quantities.

$$\mathbf{d}(x,y,z) = \epsilon \, \mathbf{e} = \epsilon \, e_0 \sum_{n \geq 0}^{\infty} \varepsilon^n \left[\, \tilde{e}_x^{(n-2)}(x,y,z) \, \hat{\mathbf{i}} + \tilde{e}_y^{(n-2)}(x,y,z) \, \hat{\mathbf{j}} + \tilde{e}_z^{(n)}(x,y,z) \, \hat{\mathbf{k}} \, \right] \tag{4.33}$$

These expressions are now substituted in the governing equations and the procedure to derive the leading order expressions corresponding to one of the equations

[20]For fields where a relative ordering of components cannot be determined, all components are assumed to be leading order. Substituting these expansions in the governing equations provides more information.

(Faraday's Law) is demonstrated. Similar procedure is applied to all the governing equations to deduce the complete leading order problem.

Expanding this equation into x,y and z components and substituting the expansions presented in equations (4.31) and (4.33).

The tildes are dropped by noting the fact that all the quantities presented below are nondimensional. The x-component of Faraday's law upto second order terms i.e., ε^2 terms

$$\left(A_0 \frac{\partial e_z^{(0)}}{\partial y} + \frac{\partial h_x^{(0)}}{\partial t} \right) + \varepsilon \left(A_0 \frac{\partial e_z^{(1)}}{\partial y} - A_0 e_y^{(0)} + \frac{\partial h_x^{(1)}}{\partial t} \right)$$
$$+ \varepsilon^2 \left(A_0 \frac{\partial e_z^{(2)}}{\partial y} - 2A_0 e_y^{(1)} + \frac{\partial h_x^{(2)}}{\partial t} \right) + \text{higher order terms} = 0 \tag{4.34}$$

The leading order terms, i.e., coefficients of ε^0, are assumed to correspond to the most dominant physical effects. Thus as an initial approximation we solve this system by ignoring all the higher order effects. The solution can be improved by incorporating higher order terms. The leading order approximation corresponding to this equation is

$$A_0 \frac{\partial e_z^{(0)}}{\partial y} + \frac{\partial h_x^{(0)}}{\partial t} = 0 \tag{4.35}$$

This procedure is repeated for all the equations and boundary conditions to deduce the leading order system. The equations that arise from these approximations gives rise to a 2-D system where the leading order coefficients are independent of z. The complete leading order equations for the electro-magneto-mechanical system are listed

below.

$$\frac{\partial h_x^{(0)}}{\partial x} + \frac{\partial h_y^{(0)}}{\partial y} = 0, \qquad -A_0 \frac{\partial e_z^{(0)}}{\partial x} + j\omega h_y^{(0)} = 0, \qquad A_0 \frac{\partial e_z^{(0)}}{\partial y} + j\omega h_x^{(0)} = 0, \quad (4.36)$$

$$\frac{\partial e_z^{(0)}}{\partial z} = 0, \qquad E_0 \left(\frac{\partial h_y^{(0)}}{\partial x} - \frac{\partial h_x^{(0)}}{\partial y} \right) = \frac{\partial d_z^{(0)}}{\partial t}, \quad (4.37)$$

$$D_{11} \frac{\partial^4 u_z^{(0)}}{\partial x^4} + 2D_{12} \frac{\partial^4 u_z^{(0)}}{\partial y^2 \partial x^2} + D_{22} \frac{\partial^4 u_z^{(0)}}{\partial y^4} + \rho f_z^{ext} = 0. \quad (4.38)$$

The leading order equations governing a single layer dielectric sheet under electro-magneto-mechanical loads reduce to the cavity model for electromagnetic analysis [47] and the classical plate theory for structural analysis [66], validating the theoretical model for the load-bearing antenna structure. Solving these equations provides a good initial estimate for the response of such a system and can allow for parametric studies in improving the existing designs. In the following section, an analytical solution for this basic model is presented and is used to study the electro-magnetic and structural properties of the antenna.

4.6 Results and Discussions

The leading order system of equations deduced in equations (4.36) - (4.38) can be further reduced to 2 sets of uncoupled mechanical and electromagnetic problems. Both these systems are presented and their analytical solutions. The technique to extend this analysis to a multilayer structure is then demonstrated.

Structural Analysis

The mathematical model for this problem is

$$D_{11} \frac{\partial^4 w}{\partial x^4} + 2D_{12} \frac{\partial^4 w}{\partial y^2 \partial x^2} + D_{22} \frac{\partial^4 w}{\partial y^4} + \rho f_z^{ext} = \frac{\partial^2 w}{\partial t^2} \quad (4.39)$$

$$w = 0 \text{ for } x = 0, a \text{ and } y = 0, b$$

where D_{ij} represents flexular rigidity of the material and depends on Young's modulus and Poisson's ratios

This theory, as expected, reduces to classical plate theory and it can be extended to a multilayer composite structure by calculating the effective material constants for this structure. Flexular rigidity constant for the composite structure can be derived using standard laminate theory [66].

$$D_{ij} = \frac{1}{3}\sum_{k=1}^{N} Q_{ij}^{(k)}(z_{k+1}^3 - z_k^3), \tag{4.40}$$

where,

$$\begin{aligned} &Q_{11}^{(k)} = \frac{E_1^{(k)}}{1-\nu_{12}^{(k)}\nu_{21}^{(k)}}, \;\; Q_{12}^{(k)} = \frac{\nu_{21}^{(k)}E_1^{(k)}}{1-\nu_{12}^{(k)}\nu_{21}^{(k)}}, \;\; Q_{22}^{(k)} = \frac{E_2^{(k)}}{1-\nu_{12}^{(k)}\nu_{21}^{(k)}}, \\ &Q_{16}^{(k)} = Q_{26}^{(k)} = 0, \;\; Q_{66}^{(k)} = G_{12}^{(k)}, \;\; Q_{44}^{(k)} = G_{23}^{(k)}, \;\; Q_{55}^{(k)} = G_{13}^{(k)} \end{aligned} \tag{4.41}$$

This system can be solved for plate deformations under static loading (i.e., the term on RHS of equation (4.39) is zero), and simply supported boundary condition on all the four corners. The analytical solution is

$$u_z(x,y) = \sum_{m=1}^{\infty}\sum_{n=1}^{\infty} \frac{16(f_z^{ext})}{\pi^2 mn} sin(\frac{m\pi x}{a})\, sin(\frac{n\pi y}{b}) \tag{4.42}$$

The center displacements are plotted for different choices of substrate and superstrate materials as a function of the plate aspect ratio. All the displacements plotted in Fig. 4.3 are nondimensionalized as $\bar{w} = w_0(0,0)\left(\frac{E_2 h^3}{a^4 f_0}\right)$

The plots demonstrate alumina has much superior structural properties compared to other dielectrics.

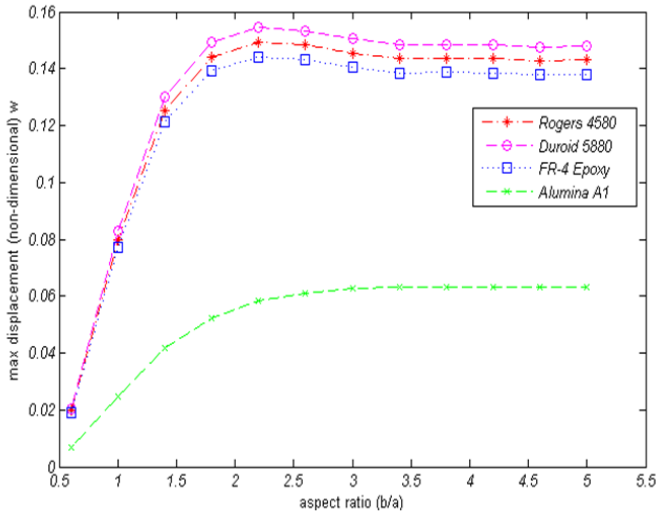

Figure 4.3: A Plot of Load-Bearing Antenna Center Displacement vs Plate Aspect Ratio for 4 different Substrate Material Choices

Electromagnetic Analysis

The complete mathematical model for electromagnetic analysis reduces to

$$\frac{\partial^2 e_z}{\partial z^2} + k_{mn}^2 e_z = J_z, \tag{4.43}$$

$$\frac{\partial e_z}{\partial x} = 0 \text{ on } y = 0, W \quad \text{and} \quad \frac{\partial e_z}{\partial y} = 0 \text{ on } x = 0, L. \tag{4.44}$$

where, $k_{mn} = \left(\frac{m\pi}{L}\right)^2 + \left(\frac{n\pi}{W}\right)^2$.

Analytical solution for this antenna is given by the expansion:

$$e_z = j\omega\mu \sum_{m,n} \frac{1}{k^2 - k_{mn}^2} \frac{< J, \nu_{mn} >}{< \nu_{mn}, \nu_{mn} >} \nu_{mn} \tag{4.45}$$

where the inner product is defined as $< a, b >= \int abdv$, k_{mn} are the eigenvalues and ν_{mn} are the corresponding eigenfunctions.

This theory reduces to the cavity model for single layer patch antenna [47] which validates our framework. By using this perturbation framework, a well known approximate theory for patch antenna was been deduced.

Using Eq. (4.45) fields inside the cavity are solved. To determine the radiated electromagnetic fields Huygen's equivalence principle is used [2]. The sources for this antenna are now defined with an equivalent system with magnetic currents source on the magnetic current wall C (sum of edges of the patch) as:

$$\mathbf{K} = 2\hat{\mathbf{n}} \times E_z \, \hat{\mathbf{e}}_z \tag{4.46}$$

where, $\hat{\mathbf{n}}$ represents normal to the surface C.

From this point onwards the standard antenna design literature based on cavity model is used to solve for the radiation fields. The electric field describing the radiation pattern for perpendicular polarization of incident electric field (TE incidence) [1]:

$$E_\phi = \frac{2jV_0 e^{-jk_0 r}}{\pi r} \, sin\phi \, \frac{sinY}{Y} \, \frac{sinZ}{Z} \, N(\theta) \tag{4.47}$$

where, $Y = 0.5\, k_0 W \, sin\theta \, sin\phi$ and $Z = 0.5\, k_0 h \, cos\theta$

Also, h is the thickness of the dielectric, r is the radial distance of observation point from the origin placed on antenna structure, $V_0 = hK_0$ and ϕ, θ are the polar coordinates. Unlike structural analysis, radiation analysis of the multilayer composite structure is not a straightforward extension of the single layer antenna. The radiation pattern of the antenna is modified by the presence of composite layers (non-actuated). In Equation (4.47) the function $N(\theta)$ represents current at $z = h/2$ at the mid-point of the radiation slot at $x = 0$. To calculate the radiation fields for the multilayer system this function is calculated using the formulation presented in [1]. Assuming

plane wave propagation for layers above the antenna, the effective electric fields and the electromagnetic gain resulting from this system are calculated. The following boundary conditions are solved:

$$V_i(z) = V_i^+ \, e^{-j\beta_i z} + V_i^- \, e^{j\beta_i z}, \tag{4.48}$$

$$I_i(z) = \frac{1}{Z_{C_i}} \left(V_i^+ \, e^{-j\beta_i z} - V_i^- \, e^{j\beta_i z} \right) \tag{4.49}$$

where, β_i and Z_{C_i} are medium propagation constants and are dependent on the medium constants permittivity, permeability, and the nature of polarization (parallel or perpendicular) [2]. Also, $V_1^+ = -V_1^-$, i.e., zero voltage on ground plane $z = 0$, and $V_4^+/Z_{C_4} = cos\theta$ or $= 1$ depending on perpendicular (TE) or parallel (TM) polarization. The corresponding electromagnetic gain is calculated using the formula:

$$\text{Gain}(\phi, \theta) = \frac{4\pi I}{\int_0^{2\pi} \int_0^{\pi/2} I sin(\theta) \, d\theta \, d\phi}, \tag{4.50}$$

$$\text{where } \; I = cos^2(X) \frac{sin^2(Y)}{Y^2} \left(sin^2(\phi) |N(\theta)|^2 + cos^2(\phi) |Q(\theta)|^2 \right) \tag{4.51}$$

where $N(\theta)$ and $Q(\theta)$ are currents at $z = h/2$ for TE and TM wave incidence respectively. These quantities are calculated and plotted for 4 different substrate materials as shown in Fig. 4.4.

4.7 Two Dimensional Plate Theory for Coupled Electro - Magneto-Mechanical Behavior

In this section, a 2-D model for novel multifunctional materials is developed with coupled electromagnetic and thermomechanical capabilities. The models developed in earlier sections are extended to formulate the theory for coupled electro-magneto-mechanical behavior and the corresponding finite element formulation is developed.

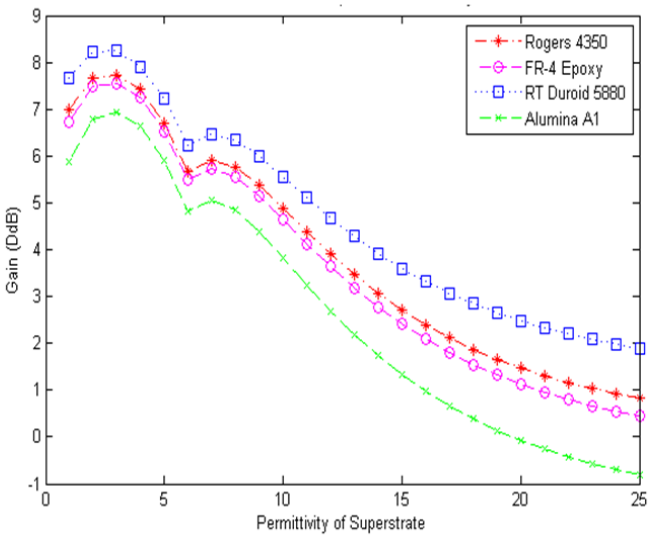

Figure 4.4: A Plot of Load-Bearing Antenna Gain vs Superstrate Permittivity for 4 different Substrate Material Choices

This framework is intended to be applicable to design and optimization of multifunctional structures.

Finite element analysis has been used widely to model smart materials in various multifunctional devices. Most of these models assume static electromagnetic fields, and the variational principle or the weak form is formulated in terms of scalar electric and magnetic potentials. Dynamic fields have been solved for the special cases of magneto-mechanical materials (Magnetostrictive materials like Terfenol-D, Galfenol, ferromagnetic materials, piezomagnetic), electro-mechanical materials (electrostrictive materials, piezoelectric) where only one of the electric or magnetic fields is dominant. Particularly, the modeling of smart materials ignores the dynamic nature of

electromagnetic fields. This assumption, although valid for smart material based actuators, may not be able to predict the behavior of high frequency electromagnetic fields that are created by radiating systems like antennas. This work aims at modeling the behavior of coupled electro-magneto-mechanical functionality of load-bearing antennas using smart structures to predict improved designs. More specifically, the behavior of a single layer antenna is studied to optimize the material behavior for substrate.

4.7.1 Assumptions on Governing Equations

Using the results of regime analysis presented in earlier sections, the following restrictions are placed on the governing equations

1. Lorentz body forces negligible compared to aerodynamic forces.
2. Coupling of electromagnetic and mechanical fields through constitutive equations.
3. Linear constitutive behavior with coupled electro-magneto-mechanical functionalities.
4. Thermal effects are ignored.

For coupled electro-magneto-mechanical constitutive behavior, that the assumption that electromagnetic and mechanical fields vary at different frequencies may not valid. Infact, the electromagnetic fields generated by the antenna act as an input to the mechanical structure, which reduced to a forced vibration model.

Assumptions on the Antenna Structure

1. Thin geometry: Thickness much smaller than the other 2 dimensions. Thin geometry is utilized to reduce the equations to a 2-D formulation by assuming an expansion in z.

2. Electromagnetic and mechanical fields in the substrate (bounded by metallic patch and ground plane) are simulated.

3. Electric walls B.C. on the metallic surfaces and magnetic walls B.C. on the boundary of the patch are assumed.

4.8 The 3-Dimensional Model for Load-Bearing Antenna Structure

Considering all the assumptions specified above, the mathematical model can be presented as follows:

Governing Equations

The behavior of load-bearing antenna structure presented in this work is given by Maxwell's equations and linear momentum equations coupled by linear electro-magneto-mechanical constitutive law, i.e.,

$$\textit{Electromagnetic}: \nabla \times \mathbf{h} \;=\; \frac{\partial \mathbf{d}}{\partial t} + \mathbf{j}, \quad \nabla \times \mathbf{e} \;=\; -\frac{\partial \mathbf{b}}{\partial t} \tag{4.52}$$

$$\textit{Mechanical}: \nabla \cdot \mathbf{T} + \mathbf{f}_e \;=\; \frac{\partial^2 \mathbf{u}}{\partial t^2} \tag{4.53}$$

Time harmonic electromagnetic fields is assumed i.e.,

$$\mathbf{e}^*(x,y,z,t) = \mathbf{e}(x,y,z)\, e^{j\omega t}; \qquad \mathbf{h}^*(x,y,z,t) = \mathbf{h}(x,y,z)\, e^{j\omega t} \tag{4.54}$$

Constitutive Equations

In order to close the mathematical model, the electrical, magnetic and mechanical variables are assumed to be related through coupled linear constitutive relations, i.e.,

$$T_{ij} = C_{ijkl}S_{kl} - q^m_{kij}h^*_k - q^e_{kij}e^*_k \tag{4.55}$$

$$d_i = q^e_{ikl}S_{kl} + \epsilon_{ik}e^*_k + \beta_{ik}h^*_k \tag{4.56}$$

$$b_i = q^m_{ikl}S_{kl} + \beta_{ik}e^*_k + \mu_{ik}h^*_k \tag{4.57}$$

where, the strain field $\mathbf{S}$ is related to displacement vector $\mathbf{u}$ as:

$$S_{ij} = \frac{1}{2}(u_{i,j} + u_{j,i}) \tag{4.58}$$

4.8.1 Boundary Conditions

The antenna is excited with incident electric field along the thickness (or potential difference across the thickness). Again, simply supported boundary conditions are assumed on all four edges of the plate. Since metallic patch and ground plane are conducting surface, electric walls boundary condition is assumed on these surfaces ($\mathbf{e} \times \mathbf{n} = 0$). The governing equations describing the coupled behavior of this load-bearing antenna are given by equations (4.1) - (4.7), along with constitutive relations and boundary conditions for mechanical fields and electromagnetic fields, to close the set of equations.

4.9 Variational Principle: The Weak Form of Governing Equations

Before deriving the weak form of the governing equations, the constitutive laws are substituted in the governing laws. The terms $\mathbf{T}$, $\mathbf{d}$ and $\mathbf{b}$ are eliminated using

Eqs. (4.55) - (4.57). This reduces the total number of unknowns to 3 vector fields **e**, **h** and **u**. The number of equations to be solved are also reduced to 3 vector equations, thus closing the mathematical model.

$$\nabla \times \mathbf{h} \;=\; \bar{\beta} \cdot \frac{\partial \mathbf{h}}{\partial t} \;+\; \bar{\epsilon} \cdot \frac{\partial \mathbf{e}}{\partial t} \;+\; \frac{1}{2}\, \bar{q}^{e} \cdot \left(\frac{\partial \nabla \mathbf{u}}{\partial t} \;+\; \frac{\partial \nabla \mathbf{u}^{T}}{\partial t} \right) \;+\; \mathbf{j} \tag{4.59}$$

$$\nabla \times \mathbf{e} \;=\; -\bar{\beta} \cdot \frac{\partial \mathbf{e}}{\partial t} \;-\; \bar{\mu} \cdot \frac{\partial \mathbf{h}}{\partial t} \;-\; \frac{1}{2}\, \bar{q}^{m} \cdot \left(\frac{\partial \nabla \mathbf{u}}{\partial t} \;+\; \frac{\partial \nabla \mathbf{u}^{T}}{\partial t} \right) \tag{4.60}$$

$$\nabla \cdot \left(\frac{1}{2}\, \bar{C} \cdot (\nabla \mathbf{u} + \nabla \mathbf{u}^{T}) \;+\; \bar{q}^{e} \cdot \mathbf{e} \;+\; \bar{q}^{m} \cdot \mathbf{h} \right) + \mathbf{f} \;+\; \mathbf{f}_{e} \;=\; \frac{\partial^{2} \mathbf{u}}{\partial t^{2}} \tag{4.61}$$

The time scales of electromagnetic fields and mechanical fields vary largely in an antenna structure. The electromagnetic fields vary at a MHz - GHz frequencies whereas the mechanical fields vary at considerably lower frequencies. It can be shown through nondimensional analysis that the displacement terms in Maxwell's equations and the electromagnetic body forces in the linear momentum equation are negligible.

Thus the system reduces to an uncoupled set of electromagnetic equations, which can be solved first and used as an input to the momentum equation to solve for displacement fields. Two variational statements corresponding to electromagnetic and mechanical analysis are presented.

The weak form for the electromagnetic system is now presented (derived from method of weighted residuals [37])

$$F(\mathbf{e}, \mathbf{w}) = \int_{V_{em}} \left[\left(\nabla \times \mathbf{w} \;+\; j\omega\, \bar{\beta} \cdot \mathbf{w} \right) \cdot \left(\nabla \times \mathbf{e} \;+\; j\omega\, \bar{\beta} \cdot \mathbf{e} \right) \;+\; \omega^{2}\, (\bar{\mu} \cdot \bar{\epsilon}) \cdot \mathbf{w} \cdot \mathbf{e} \right] dV$$

$$+ \int_{V_{em}} j\omega\, \bar{\mu} \cdot \mathbf{w} \cdot \mathbf{j}\; dV \;+\; \int_{S_{em}} \bar{\mu} \cdot (\hat{\mathbf{n}} \times \mathbf{w})^{*} \cdot \left[\bar{\mu}^{-1} \cdot \left(\nabla \times \mathbf{e} \;+\; j\omega\, \bar{\beta} \cdot \mathbf{e} \right) \right] dS \tag{4.62}$$

Similarly, the weak form governing the structural behavior is represented as:

$$F_{u}(\mathbf{u}, \mathbf{u}^{a}) = \int_{V_{u}} \left[\mathbf{T} \cdot \nabla \mathbf{u}^{a} + \rho\, \frac{\partial^{2} \mathbf{u}}{\partial t^{2}} \cdot \mathbf{u}^{a} - \mathbf{f}^{eff} \cdot \mathbf{u}^{a} \right] dV \;-\; \int_{S_{u}} (\mathbf{T} \cdot \mathbf{n}) \cdot \mathbf{u}^{a} dS \tag{4.63}$$

For the boundary conditions specified for this problem the boundary integrals over S_{em} and S_u vanish and the complete problem is characterized by the volume integral only.

4.9.1 Two Dimensional Theory: Perturbation Ansatz

Owing to the thin geometry of the antenna (i.e., $z_0 << x_0, y_0$), the following expansions are assumed for electric field $\mathbf{e}$, displacement field $\mathbf{u}$ and their corresponding adjoint fields:

$$\mathbf{e}(x,y,z) = \sum_{n=0}^{n=\infty} z^n \, \mathbf{e}^{(n)}(x,y), \quad \mathbf{e}^a(x,y,z) = \sum_{n=0}^{n=\infty} z^n \, \mathbf{w}^{(n)}(x,y) \tag{4.64}$$

$$\mathbf{u}(x,y,z) = \sum_{n=0}^{n=\infty} z^n \, \mathbf{u}^{(n)}(x,y), \quad \mathbf{u}^a(x,y,z) = \sum_{n=0}^{n=\infty} z^n \, \mathbf{u}^{a(n)}(x,y) \tag{4.65}$$

The series expansions (4.64)-(4.65) are substituted in the weak forms (4.62)-(4.63) to derive the 2-D variational principle. The final form of the 2-D equation reduces to

$$\begin{aligned}
&\int_{V_{em}} \left[\left(\nabla \times \mathbf{w} + j\omega \, \bar{\beta} \cdot \mathbf{w} \right) \cdot \left(\nabla \times \mathbf{e} + j\omega \, \bar{\beta} \cdot \mathbf{e} \right) + \omega^2 \, (\bar{\mu} \cdot \bar{\epsilon}) \cdot \mathbf{w} \cdot \mathbf{e} + j\omega \, \bar{\mu} \cdot \mathbf{w} \cdot \mathbf{j} \right] dV \\
&= \int_{V_{em}} \sum_{n,m} z^{n+m} \left[\{ \frac{\partial e_z^{(n)}}{\partial y} - \frac{n+1}{b} \, e_y^{(n+1)} + j\omega(\beta_{11} e_x^{(n)} + \beta_{12} e_y^{(n)} + \beta_{13} e_z^{(n)}) \} \cdot \{ \frac{\partial w_z^{(m)}}{\partial y} \right. \\
&\quad - \frac{m+1}{b} \, w_y^{(m+1)} + j\omega(\beta_{11} w_x^{(m)} + \beta_{12} w_y^{(m)} + \beta_{13} w_z^{(m)}) \} \; + \; \{ \frac{n+1}{b} \, e_x^{(n+1)} - \frac{\partial e_z^{(n)}}{\partial x} \\
&\quad + j\omega(\beta_{21} e_x^{(n)} + \beta_{22} e_y^{(n)} + \beta_{23} e_z^{(n)}) \} \cdot \{ \frac{n+1}{b} \, w_x^{(m+1)} - \frac{\partial w_z^{(m)}}{\partial x} + j\omega(\beta_{21} w_x^{(m)} + \beta_{22} w_y^{(m)} \\
&\quad + \beta_{23} w_z^{(m)}) \} \; + \; \{ \frac{\partial e_y^{(n)}}{\partial x} - \frac{\partial e_x^{(n)}}{\partial y} + j\omega(\beta_{31} e_x^{(n)} + \beta_{32} e_y^{(n)} + \beta_{33} e_z^{(n)}) \} \cdot \{ \frac{\partial w_y^{(m)}}{\partial x} - \frac{\partial w_x^{(m)}}{\partial y} \\
&\quad \left. + \; j\omega(\beta_{31} w_x^{(m)} + \beta_{32} w_y^{(m)} + \beta_{33} w_z^{(m)}) \} \right] dx \, dy \, dz
\end{aligned} \tag{4.66}$$

Interchanging the order of summation and integral and integrating the above expression with respect to z, the dependence on z can be eliminated from the variational

principle. Since the coefficients of z^{n+m} are independent of z, it can be shown the electromagnetic variational functional (4.66), reduces to the form

$$F_{em}(\mathbf{e},\mathbf{w}) = \sum_{n,m} B_{mn} \int_{x,y} f_{nm}(x,y)\, dx\, dy \tag{4.67}$$

where $f_{nm}(x,y)$ is the coefficient of z^{n+m} within the integral in equation (4.62). The variational form governing the mechanical behavior of the plate can be evaluated similarly,

$$\int_{V_u} \sum_{n} \left(T_{ij}^{(n)} \; - \; n\, T_{ij}^{(n-1)} \; + \; B_n\, T_j^{(n)} + \rho\omega^2 \sum_{m} B_{nm} \ddot{u}_j^{(m)} - \; f^{ext} \right) \delta u_j^{(n)} dx\, dy \tag{4.68}$$

where,

$$\begin{aligned} T_{ij}^{(n)} = \int_{-h/2}^{h/2} z^n\, T_{ij}\, dz \; &= \; \int_{-h/2}^{h/2} z^n \; \left(C_{ijkl}\, S_{kl} \; - \; q_{kij}^{m} h_k \; - \; q_{kij}^{e} e_k \right) \, dz \\ &= \int_{-h/2}^{h/2} z^{n+m} \sum_{m} \left(C_{ijkl}\, S_{kl}^{(0)} \; - \; q_{kij}^{m} h_k^{(0)} \; - \; q_{kij}^{e} e_k^{(0)} \right) \, dz \\ &= \sum_{m} B_{mn} \left(C_{ijkl}\, S_{kl}^{(0)} \; - \; q_{kij}^{m} h_k^{(0)} \; - \; q_{kij}^{e} e_k^{(0)} \right) \end{aligned} \tag{4.69}$$

and

$$\begin{aligned} B_{mn} &= \frac{2\, b^{n+m+1}}{n+m+1} \qquad \text{for } n+m \text{ even} \\ &= 0 \qquad \text{otherwise} \end{aligned}$$

4.10 Finite Element Analysis of the 2-D Piezoelectric\magnetic Laminate

As an initial estimate this system is solved for zero order $(n+m=0)$ electromagnetic system and first order mechanical plate theory; this system is solved for

vibration analysis of the system assuming a harmonic time dependence.

$$u(x,y,z,t) = u_0(x,y,t) \; + \; z\phi_x(x,y,t) \tag{4.70}$$

$$v(x,y,z,t) = v_0(x,y,t) \; + \; z\phi_y(x,y,t) \tag{4.71}$$

$$w(x,y,z,t) = w_0(x,y,t) \tag{4.72}$$

$$e_z(x,y,z,t) = e_0(x,y)\, e^{j\omega t} \tag{4.73}$$

Dropping the superscripts and generating a 2-D mesh with linear rectangular elements within the boundaries of the patch for electromagnetic system and boundaries of the plate for the mechanical system. The electric and mechanical fields within each element are approximated as linear interpolations of nodal values, i.e.,

$$e_0(x,y) = \sum_{i=1}^{4} N_i^e(x,y)\, e_{0i}^e(t), \qquad w_0(x,y,t) = \sum_{i=1}^{4} N_i^e(x,y)\, w_{0i}^e(t) \tag{4.74}$$

$$u_0(x,y) = \sum_{i=1}^{4} N_i^e(x,y)\, u_{0i}^e(t), \qquad v_0(x,y) = \sum_{i=1}^{4} N_i^e(x,y)\, v_{0i}^e(t) \tag{4.75}$$

$$\phi_x(x,y) = \sum_{i=1}^{4} N_i^e(x,y)\, \phi_{x_i}^e(t), \qquad \phi_y(x,y) = \sum_{i=1}^{4} N_i^e(x,y)\, \phi_{y_i}^e(t) \tag{4.76}$$

Different shape functions can be used for the interpolation functions, but in our present formulation Lagrange interpolation functions are used for all of the 6 unknowns. These interpolation functions are expressed in terms of the element coordinates (ζ, η), called the natural coordinates.

$$\begin{bmatrix} N_1^e \\ N_2^e \\ N_3^e \\ N_4^e \end{bmatrix} = \frac{1}{4} \begin{bmatrix} (1-\zeta)(1-\eta) \\ (1+\zeta)(1-\eta) \\ (1+\zeta)(1+\eta) \\ (1-\zeta)(1+\eta) \end{bmatrix}$$

The derivatives can be related using the Jacobian $[J]$ given by

$$\begin{bmatrix} \dfrac{\partial N_i^e}{\partial x} \\ \dfrac{\partial N_i^e}{\partial y} \end{bmatrix} = [J]^{-1} \begin{bmatrix} \dfrac{\partial N_i^e}{\partial \zeta} \\ \dfrac{\partial N_i^e}{\partial \eta} \end{bmatrix}$$

and the Jacobian is calculated as:

$$[J] = \begin{bmatrix} \sum_{i=1}^{4} x_i \frac{\partial N_i^e}{\partial \zeta} & \sum_{i=1}^{4} y_i \frac{\partial N_i^e}{\partial \zeta} \\ \sum_{i=1}^{4} x_i \frac{\partial N_i^e}{\partial \eta} & \sum_{i=1}^{4} y_i \frac{\partial N_i^e}{\partial \eta} \end{bmatrix} \tag{4.77}$$

Substituting equations (4.74) - (4.76) into variational forms (4.66) and (4.68) and truncating the expansions, these expansions can be reduced to the form

$$[\mathbf{M}]_{ij}\ddot{\Delta}_j + [\mathbf{K}]_{ij}\Delta_j = \{F^e\} + \{F^m\} + \left\{F^{ext}\right\} \tag{4.78}$$

where, $\Delta = \{u_0,\, v_0,\, w_0,\, \phi_x,\, \phi_y,\, e_z\}^T$.

Thus, the 2-D finite element formulation for this fully coupled electro-magneto-mechanical fields in a high frequency system is set up here. This formulation can be used for design and analysis of many applications like macrofiber composites, load-bearing antennas, etc., which will be a future direction for this work.

4.11 Conclusion

The complete set of equations governing the fully coupled TEMM behavior are presented in this chapter. These governing equations are utilized to demonstrate novel modeling techniques for load-bearing antenna. They are presented in nondimensional form and the corresponding nondimensional groups are deduced. Each nondimensional group quantifies a corresponding physical effect. The order or magnitude of these nondimensional groups for a particular regime are derived by determining the characteristic scales of all the parameters involved in the process. The relative ordering of these nondimensional groups identifies the dominant effects of the regime. By ignoring higher order terms, the mathematical structure of leading order governing equations corresponding to the regime is derived. Thus, a unique framework has been

demonstrated to derive regimes and analyze the behavior of coupled electo-magneto-mechanical systems for a given design or application. The need for such a theoretical framework becomes more apparent for highly complex systems, as this work provides a methodical way of identifying the dominant physical effects and making appropriate approximations to the system. This theory can be applied to practical fields like design and modeling of novel multifunctional materials.

Chapter 5: Conclusion

The central aim of this work is to develop a unified continuum framework for fully coupled thermo-electro-magneto-mechanical systems applicable to smart materials, multifunctional structures, adaptive systems, and intelligent devices. This framework is developed from a unified perspective by integrating lexicon and concepts from continuum thermomechanics, classical electromagnetism, and classical thermodynamics. And, for the sake of generality, it is developed with minimal assumptions: it is three-dimensional, fully coupled, and capable of accommodating anisotropy, multiphysics, dynamic effects, strong electrical and magnetic fields, finite deformations, and other nonlinearities.

One of the major challenges in developing such a unified framework is to bridge the two separate worlds of *electrodynamics* and *continuum mechanics*. They have been traditionally considered as two separate branches of physics, as electrodynamics deals with study of electric charges in motion, whereas continuum mechanics deals with deformation and flow of matter. Electrodynamics governed by Maxwell equations and continuum mechanics governed by thermo-mechanical conservation laws (i.e., mass, momentum, angular momentum, and energy conservation laws) cover a broad range of phenomena occurring at different time scales, and were utilized for widely disparate applications. With the rise of new applications and novel multifunctional

materials with coupled electromagnetic and mechanical properties, there is need to explore the fully coupled theories that describe the unification of these two branches.

To this end, in this dissertation, a fully coupled TEMM framework applicable to multifunctional materials and structures was delivered. The research objectives accomplished in this dissertation can be classified as (i) Development of a unified thermodynamic framework that can be used to model and design a broad range of multifunctional materials and structures, (ii) Development of analytical and computational techniques to model novel multifunctional systems in regimes not explored previously in literature. More specifically, asymptotic theories applicable to special geometries or specific unexplored regimes of behavior were developed, which can have applications in designing and developing new multifunctional technology. In other words, this dissertation focuses on development of unified modeling framework that can integrate the techniques and terminology used in structural dynamics and electrodynamics to model and design the new generation of materials, structures and intelligent devices.

5.1 Unified Thermodynamic Framework for Fully Coupled TEMM Processes

A fully coupled continuum framework was developed for modeling and characterizing thermo-electro-magneto-mechanical processes. This framework consists of two parts: (i) a comprehensive catalogue of state variables, thermodynamic potentials, and state equations (ii) development of constitutive functions for linear-reversible, transport, and hysteretic processes. This framework was presented from a unified perspective, integrating lexicon and concepts from continuum thermomechanics, classical electromagnetism, and classical thermodynamics. And, for the sake of generality, it

was developed with minimal assumptions: it is three-dimensional, multiphysics, fully coupled, and capable of accommodating anisotropy, dynamic effects, strong electrical and magnetic fields, finite deformations, and other nonlinearities.

Central to the development of part (i) is the fundamental energetic process, which, *analogous to classical thermodynamics,* features extensive independent variables, intensive dependent variables, and specific internal energy as the characterizing thermodynamic potential. Collectively, the extensive independent variables, the specific internal energy, and the set of state equations rendered by the second law of thermodynamics constitute the fundamental energetic formulation. *The fundamental energetic formulation was used as the thermodynamically consistent starting point from which all alternative energetic formulations were derived.* These alternative formulations were classified as either those whose thermodynamic energy potentials use any or all of the conjugate intensive quantities as independent variables, or those whose energy potentials use one or more non-conjugate (auxiliary) electromagnetic quantities as independent variables. The former were introduced using Legendre transformations of the internal energy, the latter using novel Legendre-type transformations. This formalism was then extended to formulations that employ entropy rather than energy as the characterizing thermodynamic potential. Many of the thermodynamic potentials appearing in our catalogue, both energetic and entropic, were introduced for the first time.

Each of the TEMM processes catalogued in part (i) correlates with a set of experiments, the independent variables being controlled and the dependent variables being the measured responses. The breadth of our catalogue aims to provide experimentalists with optimal flexibility in their approach to designing and characterizing

materials: energy or entropy landscapes can be constructed to achieve targeted performance properties expressed mathematically in the language of any set of TEMM quantities, or material properties can be deduced by working with a set of state equations that corresponds to a particular set of experiments. Our catalogue also represents a starting point for characterizing constrained TEMM materials and processes; it is particularly compatible with modeling approaches that regard constraints (e.g., incompressibility) as constitutive limits, i.e., restrictions on the constitutive behavior of the material as described by the thermodynamic potential [68].

In part (ii), the second law statement and state equations developed in part (i) were utilized to derive constitutive equations for a broad range of material behavior. The restrictions imposed by invariance and angular momentum balance were addressed. Linearization and Taylor series expansion techniques were further used to develop constitutive equations for reversible processes (near equilibrium processes). The residual inequality of second law statement was then utilized to develop constitutive restrictions on transport processes.

To develop constitutive models for materials that undergo hysteresis, the formalism described above is insufficient. An additional set of independent variables are needed to describe the energy losses caused by hysteresis and the associated microstructural changes in material. These additional independent variables, known as order-parameters, are associated with the particular microstructural changes. In this work, to accommodate hysteresis, the statement of second law was modified using a framework developed by Gurtin & Fried [23, 24] and was extended to fully coupled TEMM system to develop unified energy models for this system.

Although issues of coupling are treated in this work at a continuum level, physically coupling occurs at crystal level. In order to develop constitutive equations quantifying hysteresis or other material specific behavior, crystallographic and microstructural details need to be coupled with this continuum framework.

5.2 Asymptotic 2-D theories for multifunctional structures, with applications to load-bearing antenna structures

This chapter detailed the systematic derivation of leading-order models for multifunctional materials and structures using nondimensionalization and perturbation theories. This mathematical framework was deduced starting from the comprehensive TEMM theory [34], to derive regime and structure specific models using nondimensionalization and perturbation techniques. Perturbation techniques and asymptotic regime analysis were used in two different ways; (i) Given a particular design and its operating regime, the leading order equations were derived and solved for performance analysis, (ii) Given a set of targeted properties, mathematical formulation to design the structure that gives the most optimal performance was developed. Both these formalisms were explored, especially with regards to design and analysis of load-bearing antenna structures.

The load-bearing antenna structure is subjected to mechanical forces, temperature gradients, and electromagnetic fields, giving rise to highly-coupled nonlinear thermo-electro-magneto-mechanical (TEMM) behavior. In order to improve its design, the nature of structural deformations and electromagnetic radiations of this design need to be optimized. This can be achieved by developing analytical techniques and computational tools for multi-scale, multi-physics modeling of composite load-bearing antennas.

Due to the complexity of this system, there is a limited literature available on modeling techniques for load-bearing antennas. Computational and analytical modeling techniques for single functional antennas in stationary media have been developed extensively in literature [47, 63, 39] but integration of antenna with mechanical structure interferes with its electrical performance and these models are no longer valid for aerodynamic external conditions. Mathematical models were developed in this chapter, for analysis of fully coupled behavior of load-bearing antennas.

Using our mathematical framework, the operating regime and leading order models for load-bearing antenna were derived and solved analytically. These analytical solutions were then utilized to calculate deflections and antenna gain for various materials and the results were compared. For more complex systems involving coupled constitutive behavior, a unique coupled electro-magneto-mechanical plate theory was developed for high frequency systems, using perturbation techniques. The variational form for this system was further developed and the finite element formulation was set up.

The major contributions of this work can be summarized as:

- Development of unified continuum thermodynamic framework for fully coupled thermo-electro-magneto-mechanical behavior, consistent with classical thermodynamics principles

- Development of a comprehensive catalogue of free energies for fully coupled TEMM processes with all possible combinations of independent variables

- Derivation of thermodynamic state equations corresponding to the free energies, and application of these state equations to derive constitutive equations for equilibrium and transport processes

- Modifying the Clausius-Duhem inequality statement to include addition terms characterizing hysteresis in polarizable, magnetizable or deformable media, using framework developed by Gurtin & Fried

- Derivation of the complete set of nondimensional equations for fully coupled TEMM systems and the corresponding nondimensional groups

- Demonstrating the use of regime analysis on this system to model various multifunctional structures

- Using this framework to develop leading order equations governing the coupled behavior of load-bearing antennas

- Development of a fully coupled electro-magneto-mechanical plate theory for dynamic high frequency systems like antennas along with its finite element formulation

5.3 Future Work

To conclude, unified framework to model and characterize the new generation of intelligent structures, devices, and adaptive materials has been developed. This work can be utilized for design and analysis of a broad range of multifunctional materials and structures. Some examples and possible future directions are explored in this section.

Design of multifunctional materials and structures - The "Inverse Problem"

Design of structures is usually accomplished using minimum energy or maximum entropy postulate. By developing energy models for active materials that are applicable to a broader regime of operation, the structure can be optimized to attain the best possible combination of thermal, electrical, magnetic or mechanical behavior.

The current trend in developing multifunctional structures is to develop novel man-made materials designed to have customized material properties like permeability and permittivity. Some examples of such man-made materials include metamaterials, photonic crystals [38]. The theoretical framework developed in this work can be utilized in such a design and by doing so, it would greatly reduce the number of experiments needed to develop the material.

This can be achieved by expressing the desired meso-scale properties in terms of material functions relating the state variables. Material response functions will be converted into conditions on the constitutive energy function through our state equations. By integrating these conditions, the energy function can be constructed which provides the necessary "recipe" for material design. This procedure can be termed as an "Inverse Problem", wherein the materials are designed and manufactured to meet targeted meso-scale properties.

Constrained Material Processes and Stability

Our catalogue also represents a starting point for characterizing constrained TEMM materials and processes (e.g., incompressibility); it is particularly suitable for approaches that model constraints as constitutive limits, i.e., restrictions on the constitutive behavior of the material as described by a thermodynamic potential [68].

A constrained theory is one in which it is assumed a priori that not all processes are possible: only those processes satisfying a prescribed relation between mechanical and thermal quantities are allowable. Such idealized models are created to exploit observed behavior of particular classes of materials under particular classes of TEMM loadings. Their use has two powerful advantages: the governing equations produced by a constrained theory are in general easier to solve than those produced by the full theory, and less experiments are necessary to characterize the material in the context of the constrained model. A framework describing purely thermomechanical constrained processes was developed in [68]. Following a similar approach for fully coupled TEMM, these forms can be utilized to study specific material constraints like incompressibility in TEMM solids. Depending on the constraint, stability of the thermodynamic process can be further investigated.

Appendix A: Appendix A

A.1 Energy and Entropy Formulations

Table A.1: Fully Coupled State Equations for Energy Family 1

Residual Inequality: $\mathbf{j}^* \cdot \mathbf{e}^* - \frac{1}{\theta}\,\mathbf{q} \cdot \operatorname{grad}\theta \geq 0$			
Energy Potential	State Equations		
ε	$\mathbf{P} = \rho_R \dfrac{\partial \varepsilon}{\partial \mathbf{F}} - J\,(\mathbf{e}^* \cdot \mathbf{p}^* + \mu_o \mathbf{h}^* \cdot \mathbf{m}^*)\,\mathbf{F}^{-\mathrm{T}}$		
	$\theta = \dfrac{\partial \varepsilon}{\partial \eta}$	$\mathbf{e}^* = \rho \dfrac{\partial \varepsilon}{\partial \mathbf{p}^*}$	$\mathbf{h}^* = \dfrac{\rho}{\mu_o} \dfrac{\partial \varepsilon}{\partial \mathbf{m}^*}$
$E^{F\eta em} = \varepsilon - \frac{1}{\rho}\,\mathbf{e}^* \cdot \mathbf{p}^*$	$\mathbf{P} = \rho_R \dfrac{\partial E^{F\eta em}}{\partial \mathbf{F}} - \mu_o\, J\,(\mathbf{h}^* \cdot \mathbf{m}^*)\,\mathbf{F}^{-\mathrm{T}}$		
	$\theta = \dfrac{\partial E^{F\eta em}}{\partial \eta}$	$\mathbf{p}^* = -\rho \dfrac{\partial E^{F\eta em}}{\partial \mathbf{e}^*}$	$\mathbf{h}^* = \dfrac{\rho}{\mu_o} \dfrac{\partial E^{F\eta em}}{\partial \mathbf{m}^*}$
$E^{F\eta ph} = \varepsilon - \frac{\mu_o}{\rho}\,\mathbf{h}^* \cdot \mathbf{m}^*$	$\mathbf{P} = \rho_R \dfrac{\partial E^{F\eta ph}}{\partial \mathbf{F}} - J\,(\mathbf{e}^* \cdot \mathbf{p}^*)\,\mathbf{F}^{-\mathrm{T}}$		
	$\theta = \dfrac{\partial E^{F\eta ph}}{\partial \eta}$	$\mathbf{e}^* = \rho \dfrac{\partial E^{F\eta ph}}{\partial \mathbf{p}^*}$	$\mathbf{m}^* = -\dfrac{\rho}{\mu_o} \dfrac{\partial E^{F\eta ph}}{\partial \mathbf{h}^*}$
$E^{F\eta eh} = \varepsilon - \frac{1}{\rho}\,\mathbf{e}^* \cdot \mathbf{p}^* - \frac{\mu_o}{\rho}\,\mathbf{h}^* \cdot \mathbf{m}^*$	$\mathbf{P} = \rho_R \dfrac{\partial E^{F\eta eh}}{\partial \mathbf{F}}$		
	$\theta = \dfrac{\partial E^{F\eta eh}}{\partial \eta}$	$\mathbf{p}^* = -\rho \dfrac{\partial E^{F\eta eh}}{\partial \mathbf{e}^*}$	$\mathbf{m}^* = -\dfrac{\rho}{\mu_o} \dfrac{\partial E^{F\eta eh}}{\partial \mathbf{h}^*}$

Table A.2: Fully Coupled State Equations for Energy Family 1 (with Auxiliary Electromagnetic IVs)

Residual Inequality: $\mathbf{j}^* \cdot \mathbf{e}^* - \frac{1}{\theta}\,\mathbf{q} \cdot \operatorname{grad}\theta \geq 0$			
Energy Potential	State Equations		
$E^{F\eta dm} = \varepsilon + \frac{\epsilon_o}{2\rho}\,\mathbf{e}^* \cdot \mathbf{e}^*$	$\mathbf{P} = \rho_R \dfrac{\partial E^{F\eta dm}}{\partial \mathbf{F}} - J\left(\mathbf{e}^* \cdot \mathbf{d}^* + \mu_o \mathbf{h}^* \cdot \mathbf{m}^* - \frac{1}{2}\epsilon_o \mathbf{e}^* \cdot \mathbf{e}^*\right)\mathbf{F}^{-\mathrm{T}}$		
	$\theta = \dfrac{\partial E^{F\eta dm}}{\partial \eta}$	$\mathbf{e}^* = \rho \dfrac{\partial E^{F\eta dm}}{\partial \mathbf{d}^*}$	$\mathbf{h}^* = \dfrac{\rho}{\mu_o}\dfrac{\partial E^{F\eta dm}}{\partial \mathbf{m}^*}$
$E^{F\eta pb} = \varepsilon + \frac{\mu_o}{2\rho}\,\mathbf{h}^* \cdot \mathbf{h}^*$	$\mathbf{P} = \rho_R \dfrac{\partial E^{F\eta pb}}{\partial \mathbf{F}} - J\left(\mathbf{e}^* \cdot \mathbf{p}^* + \mathbf{h}^* \cdot \mathbf{b}^* - \frac{1}{2}\mu_o \mathbf{h}^* \cdot \mathbf{h}^*\right)\mathbf{F}^{-\mathrm{T}}$		
	$\theta = \dfrac{\partial E^{F\eta pb}}{\partial \eta}$	$\mathbf{e}^* = \rho \dfrac{\partial E^{F\eta pb}}{\partial \mathbf{p}^*}$	$\mathbf{h}^* = \rho \dfrac{\partial E^{F\eta pb}}{\partial \mathbf{b}^*}$
$E^{F\eta dh} = \varepsilon + \frac{\epsilon_o}{2\rho}\,\mathbf{e}^* \cdot \mathbf{e}^* - \frac{\mu_o}{\rho}\,\mathbf{h}^* \cdot \mathbf{m}^*$	$\mathbf{P} = \rho_R \dfrac{\partial E^{F\eta dh}}{\partial \mathbf{F}} - J\left(\mathbf{e}^* \cdot \mathbf{d} - \frac{1}{2}\epsilon_o \mathbf{e}^* \cdot \mathbf{e}^*\right)\mathbf{F}^{-\mathrm{T}}$		
	$\theta = \dfrac{\partial E^{F\eta dh}}{\partial \eta}$	$\mathbf{e}^* = \rho \dfrac{\partial E^{F\eta dh}}{\partial \mathbf{d}^*}$	$\mathbf{m}^* = -\dfrac{\rho}{\mu_o}\dfrac{\partial E^{F\eta dh}}{\partial \mathbf{h}^*}$
$E^{F\eta eb} = \varepsilon - \frac{1}{\rho}\,\mathbf{e}^* \cdot \mathbf{p} + \frac{\mu_o}{2\rho}\,\mathbf{h}^* \cdot \mathbf{h}^*$	$\mathbf{P} = \rho_R \dfrac{\partial E^{F\eta eb}}{\partial \mathbf{F}} - J\left(\mathbf{h}^* \cdot \mathbf{b}^* - \frac{1}{2}\mu_o \mathbf{h}^* \cdot \mathbf{h}^*\right)\mathbf{F}^{-\mathrm{T}}$		
	$\theta = \dfrac{\partial E^{F\eta eb}}{\partial \eta}$	$\mathbf{p}^* = -\rho \dfrac{\partial E^{F\eta eb}}{\partial \mathbf{e}^*}$	$\mathbf{h}^* = \rho \dfrac{\partial E^{F\eta eb}}{\partial \mathbf{b}^*}$
$E^{F\eta db} = \varepsilon + \frac{\epsilon_o}{2\rho}\,\mathbf{e}^* \cdot \mathbf{e}^* + \frac{\mu_o}{2\rho}\,\mathbf{h}^* \cdot \mathbf{h}^*$	$\mathbf{P} = \rho_R \dfrac{\partial E^{F\eta db}}{\partial \mathbf{F}} - J\left(\mathbf{e}^* \cdot \mathbf{d}^* + \mathbf{h}^* \cdot \mathbf{b}^* - \frac{1}{2}\epsilon_o \mathbf{e}^* \cdot \mathbf{e}^* - \frac{1}{2}\mu_o \mathbf{h}^* \cdot \mathbf{h}^*\right)\mathbf{F}^{-\mathrm{T}}$		
	$\theta = \dfrac{\partial E^{F\eta db}}{\partial \eta}$	$\mathbf{e}^* = \rho \dfrac{\partial E^{F\eta db}}{\partial \mathbf{d}^*}$	$\mathbf{h}^* = \rho \dfrac{\partial E^{F\eta db}}{\partial \mathbf{b}^*}$

Table A.3: Fully Coupled State Equations for Energy Family 2

Residual Inequality: $\mathbf{j}^* \cdot \mathbf{e}^* - \frac{1}{\theta}\,\mathbf{q} \cdot \operatorname{grad}\theta \geq 0$			
Energy Potential	State Equations		
$E^{F\theta pm} = \varepsilon - \theta\eta$	$\mathbf{P} = \rho_R \dfrac{\partial E^{F\theta pm}}{\partial \mathbf{F}} - J\left(\mathbf{e}^* \cdot \mathbf{p}^* + \mu_o \mathbf{h}^* \cdot \mathbf{m}^*\right)\mathbf{F}^{-\mathrm{T}}$		
	$\eta = -\dfrac{\partial E^{F\theta pm}}{\partial \theta}$	$\mathbf{e}^* = \rho \dfrac{\partial E^{F\theta pm}}{\partial \mathbf{p}^*}$	$\mathbf{h}^* = \dfrac{\rho}{\mu_o}\dfrac{\partial E^{F\theta pm}}{\partial \mathbf{m}^*}$
$E^{F\theta em} = \varepsilon - \theta\eta - \frac{1}{\rho}\,\mathbf{e}^* \cdot \mathbf{p}^*$	$\mathbf{P} = \rho_R \dfrac{\partial E^{F\theta em}}{\partial \mathbf{F}} - \mu_o\, J\left(\mathbf{h}^* \cdot \mathbf{m}^*\right)\mathbf{F}^{-\mathrm{T}}$		
	$\eta = -\dfrac{\partial E^{F\theta em}}{\partial \theta}$	$\mathbf{p}^* = -\rho \dfrac{\partial E^{F\theta em}}{\partial \mathbf{e}^*}$	$\mathbf{h}^* = \dfrac{\rho}{\mu_o}\dfrac{\partial E^{F\theta em}}{\partial \mathbf{m}^*}$
$E^{F\theta ph} = \varepsilon - \theta\eta - \frac{\mu_o}{\rho}\,\mathbf{h}^* \cdot \mathbf{m}^*$	$\mathbf{P} = \rho_R \dfrac{\partial E^{F\theta ph}}{\partial \mathbf{F}} - J\left(\mathbf{e}^* \cdot \mathbf{p}^*\right)\mathbf{F}^{-\mathrm{T}}$		
	$\eta = -\dfrac{\partial E^{F\theta ph}}{\partial \theta}$	$\mathbf{e}^* = \rho \dfrac{\partial E^{F\theta ph}}{\partial \mathbf{p}^*}$	$\mathbf{m}^* = -\dfrac{\rho}{\mu_o}\dfrac{\partial E^{F\theta ph}}{\partial \mathbf{h}^*}$
$E^{F\theta eh} = \varepsilon - \theta\eta - \frac{1}{\rho}\,\mathbf{e}^* \cdot \mathbf{p}^* - \frac{\mu_o}{\rho}\,\mathbf{h}^* \cdot \mathbf{m}^*$	$\mathbf{P} = \rho_R \dfrac{\partial E^{F\theta eh}}{\partial \mathbf{F}}$		
	$\eta = -\dfrac{\partial E^{F\theta eh}}{\partial \theta}$	$\mathbf{p}^* = -\rho \dfrac{\partial E^{F\theta eh}}{\partial \mathbf{e}^*}$	$\mathbf{m}^* = -\dfrac{\rho}{\mu_o}\dfrac{\partial E^{F\theta eh}}{\partial \mathbf{h}^*}$

Table A.4: Fully Coupled State Equations for Energy Family 2 (with Auxiliary Electromagnetic IVs)

Residual Inequality: $\mathbf{j}^* \cdot \mathbf{e}^* - \frac{1}{\theta}\,\mathbf{q} \cdot \operatorname{grad}\theta \geq 0$			
Energy Potential	State Equations		
$E^{F\theta dm} = \varepsilon - \theta\eta + \frac{\epsilon_o}{2\rho}\,\mathbf{e}^* \cdot \mathbf{e}^*$	$\mathbf{P} = \rho_R \dfrac{\partial E^{F\theta dm}}{\partial \mathbf{F}} - J\left(\mathbf{e}^* \cdot \mathbf{d}^* + \mu_o \mathbf{h}^* \cdot \mathbf{m}^* - \frac{1}{2}\epsilon_o \mathbf{e}^* \cdot \mathbf{e}^*\right)\mathbf{F}^{-\mathrm{T}}$		
	$\eta = -\dfrac{\partial E^{F\theta dm}}{\partial \theta}$	$\mathbf{e}^* = \rho \dfrac{\partial E^{F\theta dm}}{\partial \mathbf{d}^*}$	$\mathbf{h}^* = \dfrac{\rho}{\mu_o}\dfrac{\partial E^{F\theta dm}}{\partial \mathbf{m}^*}$
$E^{F\theta pb} = \varepsilon - \theta\eta + \frac{\mu_o}{2\rho}\,\mathbf{h}^* \cdot \mathbf{h}^*$	$\mathbf{P} = \rho_R \dfrac{\partial E^{F\theta pb}}{\partial \mathbf{F}} - J\left(\mathbf{e}^* \cdot \mathbf{p}^* + \mathbf{h}^* \cdot \mathbf{b}^* - \frac{1}{2}\mu_o \mathbf{h}^* \cdot \mathbf{h}^*\right)\mathbf{F}^{-\mathrm{T}}$		
	$\eta = -\dfrac{\partial E^{F\theta pb}}{\partial \theta}$	$\mathbf{e}^* = \rho \dfrac{\partial E^{F\theta pb}}{\partial \mathbf{p}^*}$	$\mathbf{h}^* = \rho \dfrac{\partial E^{F\theta pb}}{\partial \mathbf{b}^*}$
$E^{F\theta dh} = \varepsilon - \theta\eta + \frac{\epsilon_o}{2\rho}\,\mathbf{e}^* \cdot \mathbf{e}^* - \frac{\mu_o}{\rho}\,\mathbf{h}^* \cdot \mathbf{m}^*$	$\mathbf{P} = \rho_R \dfrac{\partial E^{F\theta dh}}{\partial \mathbf{F}} - J\left(\mathbf{e}^* \cdot \mathbf{d} - \frac{1}{2}\epsilon_o \mathbf{e}^* \cdot \mathbf{e}^*\right)\mathbf{F}^{-\mathrm{T}}$		
	$\eta = -\dfrac{\partial E^{F\theta dh}}{\partial \theta}$	$\mathbf{e}^* = \rho \dfrac{\partial E^{F\theta dh}}{\partial \mathbf{d}^*}$	$\mathbf{m}^* = -\dfrac{\rho}{\mu_o}\dfrac{\partial E^{F\theta dh}}{\partial \mathbf{h}^*}$
$E^{F\theta eb} = \varepsilon - \theta\eta - \frac{1}{\rho}\,\mathbf{e}^* \cdot \mathbf{p} + \frac{\mu_o}{2\rho}\,\mathbf{h}^* \cdot \mathbf{h}^*$	$\mathbf{P} = \rho_R \dfrac{\partial E^{F\theta eb}}{\partial \mathbf{F}} - J\left(\mathbf{h}^* \cdot \mathbf{b}^* - \frac{1}{2}\mu_o \mathbf{h}^* \cdot \mathbf{h}^*\right)\mathbf{F}^{-\mathrm{T}}$		
	$\eta = -\dfrac{\partial E^{F\theta eb}}{\partial \theta}$	$\mathbf{p}^* = -\rho \dfrac{\partial E^{F\theta eb}}{\partial \mathbf{e}^*}$	$\mathbf{h}^* = \rho \dfrac{\partial E^{F\theta eb}}{\partial \mathbf{b}^*}$
$E^{F\theta db} = \varepsilon - \theta\eta + \frac{\epsilon_o}{2\rho}\,\mathbf{e}^* \cdot \mathbf{e}^* + \frac{\mu_o}{2\rho}\,\mathbf{h}^* \cdot \mathbf{h}^*$	$\mathbf{P} = \rho_R \dfrac{\partial E^{F\theta db}}{\partial \mathbf{F}} - J\left(\mathbf{e}^* \cdot \mathbf{d}^* + \mathbf{h}^* \cdot \mathbf{b}^* - \frac{1}{2}\epsilon_o \mathbf{e}^* \cdot \mathbf{e}^* - \frac{1}{2}\mu_o \mathbf{h}^* \cdot \mathbf{h}^*\right)\mathbf{F}^{-\mathrm{T}}$		
	$\eta = -\dfrac{\partial E^{F\theta db}}{\partial \theta}$	$\mathbf{e}^* = \rho \dfrac{\partial E^{F\theta db}}{\partial \mathbf{d}^*}$	$\mathbf{h}^* = \rho \dfrac{\partial E^{F\theta db}}{\partial \mathbf{b}^*}$

Table A.5: Fully Coupled State Equations for Energy Family 3

Residual Inequality: $\mathbf{j}^* \cdot \mathbf{e}^* - \frac{1}{\theta}\,\mathbf{q} \cdot \operatorname{grad}\theta \;\geq\; 0$		
Energy Potential	State Equations	
$E^{P\eta pm} = \varepsilon - \frac{1}{\rho_R}\,\mathbf{P}\cdot\mathbf{F}$	$\mathbf{F} = -\rho_R \dfrac{\partial E^{P\eta pm}}{\partial \mathbf{P}}$	$\theta = \dfrac{\partial E^{P\eta pm}}{\partial \eta}$
	$\mathbf{e}^* = \dfrac{\partial E^{P\eta pm}}{\partial(\frac{\mathbf{p}^*}{\rho})}$	$\mathbf{h}^* = \dfrac{1}{\mu_o}\dfrac{\partial E^{P\eta pm}}{\partial(\frac{\mathbf{m}^*}{\rho})}$
$E^{P\eta em} = \varepsilon - \frac{1}{\rho_R}\,\mathbf{P}\cdot\mathbf{F} - \mathbf{e}^*\cdot\dfrac{\mathbf{p}^*}{\rho}$	$\mathbf{F} = -\rho_R \dfrac{\partial E^{P\eta em}}{\partial \mathbf{P}}$	$\theta = \dfrac{\partial E^{P\eta em}}{\partial \eta}$
	$\mathbf{p}^* = -\rho \dfrac{\partial E^{P\eta em}}{\partial \mathbf{e}^*}$	$\mathbf{h}^* = \dfrac{1}{\mu_o}\dfrac{\partial E^{P\eta em}}{\partial(\frac{\mathbf{m}^*}{\rho})}$
$E^{P\eta ph} = \varepsilon - \frac{1}{\rho_R}\,\mathbf{P}\cdot\mathbf{F} - \mu_o\,\mathbf{h}^*\cdot\dfrac{\mathbf{m}^*}{\rho}$	$\mathbf{F} = -\rho_R \dfrac{\partial E^{P\eta ph}}{\partial \mathbf{P}}$	$\theta = \dfrac{\partial E^{P\eta ph}}{\partial \eta}$
	$\mathbf{e}^* = \dfrac{\partial E^{P\eta ph}}{\partial(\frac{\mathbf{p}^*}{\rho})}$	$\mathbf{m}^* = -\dfrac{\rho}{\mu_o}\dfrac{\partial E^{P\eta ph}}{\partial \mathbf{h}^*}$
$E^{P\eta eh} = \varepsilon - \frac{1}{\rho_R}\,\mathbf{P}\cdot\mathbf{F} - \mathbf{e}^*\cdot\dfrac{\mathbf{p}^*}{\rho} - \mu_o\,\mathbf{h}^*\cdot\dfrac{\mathbf{m}^*}{\rho}$	$\mathbf{F} = -\rho_R \dfrac{\partial E^{P\eta eh}}{\partial \mathbf{P}}$	$\theta = \dfrac{\partial E^{P\eta eh}}{\partial \eta}$
	$\mathbf{p}^* = -\rho \dfrac{\partial E^{P\eta eh}}{\partial \mathbf{e}^*}$	$\mathbf{m}^* = -\dfrac{\rho}{\mu_o}\dfrac{\partial E^{P\eta eh}}{\partial \mathbf{h}^*}$

Table A.6: Fully Coupled State Equations for Energy Family 4

Residual Inequality: $\mathbf{j}^* \cdot \mathbf{e}^* - \frac{1}{\theta}\,\mathbf{q} \cdot \operatorname{grad}\theta \geq 0$		
Energy Potential	State Equations	
$E^{P\theta pm} = \varepsilon - \frac{1}{\rho_R}\mathbf{P}\cdot\mathbf{F} - \theta\eta$	$\mathbf{F} = -\rho_R \dfrac{\partial E^{P\theta pm}}{\partial \mathbf{P}}$	$\eta = -\dfrac{\partial E^{P\theta pm}}{\partial \theta}$
	$\mathbf{e}^* = \dfrac{\partial E^{P\theta pm}}{\partial(\frac{\mathbf{p}^*}{\rho})}$	$\mathbf{h}^* = \dfrac{1}{\mu_o}\dfrac{\partial E^{P\theta pm}}{\partial(\frac{\mathbf{m}^*}{\rho})}$
$E^{P\theta em} = \varepsilon - \frac{1}{\rho_R}\mathbf{P}\cdot\mathbf{F} - \theta\eta - \mathbf{e}^*\cdot\dfrac{\mathbf{p}^*}{\rho}$	$\mathbf{F} = -\rho_R \dfrac{\partial E^{P\theta em}}{\partial \mathbf{P}}$	$\eta = -\dfrac{\partial E^{P\theta em}}{\partial \theta}$
	$\mathbf{p}^* = -\rho\dfrac{\partial E^{P\theta em}}{\partial \mathbf{e}^*}$	$\mathbf{h}^* = \dfrac{1}{\mu_o}\dfrac{\partial E^{P\theta em}}{\partial(\frac{\mathbf{m}^*}{\rho})}$
$E^{P\theta ph} = \varepsilon - \frac{1}{\rho_R}\mathbf{P}\cdot\mathbf{F} - \theta\eta - \mu_o\,\mathbf{h}^*\cdot\dfrac{\mathbf{m}^*}{\rho}$	$\mathbf{F} = -\rho_R \dfrac{\partial E^{P\theta ph}}{\partial \mathbf{P}}$	$\eta = -\dfrac{\partial E^{P\theta ph}}{\partial \theta}$
	$\mathbf{e}^* = \dfrac{\partial E^{P\theta ph}}{\partial(\frac{\mathbf{p}^*}{\rho})}$	$\mathbf{m}^* = -\dfrac{\rho}{\mu_o}\dfrac{\partial E^{P\theta ph}}{\partial \mathbf{h}^*}$
$E^{P\theta eh} = \varepsilon - \frac{1}{\rho_R}\mathbf{P}\cdot\mathbf{F} - \theta\eta - \mathbf{e}^*\cdot\dfrac{\mathbf{p}^*}{\rho} - \mu_o\,\mathbf{h}^*\cdot\dfrac{\mathbf{m}^*}{\rho}$	$\mathbf{F} = -\rho_R \dfrac{\partial E^{P\theta eh}}{\partial \mathbf{P}}$	$\eta = -\dfrac{\partial E^{P\theta eh}}{\partial \theta}$
	$\mathbf{p}^* = -\rho\dfrac{\partial E^{P\theta eh}}{\partial \mathbf{e}^*}$	$\mathbf{m}^* = -\dfrac{\rho}{\mu_o}\dfrac{\partial E^{P\theta eh}}{\partial \mathbf{h}^*}$

Table A.7: Fully Coupled State Equations for Entropy Family 1

Residual Inequality: $\mathbf{j}^* \cdot \mathbf{e}^* - \frac{1}{\theta}\,\mathbf{q} \cdot \operatorname{grad}\theta \geq 0$			
Entropy Potential	State Equations		
η	$\mathbf{P} = -\rho_R\theta\,\dfrac{\partial\eta}{\partial\mathbf{F}} - J\,(\mathbf{e}^*\cdot\mathbf{p}^* + \mu_o\mathbf{h}^*\cdot\mathbf{m}^*)\,\mathbf{F}^{-\mathrm{T}}$		
	$\dfrac{1}{\theta} = \dfrac{\partial\eta}{\partial\varepsilon}$	$\mathbf{e}^* = -\rho\theta\,\dfrac{\partial\eta}{\partial\mathbf{p}^*}$	$\mathbf{h}^* = -\dfrac{\rho\theta}{\mu_o}\,\dfrac{\partial\eta}{\partial\mathbf{m}^*}$
$\eta^{F\varepsilon em} = \eta + \frac{1}{\rho\theta}\,\mathbf{e}^*\cdot\mathbf{p}^*$	$\mathbf{P} = -\rho_R\theta\,\dfrac{\partial\eta^{F\varepsilon em}}{\partial\mathbf{F}} - J\mu_o\,(\mathbf{h}^*\cdot\mathbf{m}^*)\,\mathbf{F}^{-\mathrm{T}}$		
	$\dfrac{1}{\theta} = \dfrac{\partial\eta^{F\varepsilon em}}{\partial\varepsilon}$	$\mathbf{p}^* = \rho\dfrac{\partial\eta^{F\varepsilon em}}{\partial(\frac{\mathbf{e}^*}{\theta})}$	$\mathbf{h}^* = -\dfrac{\rho\theta}{\mu_o}\,\dfrac{\partial\eta^{F\varepsilon em}}{\partial\mathbf{m}^*}$
$\eta^{F\varepsilon ph} = \eta + \frac{\mu_o}{\rho\theta}\,\mathbf{h}^*\cdot\mathbf{m}^*$	$\mathbf{P} = -\rho_R\theta\,\dfrac{\partial\eta^{F\varepsilon ph}}{\partial\mathbf{F}} - J\,(\mathbf{e}^*\cdot\mathbf{p}^*)\,\mathbf{F}^{-\mathrm{T}}$		
	$\dfrac{1}{\theta} = \dfrac{\partial\eta^{F\varepsilon ph}}{\partial\varepsilon}$	$\mathbf{e}^* = -\rho\theta\,\dfrac{\partial\eta^{F\varepsilon ph}}{\partial\mathbf{p}^*}$	$\mathbf{m}^* = \dfrac{\rho}{\mu_o}\,\dfrac{\partial\eta^{F\varepsilon ph}}{\partial(\frac{\mathbf{h}^*}{\theta})}$
$\eta^{F\varepsilon eh} = \eta + \frac{1}{\rho\theta}\,\mathbf{e}^*\cdot\mathbf{p}^* + \frac{\mu_o}{\rho\theta}\,\mathbf{h}^*\cdot\mathbf{m}^*$	$\mathbf{P} = -\rho_R\theta\,\dfrac{\partial\eta^{F\varepsilon eh}}{\partial\mathbf{F}}$		
	$\dfrac{1}{\theta} = \dfrac{\partial\eta^{F\varepsilon eh}}{\partial\varepsilon}$	$\mathbf{p}^* = \rho\,\dfrac{\partial\eta^{F\varepsilon eh}}{\partial(\frac{\mathbf{e}^*}{\theta})}$	$\mathbf{m}^* = \dfrac{\rho}{\mu_o}\,\dfrac{\partial\eta^{F\varepsilon eh}}{\partial(\frac{\mathbf{h}^*}{\theta})}$

Table A.8: Fully Coupled State Equations for Entropy Family 2

Residual Inequality: $\mathbf{j}^* \cdot \mathbf{e}^* - \frac{1}{\theta}\,\mathbf{q} \cdot \operatorname{grad}\theta \geq 0$		
Entropy Potential	State Equations	
$\eta^{F\theta pm} = \eta - \dfrac{\varepsilon}{\theta}$	$\mathbf{P} = -\rho_R\theta \dfrac{\partial \eta^{F\theta pm}}{\partial \mathbf{F}} - J\left(\mathbf{e}^* \cdot \mathbf{p}^* + \mu_o \mathbf{h}^* \cdot \mathbf{m}^*\right)\mathbf{F}^{-\mathrm{T}}$	$\mathbf{e}^* = -\rho\theta \dfrac{\partial \eta^{F\theta pm}}{\partial \mathbf{p}^*}$
	$\varepsilon = \theta^2 \dfrac{\partial \eta^{F\theta pm}}{\partial \theta}$	$\mathbf{h}^* = -\dfrac{\rho\theta}{\mu_o} \dfrac{\partial \eta^{F\theta pm}}{\partial \mathbf{m}^*}$
$\eta^{F\theta em} = \eta - \dfrac{\varepsilon}{\theta} + \dfrac{\mathbf{p}^*}{\rho} \cdot \dfrac{\mathbf{e}^*}{\theta}$	$\mathbf{P} = -\rho_R\theta \dfrac{\partial \eta^{F\theta em}}{\partial \mathbf{F}} - J\mu_o\left(\mathbf{h}^* \cdot \mathbf{m}^*\right)\mathbf{F}^{-\mathrm{T}}$	$\mathbf{p}^* = \rho\theta \dfrac{\partial \eta^{F\theta em}}{\partial \mathbf{e}^*}$
	$\varepsilon = \theta^2 \dfrac{\partial \eta^{F\theta em}}{\partial \theta} + \dfrac{1}{\rho}\,\mathbf{e}^* \cdot \mathbf{p}^*$	$\mathbf{h}^* = -\dfrac{\rho\theta}{\mu_o} \dfrac{\partial \eta^{F\theta em}}{\partial \mathbf{m}^*}$
$\eta^{F\theta ph} = \eta - \dfrac{\varepsilon}{\theta} + \mu_o \dfrac{\mathbf{m}^*}{\rho} \cdot \dfrac{\mathbf{h}^*}{\theta}$	$\mathbf{P} = -\rho_R\theta \dfrac{\partial \eta^{F\theta ph}}{\partial \mathbf{F}} - J\left(\mathbf{e}^* \cdot \mathbf{p}^*\right)\mathbf{F}^{-\mathrm{T}}$	$\mathbf{e}^* = -\rho\theta \dfrac{\partial \eta^{F\theta ph}}{\partial \mathbf{p}^*}$
	$\varepsilon = \theta^2 \dfrac{\partial \eta^{F\theta ph}}{\partial \theta} + \dfrac{\mu_o}{\rho}\,\mathbf{m}^* \cdot \mathbf{h}^*$	$\mathbf{m}^* = \dfrac{\rho\theta}{\mu_o} \dfrac{\partial \eta^{F\theta ph}}{\partial \mathbf{h}^*}$
$\eta^{F\theta eh} = \eta - \dfrac{\varepsilon}{\theta} + \dfrac{\mathbf{p}^*}{\rho} \cdot \dfrac{\mathbf{e}^*}{\theta} + \mu_o \dfrac{\mathbf{m}^*}{\rho} \cdot \dfrac{\mathbf{h}^*}{\theta}$	$\mathbf{P} = -\rho_R\theta \dfrac{\partial \eta^{F\theta eh}}{\partial \mathbf{F}}$	$\mathbf{p}^* = \rho\theta \dfrac{\partial \eta^{F\theta eh}}{\partial \mathbf{e}^*}$
	$\varepsilon = \theta^2 \dfrac{\partial \eta^{F\theta eh}}{\partial \theta} + \dfrac{\mu_o}{\rho}\mathbf{m}^* \cdot \mathbf{h}^* + \dfrac{1}{\rho}\mathbf{e}^* \cdot \mathbf{p}^*$	$\mathbf{m}^* = \dfrac{\rho\theta}{\mu_o} \dfrac{\partial \eta^{F\theta eh}}{\partial \mathbf{h}^*}$

Table A.9: Fully Coupled State Equations for Entropy Family 3

Residual Inequality: $\mathbf{j}^* \cdot \mathbf{e}^* - \frac{1}{\theta}\,\mathbf{q} \cdot \operatorname{grad}\theta \;\geq\; 0$		
Entropy Potential	State Equations	
$\eta^{P\varepsilon pm} = \eta + \frac{1}{\rho_R}\mathbf{F}\cdot\frac{\mathbf{P}}{\theta}$	$\mathbf{F} = \rho_R \dfrac{\partial \eta^{P\varepsilon pm}}{\partial(\frac{\mathbf{P}}{\theta})}$	$\dfrac{1}{\theta} = \dfrac{\partial \eta^{P\varepsilon pm}}{\partial \varepsilon}$
	$\mathbf{e}^* = -\theta \dfrac{\partial \eta^{P\varepsilon pm}}{\partial(\frac{\mathbf{p}^*}{\rho})}$	$\mathbf{h}^* = -\dfrac{\theta}{\mu_o}\dfrac{\partial \eta^{P\varepsilon pm}}{\partial(\frac{\mathbf{m}^*}{\rho})}$
$\eta^{P\varepsilon em} = \eta + \frac{1}{\rho_R}\mathbf{F}\cdot\frac{\mathbf{P}}{\theta} + \frac{\mathbf{p}^*}{\rho}\cdot\frac{\mathbf{e}^*}{\theta}$	$\mathbf{F} = \rho_R \dfrac{\partial \eta^{P\varepsilon em}}{\partial(\frac{\mathbf{P}}{\theta})}$	$\dfrac{1}{\theta} = \dfrac{\partial \eta^{P\varepsilon em}}{\partial \varepsilon}$
	$\mathbf{p}^* = \rho \dfrac{\partial \eta^{P\varepsilon em}}{\partial(\frac{\mathbf{e}^*}{\theta})}$	$\mathbf{h}^* = -\dfrac{\theta}{\mu_o}\dfrac{\partial \eta^{P\varepsilon em}}{\partial(\frac{\mathbf{m}^*}{\rho})}$
$\eta^{P\varepsilon ph} = \eta + \frac{1}{\rho_R}\mathbf{F}\cdot\frac{\mathbf{P}}{\theta} + \mu_o\frac{\mathbf{m}^*}{\rho}\cdot\frac{\mathbf{h}^*}{\theta}$	$\mathbf{F} = \rho_R \dfrac{\partial \eta^{P\varepsilon ph}}{\partial(\frac{\mathbf{P}}{\theta})}$	$\dfrac{1}{\theta} = \dfrac{\partial \eta^{P\varepsilon ph}}{\partial \varepsilon}$
	$\mathbf{e}^* = -\theta \dfrac{\partial \eta^{P\varepsilon ph}}{\partial(\frac{\mathbf{p}^*}{\rho})}$	$\mathbf{m}^* = \dfrac{\rho}{\mu_o}\dfrac{\partial \eta^{P\varepsilon ph}}{\partial(\frac{\mathbf{h}^*}{\theta})}$
$\eta^{P\varepsilon eh} = \eta + \frac{1}{\rho_R}\mathbf{F}\cdot\frac{\mathbf{P}}{\theta} + \frac{\mathbf{p}^*}{\rho}\cdot\frac{\mathbf{e}^*}{\theta} + \mu_o\frac{\mathbf{m}^*}{\rho}\cdot\frac{\mathbf{h}^*}{\theta}$	$\mathbf{F} = \rho_R \dfrac{\partial \eta^{P\varepsilon eh}}{\partial(\frac{\mathbf{P}}{\theta})}$	$\dfrac{1}{\theta} = \dfrac{\partial \eta^{P\varepsilon eh}}{\partial \varepsilon}$
	$\mathbf{p}^* = \rho \dfrac{\partial \eta^{P\varepsilon eh}}{\partial(\frac{\mathbf{e}^*}{\theta})}$	$\mathbf{m}^* = \dfrac{\rho}{\mu_o}\dfrac{\partial \eta^{P\varepsilon eh}}{\partial(\frac{\mathbf{h}^*}{\theta})}$

Table A.10: Fully Coupled State Equations for Entropy Family 4

Residual Inequality: $\mathbf{j}^* \cdot \mathbf{e}^* - \frac{1}{\theta}\,\mathbf{q} \cdot \operatorname{grad}\theta \geq 0$			
Entropy Potential	State Equations		
$\eta^{P\theta pm} = \eta - \dfrac{\varepsilon}{\theta} + \dfrac{1}{\rho_R}\mathbf{F}\cdot\dfrac{\mathbf{P}}{\theta}$	$\varepsilon = \theta^2 \dfrac{\partial \eta^{P\theta pm}}{\partial \theta} + \dfrac{1}{\rho_R}\mathbf{P}\cdot\mathbf{F}$		
	$\mathbf{F} = \rho_R\theta \dfrac{\partial \eta^{P\theta pm}}{\partial \mathbf{P}}$	$\mathbf{e}^* = -\theta \dfrac{\partial \eta^{P\theta pm}}{\partial(\frac{\mathbf{p}^*}{\rho})}$	$\mathbf{h}^* = -\dfrac{\theta}{\mu_o}\dfrac{\partial \eta^{P\theta pm}}{\partial(\frac{\mathbf{m}^*}{\rho})}$
$\eta^{P\theta em} = \eta - \dfrac{\varepsilon}{\theta} + \dfrac{1}{\rho_R}\mathbf{F}\cdot\dfrac{\mathbf{P}}{\theta} + \dfrac{\mathbf{p}^*}{\rho}\cdot\dfrac{\mathbf{e}^*}{\theta}$	$\varepsilon = \theta^2 \dfrac{\partial \eta^{P\theta em}}{\partial \theta} + \dfrac{1}{\rho_R}\mathbf{P}\cdot\mathbf{F} + \dfrac{1}{\rho}\mathbf{e}^*\cdot\mathbf{p}^*$		
	$\mathbf{F} = \rho_R\theta \dfrac{\partial \eta^{P\theta em}}{\partial \mathbf{P}}$	$\mathbf{p}^* = \rho\theta \dfrac{\partial \eta^{P\theta em}}{\partial \mathbf{e}^*}$	$\mathbf{h}^* = -\dfrac{\theta}{\mu_o}\dfrac{\partial \eta^{P\theta em}}{\partial(\frac{\mathbf{m}^*}{\rho})}$
$\eta^{P\theta ph} = \eta - \dfrac{\varepsilon}{\theta} + \dfrac{1}{\rho_R}\mathbf{F}\cdot\dfrac{\mathbf{P}}{\theta} + \mu_o\dfrac{\mathbf{m}^*}{\rho}\cdot\dfrac{\mathbf{h}^*}{\theta}$	$\varepsilon = \theta^2 \dfrac{\partial \eta^{P\theta ph}}{\partial \theta} + \dfrac{1}{\rho_R}\mathbf{P}\cdot\mathbf{F} + \dfrac{\mu_o}{\rho}\mathbf{m}^*\cdot\mathbf{h}^*$		
	$\mathbf{F} = \rho_R\theta \dfrac{\partial \eta^{P\theta ph}}{\partial \mathbf{P}}$	$\mathbf{e}^* = -\theta \dfrac{\partial \eta^{P\theta ph}}{\partial(\frac{\mathbf{p}^*}{\rho})}$	$\mathbf{m}^* = \dfrac{\rho\theta}{\mu_o}\dfrac{\partial \eta^{P\theta ph}}{\partial \mathbf{h}^*}$
$\eta^{P\theta eh} = \eta - \dfrac{\varepsilon}{\theta} + \dfrac{1}{\rho_R}\mathbf{F}\cdot\dfrac{\mathbf{P}}{\theta} + \dfrac{\mathbf{p}^*}{\rho}\cdot\dfrac{\mathbf{e}^*}{\theta} + \mu_o\dfrac{\mathbf{m}^*}{\rho}\cdot\dfrac{\mathbf{h}^*}{\theta}$	$\varepsilon = \theta^2 \dfrac{\partial \eta^{P\theta eh}}{\partial \theta} + \dfrac{1}{\rho_R}\mathbf{P}\cdot\mathbf{F} + \dfrac{\mu_o}{\rho}\mathbf{m}^*\cdot\mathbf{h}^* + \dfrac{1}{\rho}\mathbf{e}^*\cdot\mathbf{p}^*$		
	$\mathbf{F} = \rho_R\theta \dfrac{\partial \eta^{P\theta eh}}{\partial \mathbf{P}}$	$\mathbf{p}^* = \rho\theta \dfrac{\partial \eta^{P\theta eh}}{\partial \mathbf{e}^*}$	$\mathbf{m}^* = \dfrac{\rho\theta}{\mu_o}\dfrac{\partial \eta^{P\theta eh}}{\partial \mathbf{h}^*}$

A.2 Characteristic scales of parameters involved in TEMM process

Characteristic Scales	**Notation**
Time scale of electromagnetic phenomena	t_{e0}
Time scale of thermo-mechanical phenomena	t_{m0}
Length scale in x-direction	x_{1o}
Length scale in y-direction	x_{2o}
Length scale in z-direction	x_{3o}
Velocity scale in x-direction	v_{1o}
Velocity scale in y-direction	v_{2o}
Velocity scale in z-direction	v_{3o}
Electric field in x-direction	e_{1o}
Electric field in y-direction	e_{2o}
Electric field in z-direction	e_{3o}
Effective electric field in x-direction	e^*_{1o}
Effective electric field in y-direction	e^*_{2o}
Effective electric field in z-direction	e^*_{3o}
Magnetic field intensity in x-direction	h_{1o}
Magnetic field intensity in y-direction	h_{2o}
Magnetic field intensity in z-direction	h_{3o}
Effective magnetic field intensity in x-direction	h^*_{1o}
Effective magnetic field intensity in y-direction	h^*_{2o}

Effective magnetic field intensity in z-direction	h^*_{3o}
Electric displacement in x-direction	d_{1o}
Electric displacement in y-direction	d_{2o}
Electric displacement in z-direction	d_{3o}
Magnetic induction in x-direction	b_{1o}
Magnetic induction in y-direction	b_{2o}
Magnetic induction in z-direction	b_{3o}
Current density in x-direction	j_{1o}
Current density in y-direction	j_{2o}
Current density in z-direction	j_{3o}
Charge density	σ_o
Mass density	ρ_o
External force in x-direction	f_{1o}
External force in y-direction	f_{2o}
External force in z-direction	f_{3o}
Electromagnetic force in x-direction	f_{e1o}
Electromagnetic force in y-direction	f_{e2o}
Electromagnetic force in z-direction	f_{e3o}

Table A.11: List of Characteristic Scales Appearing in Table.1

Component of Cauchy stress tensor	T_{11o}
Component of Cauchy stress tensor	T_{12o}
Component of Cauchy stress tensor	T_{13o}
Component of Cauchy stress tensor	T_{22o}
Component of Cauchy stress tensor	T_{13o}
Component of Cauchy stress tensor	T_{33o}
Component of skew tensor due to couple L^e	L_{11o}
Component of skew tensor due to couple L^e	L_{12o}
Component of skew tensor due to couple L^e	L_{13o}
Component of skew tensor due to couple L^e	L_{21o}
Component of skew tensor due to couple L^e	L_{22o}
Component of skew tensor due to couple L^e	L_{23o}
Component of skew tensor due to couple L^e	L_{31o}
Component of skew tensor due to couple L^e	L_{32o}
Component of skew tensor due to couple L^e	L_{33o}
Internal energy density	ε_o
Heat flux in x-function	q_{1o}
Heat flux in y-function	q_{2o}
Heat flux in z-function	q_{3o}

Table A.12: List of Characteristic Scales Appearing in Table.1

Bibliography

[1] H. Attia, L. Yousefi, and O.M. Ramahi. Analytical model for calculating the radiation field of microstrip antennas with artificial magnetic superstrates: Theory and experiment. *Antennas and Propagation, IEEE Transactions on*, 59(5):1438–1445, 2011.

[2] C.A. Balanis. *Antenna theory: analysis and design/Constantine A. Balanis*. J. Wiley, New York, 1982.

[3] J. Bataille and J. Kestin. Irreversible processes and physical interpretation of rational thermodynamics. *Journal of Non-Equilibrium Thermodynamics*, 4(4):229–258, 2009.

[4] SE Bechtel, KD Bolinger, JZ Cao, and MG Forest. Torsional effects in high-order viscoelastic thin-filament models. *SIAM Journal on Applied Mathematics*, 55(1):58–99, 1995.

[5] SE Bechtel, JZ Cao, and MG Forest. Practical application of a higher order perturbation theory for slender viscoelastic jets and fibers. *Journal of non-newtonian fluid mechanics*, 41(3):201–273, 1992.

[6] S.B. Brown, K.H. Kim, and L. Anand. An internal variable constitutive model for hot working of metals. *International Journal of Plasticity*, 5(2):95–130, 1989.

[7] W.F. Brown. *Magnetoelastic Interactions*. Springer-Verlag, New York, 1966.

[8] W.G. Cady. *Piezoelectricity*. McGraw-Hill, New York, 1946.

[9] H.B. Callen. *Thermodynamics and an Introduction to Thermostatistics*. Wiley, New York, 2nd edition, 1985.

[10] H.B. Callen. *Thermodynamics and an Introduction to Thermostatistics*. Wiley, New York, 2nd edition, 1985.

[11] L. Christodoulou and J.D. Venables. Multifunctional material systems: The first generation. *JOM: Journal of the Minerals, Metals and Materials Society*, 55(12):39–45, 2003.

[12] B.D. Coleman and W. Noll. The thermodynamics of elastic materials with heat conduction and viscosity. *Archive for Rational Mechanics and Analysis*, 13(1):167–178, 1963.

[13] Bernard D. Coleman and Ellis H. Dill. On the thermodynamics of electromagnetic fields in materials with memory. *Archive for Rational Mechanics and Analysis*, 41:132–162, 1971. 10.1007/BF00281371.

[14] Bernard D. Coleman and Ellis H. Dill. Thermodynamic restrictions on the constitutive equations of electromagnetic theory. *Zeitschrift fr Angewandte Mathematik und Physik (ZAMP)*, 22:691–702, 1971. 10.1007/BF01587765.

[15] S.R. De Groot and L.G. Suttorp. *Foundations of Electrodynamics*. North-Holland Publishing Company, Amsterdam, 1972.

[16] A. Dorfmann and RW Ogden. Nonlinear magnetoelastic deformations. *The Quarterly Journal of Mechanics and Applied Mathematics*, 57(4):599–622, 2004.

[17] A. Dorfmann, RW Ogden, and G. Saccomandi. Universal relations for nonlinear magnetoelastic solids. *International Journal of Non-Linear Mechanics*, 39(10):1699–1708, 2004.

[18] A.C. Eringen. Continuum theory of micromorphic electromagnetic thermoelastic solids. *International Journal of Engineering Science*, 41(7):653–665, 2003.

[19] A.C. Eringen and G.A. Maugin. *Electrodynamics of Continua I: Foundations and Solid Media*. Springer-Verlag, New York, 1990.

[20] P.G. Evans. *Nonlinear magnetomechanical modeling and characterization of galfenol and system-level modeling of Galfenol-based transducers*. PhD thesis, The Ohio State University, 2009.

[21] PG Evans and MJ Dapino. Efficient magnetic hysteresis model for field and stress application in magnetostrictive galfenol. *Journal of Applied Physics*, 107(6):063906–063906, 2010.

[22] R.M. Fano, L.J. Chu, and R.B. Adler. *Electromagnetic fields, energy, and forces*. The MIT Press, Cambridge, Mass., 1968.

[23] E. Fried and M.E. Gurtin. Continuum theory of thermally induced phase transitions based on an order parameter. *Physica D: Nonlinear Phenomena*, 68(3-4):326–343, 1993.

[24] E. Fried and ME Gurtin. Dynamic solid-solid transitions with phase characterized by an order parameter. *Physica D: Nonlinear Phenomena*, 72(4):287–308, 1994.

[25] A. E. Green and P. M. Naghdi. On thermodynamics and the nature of the second law. *Proceedings of the Royal Society of London. A. Mathematical and Physical Sciences*, 357(1690):253–270, 1977.

[26] A. E. Green and P. M. Naghdi. Aspects of the second law of thermodynamics in the presence of electromagnetic effects. *The Quarterly Journal of Mechanics and Applied Mathematics*, 37(2):179–193, 1984.

[27] M.E. Gurtin. *An introduction to continuum mechanics*, volume 158. Academic Pr, 1981.

[28] M.E. Gurtin. Generalized ginzburg-landau and cahn-hilliard equations based on a microforce balance. *Physica D: Nonlinear Phenomena*, 92(3-4):178–192, 1996.

[29] M.E. Gurtin. On the plasticity of single crystals: free energy, microforces, plastic-strain gradients. *Journal of the Mechanics and Physics of Solids*, 48(5):989–1036, 2000.

[30] M.E. Gurtin. On a framework for small-deformation viscoplasticity: free energy, microforces, strain gradients. *International Journal of Plasticity*, 19(1):47–90, 2003.

[31] K. Hutter. A thermodynamic theory of fluids and solids in electromagnetic fields. *Archive for Rational Mechanics and Analysis*, 64(3):269–298, 1977.

[32] K. Hutter. Thermodynamic aspects in field-matter interactions. In H. Parkus, editor, *Electromagnetic Interactions in Elastic Solids*, pages 191–242. Springer-Verlag, Wien and New York, 1979.

[33] K. Hutter and Y.H. Pao. A dynamic theory for magnetizable elastic solids with thermal and electrical conduction. *Journal of Elasticity*, 4(2):89–114, 1974.

[34] K. Hutter, A.A.F. van de Ven, and A. Ursescu. *Electromagnetic Field Matter Interactions in Thermoelastic Solids and Viscous Fluids*. Springer, Berlin and Heidelberg, 2006.

[35] S.C. Hwang and R.M. McMeeking. A finite element model of ferroelectric polycrystals. *Ferroelectrics*, 211(1):177–194, 1998.

[36] S.C. Hwang and R.M. McMeeking. A finite element model of ferroelastic polycrystals. *International Journal of Solids and Structures*, 36(10):1541–1556, 1999.

[37] J. Jin, J. Jin, and J.M. Jin. *The finite element method in electromagnetics*. Wiley New York, 1993.

[38] J.D. Joannopoulos, S.G. Johnson, J.N. Winn, and R.D. Meade. *Photonic crystals: molding the flow of light*. Princeton university press, 2008.

[39] L. Josefsson and P. Persson. *Conformal array antenna theory and design*, volume 29. Wiley-IEEE Press, 2006.

[40] SV Kankanala and N. Triantafyllidis. On finitely strained magnetorheological elastomers. *Journal of the Mechanics and Physics of Solids*, 52(12):2869–2908, 2004.

[41] L.D. Landau and E.M. Lifshitz. *Statistical Physics, Part 1*. Butterworth-Heinemann, Oxford, 3rd edition, 1980.

[42] LD Landau and EM Lifshitz. *Theory of Elasticity*. Pergamon Press, Oxford, UK, 3rd edition, 1986.

[43] C.M. Landis. Non-linear constitutive modeling of ferroelectrics. *Current Opinion in Solid State and Materials Science*, 8(1):59–69, 2004.

[44] C.M. Landis. A continuum thermodynamics formulation for micro-magneto-mechanics with applications to ferromagnetic shape memory alloys. *Journal of the Mechanics and Physics of Solids*, 56(10):3059–3076, 2008.

[45] B.-L. Lee and D.J. Inman. Multifunctional materials and structures for autonomic systems. *Proceedings of the Institution of Mechanical Engineers, Part I: Journal of Systems and Control Engineering*, 223(4):431–434, 2009.

[46] LJ Li, CH Lei, YC Shu, and JY Li. Phase-field simulation of magnetoelastic couplings in ferromagnetic shape memory alloys. *Acta Materialia*, 2011.

[47] Y. Lo, D. Solomon, and W. Richards. Theory and experiment on microstrip antennas. *Antennas and Propagation, IEEE Transactions on*, 27(2):137–145, 1979.

[48] H.A. Lorentz. *The Theory of Electrons*. Dover, New York, 2nd edition, 2004.

[49] E. Lui. Multi-physics interactions for coupled thermo-electro-magneto-mechanical effects. Master's thesis, The Ohio State University, 2011.

[50] F. Massieu. *Sur les intégrales algébriques des problèmes de mécanique*. PhD thesis, 1861.

[51] F. Massieu. Sur les fonctions des divers fluides. *Comptes Rendus de l'Académie des Sciences*, 69:858–862, 1869.

[52] G.A. Maugin. *Continuum mechanics of electromagnetic solids*. North-Holland Amsterdam, 1988.

[53] J.C. Maxwell. A dynamical theory of the electromagnetic field. *Philosophical Transactions of the Royal Society of London*, 155:459–512, 1865.

[54] J.C. Maxwell. *A Treatise on Electricity and Magnetism*. Clarendon Press, Oxford, 1873.

[55] RD Mindlin. High frequency vibrations of piezoelectric crystal plates. *International Journal of Solids and Structures*, 8(7):895–906, 1972.

[56] M.J. Moran, H.N. Shapiro, D.D. Boettner, and M.B. Bailey. *Fundamentals of Engineering Thermodynamics*. Wiley, Hoboken, N.J., 7th edition, 2010.

[57] W. Muschik, C. Papenfuss, and H. Ehrentraut. A sketch of continuum thermodynamics. *Journal of non-newtonian Fluid Mechanics*, 96(1-2):255–290, 2001.

[58] A.H. Nayfeh. *Introduction to perturbation techniques*. Wiley-VCH, 2011.

[59] R.E. Newnham. *Properties of Materials: Anisotropy, Symmetry, Structure: Anisotropy, Symmetry, Structure*. OUP Oxford, 2004.

[60] Y.-H. Pao. Electromagnetic forces in deformable continua. In S. Nemat-Nasser, editor, *Mechanics Today*, volume 4, pages 209–305. Pergamon Press, Inc., New York, 1978.

[61] Y.-H. Pao and K. Hutter. Electrodynamics for moving elastic solids and viscous fluids. *Proceedings of the IEEE*, 63(7):1011–1021, 1975.

[62] AC Pipkin and RS Rivlin. Galvanomagnetic and thermomagnetic effects in isotropic materials. *Journal of Mathematical Physics*, 1:542, 1960.

[63] D.M. Pozar and D.H. Schaubert. *Microstrip antennas: the analysis and design of microstrip antennas and arrays*. Wiley-ieee press, 1995.

[64] KR Rajagopal and M. Ružička. Mathematical modeling of electrorheological materials. *Continuum Mechanics and Thermodynamics*, 13(1):59–78, 2001.

[65] JN Reddy. On laminated composite plates with integrated sensors and actuators. *Engineering Structures*, 21(7):568–593, 1999.

[66] J.N. Reddy. *Mechanics of laminated composite plates and shells: theory and analysis*. CRC, 2003.

[67] J.R. Rice. Inelastic constitutive relations for solids: an internal-variable theory and its application to metal plasticity. *Journal of the Mechanics and Physics of Solids*, 19(6):433–455, 1971.

[68] F.J. Rooney and S.E. Bechtel. Constraints, constitutive limits, and instability in finite thermoelasticity. *Journal of Elasticity*, 74(2):109–133, 2004.

[69] K. Salonitis, J. Pandremenos, J. Paralikas, and G. Chryssolouris. Multifunctional materials: engineering applications and processing challenges. *The International Journal of Advanced Manufacturing Technology*, 49(5):803–826, 2010.

[70] A. Sihvola. Metamaterials in electromagnetics. *Metamaterials*, 1(1):2–11, 2007.

[71] D. Sinha. A micro antenna device, November 12 2008. US Patent App. 12/809,780.

[72] R.C. Smith. *Smart Material Systems: Model Development*. Society for Industrial and Applied Mathematics (SIAM), Philadelphia, 2005.

[73] R.C. Smith, M.J. Dapino, and S. Seelecke. Free energy model for hysteresis in magnetostrictive transducers. *Journal of Applied Physics*, 93(1):458–466, 2003.

[74] H.A. Sodano, G. Park, and D.J. Inman. An investigation into the performance of macro-fiber composites for sensing and structural vibration applications. *Mechanical Systems and Signal Processing*, 18(3):683–697, 2004.

[75] Y. Su and C.M. Landis. Continuum thermodynamics of ferroelectric domain evolution: Theory, finite element implementation, and application to domain wall pinning. *Journal of the Mechanics and Physics of Solids*, 55(2):280–305, 2007.

[76] RA Toupin. A dynamical theory of elastic dielectrics. *International Journal of Engineering Science*, 1(1):101–126, 1963.

[77] C. Truesdell and R. Baierlein. Rational thermodynamics. *American Journal of Physics*, 53:1020–1021, 1985.

[78] C. Truesdell and R. Toupin. *The classical field theories*. Springer, 1960.

[79] E.A. Vittoz, M.G.R. Degrauwe, and S. Bitz. High-performance crystal oscillator circuits: Theory and application. *Solid-State Circuits, IEEE Journal of*, 23(3):774–783, 1988.

[80] R.B. Williams, G. Park, D.J. Inman, and W.K. Wilkie. An overview of composite actuators with piezoceramic fibers. In *Proc. 20th International Modal Analysis Conference*, 2002.

[81] C.S. You and W. Hwang. Design of load-bearing antenna structures by embedding technology of microstrip antenna in composite sandwich structure. *Composite Structures*, 71(3-4):378–382, 2005.

[82] CS You, W. Hwang, HC Park, RM Lee, and WS Park. Microstrip antenna for sar application with composite sandwich construction: surface-antenna-structure demonstration. *Journal of composite materials*, 37(4):351–364, 2003.